UNIVERSIDADE ESTADUAL PAULISTA
"JÚLIO DE MESQUITA FILHO"
INSTITUTO DE BIOCIÊNCIAS – RIO CLARO

PROGRAMA DE PÓS-GRADUAÇÃO EM ECOLOGIA E BIODIVERSIDADE

O EFEITO DE PAISAGENS ANTROPIZADAS SOBRE A ASSIMETRIA FLUTUANTE DE LEPIDÓPTEROS

Ademir Júnior Francisco

Rio Claro – SP

2021

PROGRAMA DE PÓS-GRADUAÇÃO EM ECOLOGIA E BIODIVERSIDADE

O EFEITO DE PAISAGENS ANTROPIZADAS SOBRE A ASSIMETRIA FLUTUANTE DE LEPIDÓPTEROS

Ademir Júnior Francisco

Dissertação apresentada ao Instituto de Biociências do Câmpus de Rio Claro, Universidade Estadual Paulista, como parte dos requisitos para obtenção do título de Mestre em Ecologia e Biodiversidade.

Orientadora: Profª. Drª. Marina Corrêa Côrtes

Rio Claro – SP

2021

F819e

Francisco, Ademir Júnior
O efeito de paisagens antropizadas sobre a assimetria flutuante de lepidópteros / Ademir Júnior Francisco. -- Rio Claro, 2021
83 p. : il., tabs., fotos

Dissertação (mestrado) - Universidade Estadual Paulista (Unesp), Instituto de Biociências, Rio Claro
Orientadora: Marina Corrêa Côrtes

1. Ecologia da paisagem. 2. Borboletas. 3. Morfometria. 4. Natureza Influência do homem. I. Título.

Sistema de geração automática de fichas catalográficas da Unesp. Biblioteca do Instituto de Biociências, Rio Claro. Dados fornecidos pelo autor(a).

Essa ficha não pode ser modificada.

UNIVERSIDADE ESTADUAL PAULISTA

Câmpus de Rio Claro

CERTIFICADO DE APROVAÇÃO

TÍTULO DA DISSERTAÇÃO: INSTABILIDADE NO DESENVOLVIMENTO DE LEPIDÓPTEROS EM PAISAGENS ANTROPIZADAS

AUTOR: ADEMIR JÚNIOR FRANCISCO
ORIENTADORA: MARINA CORREA CORTES

Aprovado como parte das exigências para obtenção do Título de Mestre em ECOLOGIA E BIODIVERSIDADE, área: Biodiversidade pela Comissão Examinadora:

Profa. Dra. MARINA CORREA CORTES (Participaçao Virtual)
Departamento de Biodiversidade / IB Rio Claro

Prof. Dr. NICHOLAS FERREIRA DE CAMARGO (Participaçao Virtual)
Departamento de Ecologia / Universidade de Brasília

Prof. Dr. MILTON CEZAR RIBEIRO (Participaçao Virtual)
Departamento de Biodiversidade / IB Rio Claro

Rio Claro, 16 de dezembro de 2021

Título alterado para: "O efeito de paisagens antropizadas sobre a assimetria flutuante de lepidópteros"

AKNOWLEDGEMENTS

Thanks to my family I was able to undergraduate, for several years my father supported me so I would be the first in the family to ever conclude higher education and now to achieve a master degree, I hope one day I'll be able to secure a better life for them through the fruits of my education.

Thanks to all my various friends who supported me emotionally during very hard times on the way to develop this project, no science is produced in a vacuum separated from a human being who is a scientist, better science demands mentally healthy scientists, all my friends helped me to feel lighter in difficult times and complete this project. Some of these friends helped me more directly in the project, such as Jay Carriker, whom I would seek out whenever I needed help with English, either to understand better a sentence in a paper or to articulate properly my ideas as I was writing my thesis.

Dr. André Freitas from UNICAMP for being incredibly helpful and patient whenever we needed some information or opinion regarding butterflies and their ecology, big thanks as well to Dr. Jessie Pereira for his contribution with scores for the ITA calculations.

I'm also very thankful to the whole Lab of Vegetation Ecology (Leveg) team and Dr. Alessandra Fidelis for allowing me to use their lab dependencies and scanner.

Couldn't forget the very helpful advises coming from Hugo Benítez who was extremely nice answering my e-mails regarding missing landmarks and also offering a totally free online workshop on Geometric Morphometrics, a very important contribution to the Latin American morphometrists community.

Finally, my adviser Marina Côrtes for accepting the challenge of supervising this project and guiding me through some of the more complex parts of the scientific endeavor, getting results and making sense of them!

This study was financed in part by the Coordenação de Aperfeiçoamento de Pessoal de Nível Superior - Brasil (CAPES) - Finance Code 001.

RESUMO

A atividade humana é uma força transformadora constante do meio ambiente que pode representar situações desafiadoras para indivíduos e populações. Pequenas diferenças entre os lados direito e esquerdo em organismos com simetria bilateral (ou seja, assimetria flutuante) foram apontadas como um indicador de instabilidade de desenvolvimento devido ao estresse ambiental. Aqui, investigamos se o nível de alteração antrópica está associado à assimetria nas asas de lepidópteros frugívoros *Cissia eous* (A. Butler, 1867) e *Paryphthimoides poltys* (Prittwitz, 1865) em paisagens agrícolas brasileiras (região do Interior da Mata Atlântica). A assimetria flutuante foi medida a partir de imagens das asas usando a abordagem de morfometria geométrica. Modelamos o efeito das métricas de paisagens medidas a partir do uso e cobertura do solo em três escalas espaciais diferentes sobre a assimetria flutuante média dos indivíduos capturados. Encontramos evidências de que a assimetria flutuante em ambas as espécies está conectada às transformações induzidas pelo homem no meio ambiente. Bordas florestais, áreas antrópicas, agricultura e Índice de Transformação Antrópica (ITA) foram as principais variáveis que explicam a assimetria. As duas espécies responderam de forma diferente em termos de escala e resposta à antropização. Concluímos que, apesar de ambas as espécies serem consideradas mais adaptadas ao ambiente antrópico, a assimetria flutuante em *C. eous* 'pode ser um indicador interessante de intensificação da pressão antrópica, enquanto a antropização pode ter um efeito mais severo no fitness dos indivíduos de *P. poltys.*

Keywords: Assimetria flutuante; Nymphalidae; Morfometria geométrica; Antropização; Ecologia da paisagem; Paisagens agrícolas.

ABSTRACT

Human activity is a constant transforming force of the environment that may pose challenging situations to individuals and populations. Small differences between the right and left sides in organisms with bilateral symmetry (i.e., fluctuating asymmetry) has been pointed out as an indicator of developmental instability due to environmental stress. Here we investigate whether the level of anthropic alteration is associated with asymmetry in wings of fruit-feeding lepidopterans *Cissia eous* (A. Butler, 1867) and *Paryphthimoides poltys* (Prittwitz, 1865) in Brazilian agricultural landscapes (Atlantic Forest *Interior* region). Fluctuating asymmetry was measured from images of the wings using the geometric morphometrics approach. We modeled the effect of landscapes metrics measured from land use and cover at three different spatial scales on average fluctuating asymmetry of captured individuals. We found fluctuating asymmetry in both species to be connected to human-induced transformations on the environment. Forest edges, Anthropic areas, agriculture and Anthropic Transformation Index (ITA) were the main variables to explain asymmetry. The two species responded differently in terms of scale and response to anthropization. We conclude that despite both species being regarded as more adapted to anthropic environment, fluctuating asymmetry in *C. eous'* might be an interesting indicator of anthropic pressure intensification, while anthropization might have a harsher effect on *P. poltys individuals*' fitness.

Keywords: Fluctuating asymmetry; Nymphalidae; Geometric Morphometrics; Anthropization; Landscape Ecology; Agricultural landscape

INDEX

INTRODUCTION

Human enterprises are changing forces of the environment, in fact, the term *Anthropocene* was coined in the 2000's as reference to the global impacts caused by humans on ecosystem functioning (ZALASIEWICZ et al. 2021; KEYS et al. 2019; LEWIS & MASLIN, 2015). Landscape anthropization is a general concept that refers to all sorts of human activities that cause change in natural environments. Human induced transformation on the landscape seems to be an inevitable characteristic of humans as a species, considered an extreme example of what is called "Ecosystem Engineers", (i.e., organisms with the ability to change biotic and abiotic elements in an environment, modulating resources availability and distribution to species other than themselves) (SMITH, 2007; LAWTON & JONES, 1995).

Anthropization as a phenomenon grew in complexity along with human social development, since transformations are not produced anymore by isolated agrarian societies but a product of a global scale economic system that has shaped resource consumption in order to maintain different life standards.

To implement conservation strategies and landscape management and mitigate detrimental effects of human activities it is necessary to understand the nature and intensity of these effects on biodiversity. Lepidopterans, especially butterflies (Rhopalocera), are well established and traditional model organisms used as biological indicators of environmental conditions, ecological processes, and biodiversity patterns, many studies worldwide have employed butterflies as bioindicators to assess changes in the environment, how these changes affect organisms, and what is the general state of local biodiversity (THOMAS, 2005; RÁKOSY, 2011; VU, 2007; BROWN & FREITAS, 2000).), since they are sensitive to habitat change, are taxonomically well-known and easy to sample and identify. In addition, aspects related to biology and general life history are properly understood (McGEOCH 1998). However, this later is still incipient in the tropics, and how it relates with environmental impacts in this region, our knowledge of tropical butterflies' ecology is scarce compared to what we know about butterflies in temperate regions, which impacts the conservation and management practices employed in the tropics (BONEBRAKE et al, 2010).

Commonly, studies on the impact of landscape composition and configuration based on land uses and land cover (LULC) focus on patterns of species occurrence and species diversity (FAHRIG et al, 2011; RIBEIRO et al. 2012). However, it is also important to analyze impacts on population level patterns, such as intraspecific phenotypic variation. Intraspecific phenotypic variation partially results from the so-called phenotypic plasticity, which is defined by Stearns et al (1991) as "the set of phenotypes expressed by a single genotype across a range of environmental conditions". This property is conceptually the opposite of "canalization", which is the ability to express the same phenotype across different environmental conditions (PALMER, 1994. p. 335-364). Plasticity can occur as a response to environmental instability and heterogeneity. However, this plasticity may also manifest itself as a reaction to physical or chemical constraints that produce non-adaptive modifications (GOTTHARD & NYLIN, 1995; GHALAMBOR et al, 2007).

To understand how organisms respond to potentially stressful environmental conditions that species have never been exposed to in their evolutionary history, it is important that we detect instability in organisms' development and investigate associations with the changing environment. Developmental instability can have two originating pathways: intrinsic (genetic) and extrinsic (environmental in nature). Instability in the development results from a set of independent processes in which disruptions on the developmental precision occur, such as: random changes in the rates of division, growth and cell shape change, noise in enzymatic processes and random disparities in rates of cellular physiological processes (MARKOW, 2012). All these processes can happen on a very small scale, producing subtle and random variations (MARKOW, 2012). Conversely, development stability results from the processes that buffer against disruptive processes (noise) in development, either through negative feedback systems regulating enzymatic activity or nervous/hormonal regulation of non-contiguous structures (MARKOW, 2012). Therefore, development stability is the ability of an organism or structure to achieve an 'ideal' phenotype given certain conditions, while canalization is the ability of an organism or structure to achieve a given format under different environmental conditions (opposite of phenotypic plasticity). The greater the instability of development and the lower the canalization of a structure, the greater the chances of an organism distancing itself

from its target phenotype. So, the realized phenotype of an organism is always the outcome of these two sets of processes, while the target phenotype is unknown a priori in most cases. Bilateral symmetry offers the possibility of establishing a measurable ideal, the perfect symmetry between the left and right sides. Considering that both sides of a bilateral symmetry are subject to the same environmental conditions and result from the expression of the same genomic regions, any asymmetry can be assumed to arise from developmental instability. There are three types of asymmetries in bilaterally symmetrical animals, namely:

(i) Antisymmetry: a pattern in which some individuals present asymmetry on the left side, while other individuals present asymmetry in the right part. Antisymmetry is a bimodal distribution of asymmetry in a population, where it is possible to verify asymmetry, but it is not possible to predict bias to the side.

(ii) Directional asymmetry: asymmetric pattern for only one side of the body of individuals in a population.

(iii) Fluctuating asymmetry: small differences are observed between the left and right sides of specimens (KLINGENBERG 2015). These asymmetries, however, are categorized according to the patterns of distribution of differences between the left and right sides in a population, that is, it is only possible to identify and measure these asymmetries from the analysis of more than one individual (KLINGENBERG 2015).

Morphometry, the application of mathematical analysis of the form to describe the morphology of organisms quantitatively and comparatively (ZELDITCH et al, 2012, p.1), emerges as an interesting field to study phenotypic variation. In its most modern form, called geometric morphometrics, anatomical landmarks locate morphological structures and allow to extract, preserve, and represent the geometric information of the described structure (ZELDITCH et al, 2012, p.6). Landmarks are described as discrete (distinct from other structures) anatomical loci recognizable in all specimens. They are two- or three-dimensional points that bear cartesian coordinates. True landmarks must fulfill certain criteria: they should be homologous anatomical loci with topologically fixed positions relative to other landmarks. Homology has been pointed

out as the most important criteria in landmark's selection. In geometric morphometry *homology* refers to structures that occur in the same anatomical locus in all specimens and are functional or developmental analogous.

Within the field of morphometrics, 'fluctuating asymmetry' (FA) has been used since the 1980s as an indicator of stress in individuals and populations (FALMER & STROBECK, 1986; FARSONS 1990; MØLLER & SWADDLE, 1997). Fluctuating asymmetry has been related to inconsistencies during ontogenetic development (KLINGENBERG 2015; SWADDLE & WITTER, 1994). Small dissimilarities between the two sides of individuals in a population have been correlated with situations of stress, hybridization, and inbreeding (KLINGENBERG 2015; FALMER & STROBECK 1986). Assuming the development of the two sides in a bilateral organism is encoded by the same genomic regions in an individual, we expect both sides to be identical. So, deviations between sides are interpreted as developmental instability resulted of biological (intrinsic) – genetic basis, or environmental (extrinsic) processes (e.g., stressful conditions). Such processes interfere with the stability of developing perfectly symmetrical structures. Individual subtle asymmetry caused by populational fluctuating asymmetry can serve as a parameter to investigating the impacts of anthropogenic environmental transformation on the developmental stability in organisms. (KLINGENBERG, 2015; BENÍTEZ et al, 2020).

Identifying and measuring the extrinsic drivers of fluctuating asymmetry in natural populations is a challenging task. If human transformation of landscapes results in more stressful environmental conditions for native species, we expect that the fluctuating asymmetry correlates with the landscape's configuration and composition (ELLIS et al, 2012). Fluctuating asymmetry in wings of neotropical birds has already been positively correlated to habitat fragmentation and negatively correlated with the size of forest fragments (ANCIÃES & MARINI, 2000). In dragonflies, the degradation of riparian forests substantially increased wings fluctuating asymmetry (PINTO, 2012). Also, asymmetry in the shape of bees' wings (*Apis mellifera)* was positively associated with anthropization (NUMES et al, 2015).

In this study we used lepidoptera as model organisms to quantify fluctuating asymmetry and investigate whether it is associated with landscape structure. For this

we measured the wing shape of two fairly widespread and abundant species of fruit-feeding butterflies of the subfamily Satyrinae occurring in the Atlantic Forest: 82 *specimens of Cissia eous* (A. Butler, 1867) and 115 specimens of *Paryphthimoides poltys* (Prittwitz, 1865). We evaluate asymmetry variation at three spatial scales in agricultural landscapes with different land use and cover composition and landscape configuration. We hypothesize that fluctuating asymmetry will be stronger in individuals in more anthropogenic landscapes and that the effects will be mainly perceived at finer spatial scales, due to species limited movement.

MATERIAL AND METHODS

STUDY SYSTEM

- **Study Species**

Cissia eous (family: Nymphalidae; subfamily: Satyrinae).

Cissia eous (Figure 1A) is an exclusively South American species that occurs in Brazil, Paraguay, Uruguay and Argentina. It has a preference for lower altitudes and it is not restricted to specific habitat types, being found in open forest areas, riparian vegetation, and anthropogenic areas (ZACCA et al, 2018). It frequently occurs in shady and moist areas, forest edges, and secondary forests (ZACCA et al, 2018). Females tend to be larger (forewings length 18 – 21 mm) than males (forewings length 15 – 19 mm). Immature individuals have been reported feeding on leaves of the grass *Poa annua L*, an exotic herb native to Europe, introduced in southern and southeastern Brazil, well adapted to disturbed environments (e-Flora of South Africa. v1.21. 2018; WFO (2021), *Digitaria sanguinalis*, another poacea very invasive and allelopathic, conditioned to Brazil's climate and *Stenotaphrum secundatum* a native poacea (ZACCA et al, 2018; Canto-Dorow, 2020; EMBRAPA, 2014).

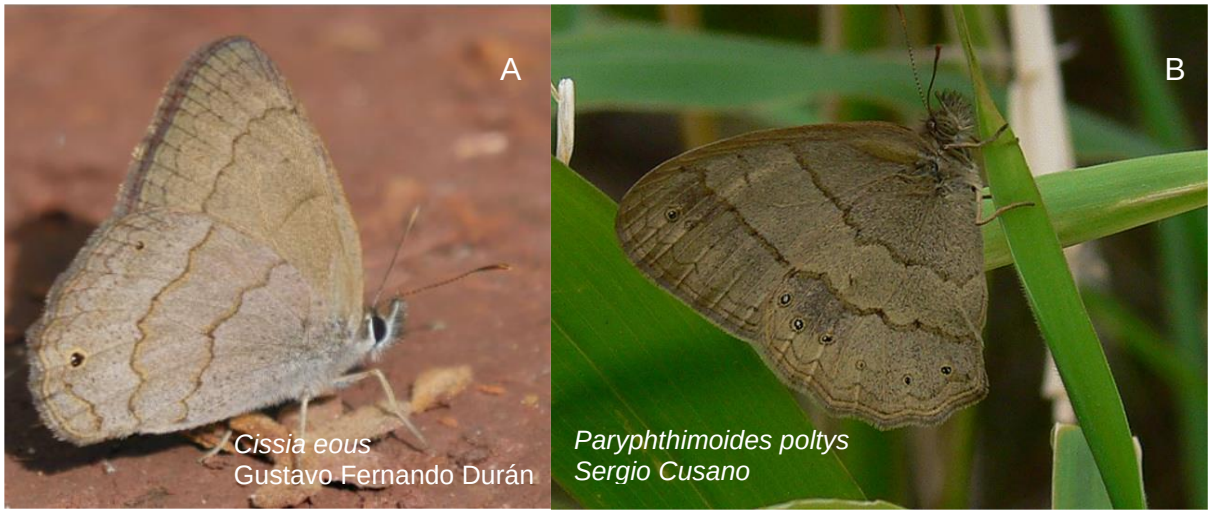

Figure 1. Photos of the two study species: A) *Cissia eous* and B) *Paryphthimoides poltys*.

Paryphthimoides poltys (family: Nymphalidae; subfamily: Satyrinae).

There are two subspecies of *P. poltys: P. poltys poltys* and *P. poltys numilia* (ZACCA et al, 2020). Given the geographic distribution of these subspecies and the location of the assemblages sampled in this study, we can say we collected *P. poltys poltys* (Figure 1B). Females are larger (forewings length 16 – 20 mm) than males (forewings length 14 – 19 mm) normally. *Paryphthimoides poltys poltys* (referred to as just *P. poltys* in the remainder of the study) occurs in midwestern and southern Brazil, Paraguay, Uruguay, Bolivia, and northern Argentina. *P. poltys* is found in open environments, edges, secondary forests, and riparian environments, and it is common in disturbed areas. Common hosts plants are *Eulesine* (Chloridoideae), *Cenchrus L,* and *Stenotaphrum* (Panicoideae) (ZACCA et al, 2020; FILGUEIRAS, 1984; WATSON et al, 1992).

- **Study Area**

The study area comprises an area of 750 thousand km² along the border between the states of São Paulo and Minas Gerais, in the whereabouts of the municipalities of Espírito Santo do Pinhal, Andradas, Águas da Prata, Poços de Caldas, Cape Verde, and Serra dos Lemes (Figure 2). The original native vegetation that makes up the Atlantic Forest biome is characterized by humid and semideciduous forests (MORELLATO & HADDAD, 2000). The Atlantic Forest is heavily impacted by human activities, and its use and land cover is deeply linked to changes in social, political, and economic dynamics (RIBEIRO, 2009; LIRA, 2012). The study region is an agro-

mosaic where agricultural activities are structuring forces of the landscape (RIBEIRO, 2011). The region is currently composed of forest fragments, pastures, monocultures (mainly coffee), and forest plantations (eucalyptus).

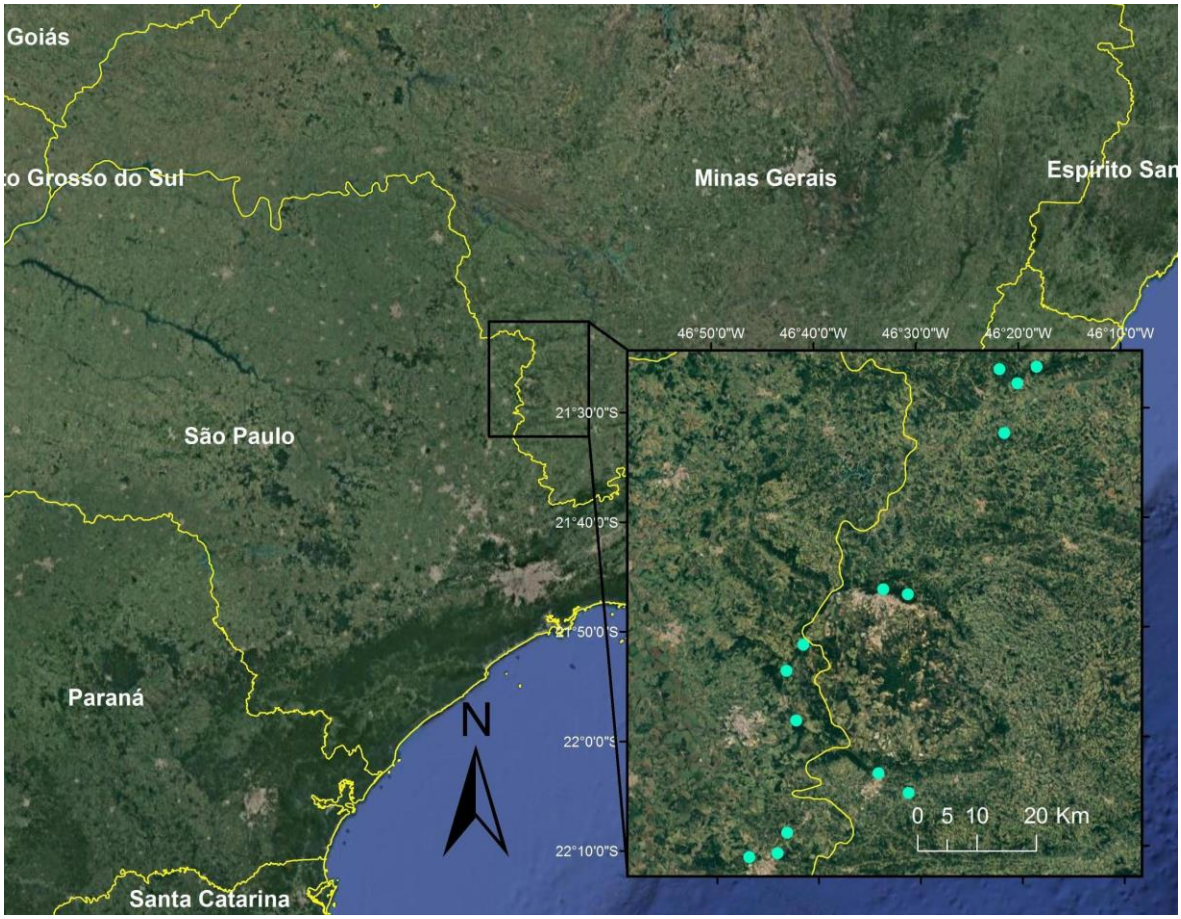

Figure 2. The satellite image shows the study area in the Atlantic Forest sub-region called the Interior, according to Silva (2003). Green dots along the border between the states of Minas Gerais and São Paulo indicate landscapes of 1 km radius where the collections of specimens of *Cissia eous* and *Paryphthimoides poltys* were done for the analysis of fluctuating asymmetry. Basemap provided by ArcMap (Source: Esri, Maxar, GeoEye, Earthstar Geographics, CNES/Airbus DS, USDA, USGS, AeroGRID, IGN, and the GIS User Community)

Lepidoptera Sampling and Material Preparation

- **Sampling**

Individuals were collected between May and June 2017, after the rainy season and before major drops in temperatures as winter approached, in 14 different sites in the study area (Figure 2). Between 10 and 15 Van Someren-Rydon (VSR) traps were placed 50 meters apart from each other in each site. Each trap was baited with a fermented mixture of banana and sugar cane juice and left in the field for 48 hours.

This trap model has been used extensively for sampling of fruit-feeding butterflies (FREITAS et al, 2021, p.106). It consists of a veil cylinder tied to a rectangular base, internally to the cylindrical veil at its lower extent stands an inverted cone.

All specimens were collected and preserved separately in glassine paper envelopes. The identification of the material collected at the species level was carried out by specialists from LABBOR - Laboratory of Ecology and Systematics of Butterflies, in the Animal Biology Department of Campinas University. 779 individuals of 47 species were collected. The most abundant and more widely distributed species were *Cissia eous* (A. Butler, 1867) (94 individuals) and *Paryphthimoides poltys* (Prittwitz, 1865) (128 individuals). These species were chosen as our model organisms because of their wide occurrence and high abundance.

- **Specimen dismemberment**

Dismemberment consisted of carefully plucking the mesothoracic wings (forewings) under the light of a stereoscopic microscope. The wings were stored separately according to side (left and right) in two different envelopes for each individual. The entire process of handling the individuals and their parts was done with two flexible aluminum tweezers suitable for handling Lepidoptera as they are light and thin, thus avoiding damaging the wings in the process. Each pair of envelopes was attached to each other and tagged with specimen data.

- **Diaphanization**

Diaphanization is a technique commonly used in biology to make tissues diaphanous (i.e., transparent) while preserving the shape of structures. This technique is especially useful in cases where the pigmentation is too dark to see the wing veins. The diaphanization protocol for lepidopteran wings was based on BIZARRO et al. (2003) and consisted of immersing them in 70% alcohol solution for one minute to dissolve the fat layer on the surface of the wings, and then they are soaked in commercial bleach (NaClO 2% - 2.5%) for about one minute until the wings are clear enough to see the veins, after which the wings are returned to alcohol to stop the bleach reaction, and finally washed in distilled water and left to dry in plastic Petri dishes.

- **Scanning, Digitizing and Accounting for Missing Landmarks**

Images of individual's pair of wings were generated in an Epson Perfection V800 Photo Flatbed - J221B Scanner, in 3200 dpi (dots per inch) resolution. The images underwent transformations in GIMP Software V. 2.10.24 (GNU Image Manipulation Program), a free and open-source raster graphic editor, so that all wings were oriented with the base to the right side, thus avoiding side bias during the digitizing process.

The digitization of the wings landmarks was done using Software TPSdig V. 2.32. Both species were digitized twice (with an interval of one to two days between one digitization and another) so that we could estimate and take into account the digitizing error produced by the observer and reduce possible biases in the asymmetry quantification.

Nineteen landmarks were selected along the entire length of the wing so that we could have adequate coverage of the structure. Landmarks are distributed over the basal region (Ba), the venal intersections of the cell area (indicated by subscript "c"), the costal and apex region (Sc and R_x), and the marginal venous endings of the termen and tornus regions (M_x, Cu_x/CuA_x and XA) (Figure 3). All the landmarks are of type 1 (tissue juxtapositions) except for the ba1 landmark, which is a type 2 landmark (point of maximum curvature in a structure) (ZELDITCH et al, 2004, 31 p).

Some of our specimens presented wings lacking certain parts, this is a very common issue when dealing with natural populations instead of lab reared individuals. We sampled individuals that have been through predators' attack attempts, and environmental induced damage, the older an individual is, the higher are the chances some incident caused the loss of body parts. Because of this, some landmarks (approximately 5% of total in both species) were missing in our sample. Arbour & Brown in their 2014 paper showed that in this case it is highly indicated that methods to estimate landmarks are used instead of simply discarding altogether all incomplete specimens from the analysis. Therefore, we used a Bayesian Principal Components Analysis (BPCA) (Oba et al, 2003) to estimate the location of all missing landmarks.

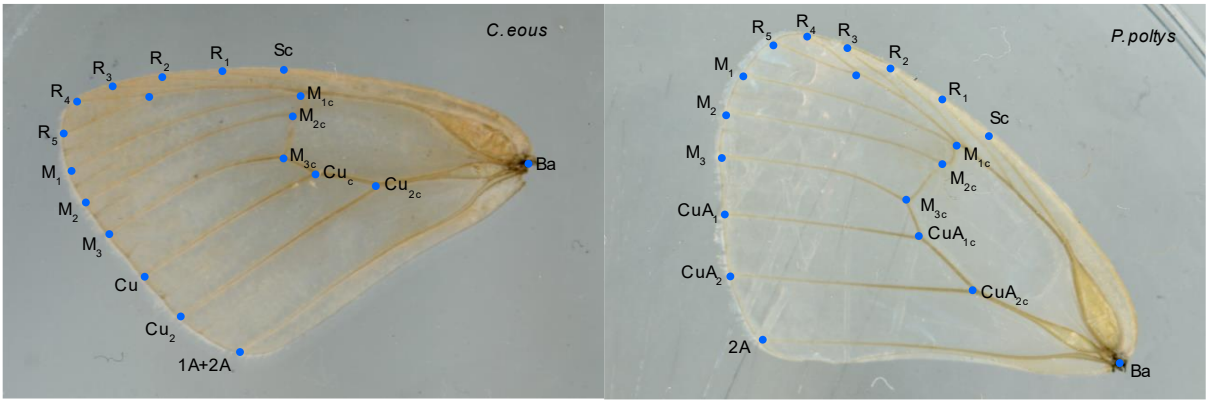

Figure 3. Landmarks configuration in diaphanized wings of *C. eous* and *P. poltys*.

MORPHOMETRIC ANALYSIS

- **Procrustes Fit**

Once digitizing was concluded, we combined the two digitized sets for each species and performed the Procrustes fit in the MorphoJ v 1.07a software (KLINGENBERG, 2011). In the raw dataset each digitized landmark corresponds to coordinates of two values (X, Y) in the Cartesian plane. The set of coordinates for each wing will define the shape, as well as information on position, rotation, and size. Procrustes fit, also called Procrustes superimposition, is a process that aims at eliminating all variation (size, rotation, position) that is not variation in shape. This process is the main paradigm of two forms of analysis: Ordinary Procrustes Analysis (SCHÖNEMANN & CARROLL, 1970) and Generalized Procrustes Analysis (GPA) (GOWER, 1975). The Generalized Procrustes Analysis is based on a series of Ordinary Procrustes Analyses (OPA) (Figure 4), which basic procedure is:

a. Reflect digitized wings to the same side

b. Scale left and right wings to a centroid size 1.0. Centroid size is a non-Euclidean unit of measurement: it is the square root of the sum of the squared distances of all landmarks to the center of gravity of the configuration. (Figure 5).

c. Superimpose one digitized wing on its pair, aligning its centroids and thus eliminating the location effect, or also called the position effect.

d. Rotate the configurations until the best fit is found among their corresponding anatomical landmarks. This eliminates the rotation effect.

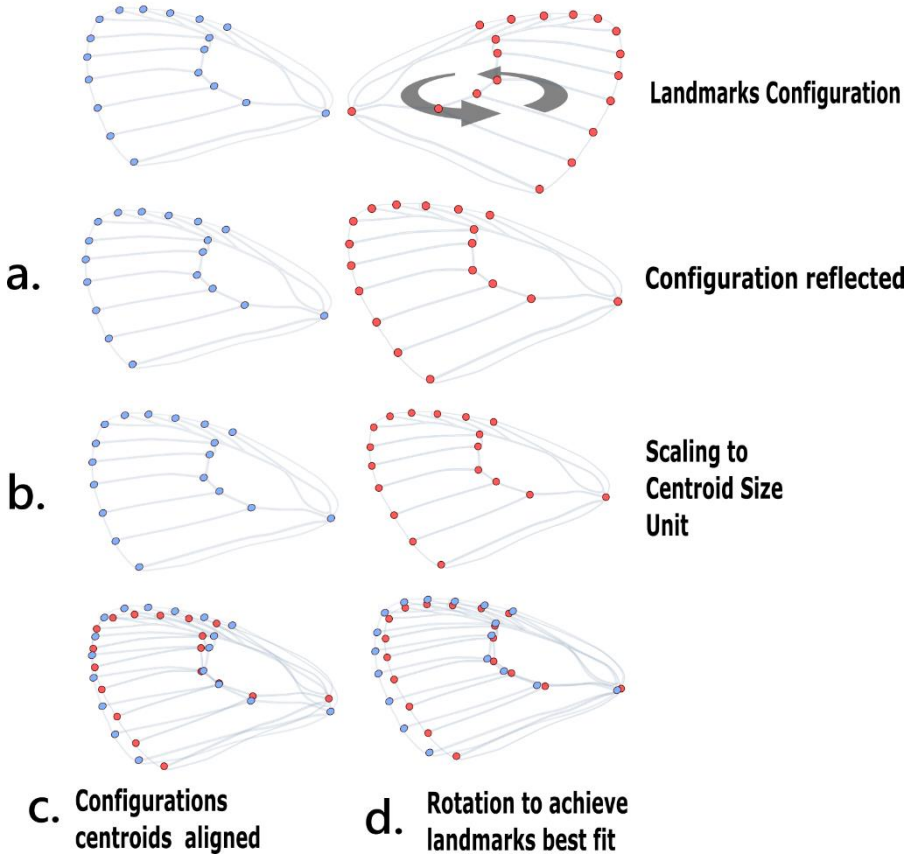

Figure 4. Steps of an Ordinary Procrustes Analysis. The basic procedure in geometric morphometrics is to eliminate variation other than shape. Blue and red dots represent landmarks in two opposite wings. Each step is described on the text above.

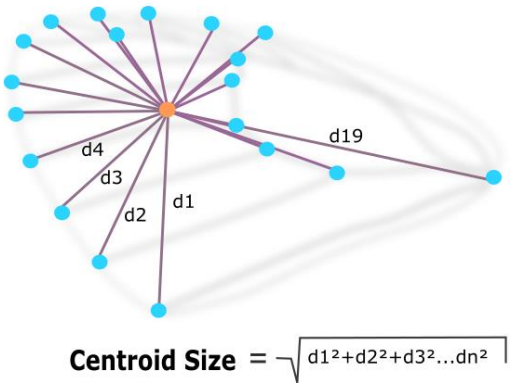

Figure 5. Calculation of centroid size where *d* = distances between landmarks and the centroid of the configuration

At the end of this process, the pair of digitized wings will have the same size, the same position, and the same rotation, so the dissimilarities between one

configuration and the other are shape variation measured as the square root of the sum of the squared distances between corresponding landmarks, which is referred to as Procrustes distance.

The operation just described is used to measure shape variation between two sides of the same individual (two configurations). When we perform analysis at the population level (three or more configurations), as in the case of this study, we must employ some additional steps, as follows:

- In the first step a random configuration from the set (sampled population) is chosen as the target configuration. All other configurations will be adjusted to it following the Ordinary Procrustes Analysis and a consensus shape is calculated from the averages of all configurations. This consensus shape is scaled to centroid size 1.0.
- That new consensus shape becomes the target shape and all configurations are adjusted to this to recalculate a new consensus that is scaled to centroid size 1.0.
- This iterative process continues until the new consensus shape no longer changes.
- The set of configurations are thus optimally fitted to their average shape, and the coordinates of their landmarks represent now the shape variations of each configuration.

In this process, the original coordinates matrix containing the variations of size, position, rotation and shape, is transformed into a new matrix of Procrustes coordinates that accounts only for the information of shape. After that, we detected possible outliers (landmarks extremely distant from their counterparts in the average shape) in each wing individually using MorphoJ, so that they could be corrected in TPSdig in case of being result of digitizing error.

- **Allometry and size correction**

The conceptual differences between size and shape have been long discussed in the field of Morphometrics, as well as the different methods to approach allometry: size-related variation in morphological traits. In Geometric Morphometrics size is often conceptualized as a scalar property that can be represented by a single number, while shape is a property related to proportions. In this perspective where shape and size are two distinct attributes of an object, allometry is understood as the correlation between both. We tested our data for the presence of allometric effect through a multivariate regression of shape on centroid size. The size correction then, is done by using the regression residuals to perform all the morphometric analysis (KLINGENBERG, 2016).

- **ANOVA Procrustes**

The ANOVA Procrustes uses the Procrustes coordinates as the basis for its mathematical process, where the factor individual (id) enters as a random effect (each individual used in the study is a random sample of a population) and the factor side enters as a fixed effect (two-level fixed factor - left/right) (KLINGENBERG, 2015). The interaction between id and side is what we interpret as fluctuating asymmetry as it is the difference between individuals in their asymmetries (WEBSTER & SHEETS 2010; KLINGENBERG & MCINTYRE, 1998; KLINGENBERG, 2015).

After running the Procrustes ANOVA, we can export the *Fluctuating Asymmetry Scores* in Procrustes distance and Mahalanobis distance. The Procrustes distance at the population level measures the deviation of each individual from the consensus shape, at the individual level it represents the difference between left and right sides. The Mahalanobis distance is a transformation of Euclidean (Procrustes) distances and the space where they are allocated to ensure an isotropic distribution of intragroup variation and avoid inconsistencies in estimates when the variation around the mean is very large. When there is no great variation around the mean, both distances offer similar results (KLINGENBERG et al, 2005).

CHARACTERIZATION OF LANDSCAPES

Landscapes are defined at three different scales; 200 meter-radius buffers around each trap (Scale 1), since satyrids are reported to respond better to changes at small scales (RIBEIRO et al, 2012).; 200 meter- radius buffers around traps merged into a single landscape at each location (Scale 2); 1 km-radius buffer around the traps centroid (Scale 3). Scales 2 and 3 comprise a total of 10 sampled landscapes, while scale 1 comprises 46 landscapes for *P. poltys* and 42 landscapes for *C. eous*. (Figure 6).

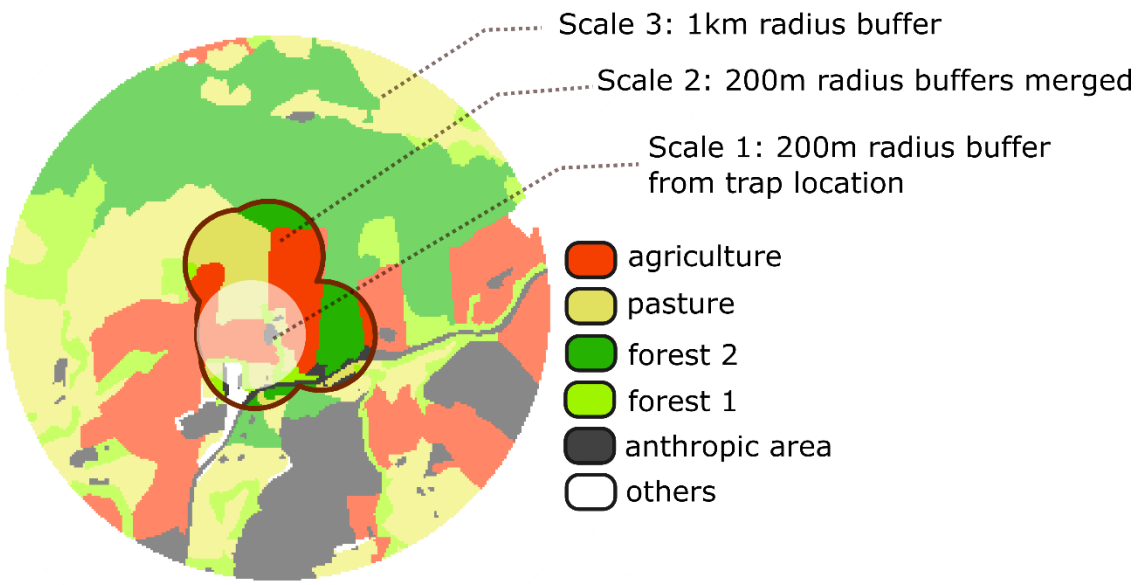

Figure 6. Three different spatial scales addressed in the study overlapped.

Land use and cover mapping was done manually at 4 meters resolution, with composite images from the Basemap provided by ArcMap (Source: Esri, Maxar, GeoEye, Earthstar Geographics, CNES/Airbus DS, USDA, USGS, AeroGRID, IGN, and the GIS User Community) as a basis for photointerpretation. The projection used

was WGS 1984 UTM 23S Zone and the Datum was WGS 1984, using 8 classes of land use and land cover (Table 1).

Table 1: Type and description of the classes of land use and land cover identified in the 1 km (scale 3) landscapes in the study area.

№	Class	Description
1	Water	Bodies of water as (artificial) lakes and rivers
2	Forest initial	Patches composed mainly by seedlings and other pioneer individuals and small patches of sparse vegetation (35 ha on average).
3	Forest advanced	Patches of denser vegetation and large areas of dense and older vegetation cover (75 ha on average)
4	Pasture	Pasture areas composed of grasses ('clean' pastures) and grazing areas that have trees and shrubs ('dirty' pastures)
5	Agriculture	Plantations of annual and perennial cycle, in this study mostly coffee
6	Silviculture	Areas of logging activity, mostly composed by eucalyptus plantations
7	Wetlands	Flooded or humid areas, usually next to bodies of water
8	Anthropic Area	Constructions in rural context, urban areas, roads and highways

From the categorical maps we extracted spatial composition and configuration metrics at the landscape and class level including:

- Percentage of Landscape (PLAND): Area of each class represented in hectare and Percentage of landscape composed by the class. These are compositional metrics that help describe the availability and extent of habitat.
- Largest Patch Index (LPI): Percentage of the landscape taken by the largest patch (area restricted to a land use/cover) of a class. Configuration metric describing spatial dominance of a land use or cover.

● Forests' Edge Density (ED): Sum of edge segments lengths of a forest type, divided by the total landscape area and multiplied by 10,000. It is considered ideal to compare amount of forest edge among differently sized landscapes.

● Euclidean Nearest-Neighbor (ENN_AM): Distance in meters between the nearest edges of patches of the same class. It is a configuration metric that allows inferences about isolation or aggregation of patches in a landscape, helping to characterize fragmentation processes.

● Forests' Connectance Index (CI): Number of functional connections between same forests patches of the same type divided by the total number of possible connections. Expressed as percentage. Functional connectedness is considered as 200 meters between patches.

● Shannon-Weaver Diversity Index (Heterogeneity): Index based on patch evenness and richness relationship. Used to describe landscape complexity (FARINA, 2008, p.59).

These metrics were extracted using software Fragstats v4.2 - Spatial Pattern Analysis Program for Categorical Maps (McGARIGAL. 2012) and are used to characterize landscapes and measure the magnitude of environmental anthropization. In addition to these metrics, we calculated the Anthropogenic Transformation Index (ITA) (LÉMECHEV, 1982; MATEO, 1991), which is calculated according to the following formula:

$$ITA = \sum(\%LULC \times weight)/100$$

Where ∑ is the sum for all classes (Table 1), *%LULC* (land use and land cover) is the percentage of the landscape covered by a class and *weight* is the value from 1 to 5 that qualifies the degree of anthropogenic transformation represented by the class in the landscape, with 5 being higher degree. Weights were defined based on the opinion of an *expert* in butterflies ecology (table 1 – Supplementary material).

STATISTICAL ANALYSIS

We fitted *Generalized Linear Models* (GLM) and *Generalized Linear Mixed Models* (GLMM) according to the scale of interest. Fluctuating Asymmetry, measured

as both Procrustes FA scores and Mahalanobis FA scores, is treated as mean individual's asymmetry and taken as dependent variable. Explanatory variables consisted of percentages of landscape covered by 6 classes (PLAND), forest connectance index for initial and advanced forest types (CONNECT), anthropic transformation index (ITA), and density of forest edges (ED). Therefore, in total there were 11 landscape variables (Figure 7) which were combined into up to 2 variables models (two landscape variables plus random factor 'landscape' for GLMMs). Models with all possible combinations of covariates were tested. Variables were tested in the same model if they were not significantly correlated ($r < |0.5|$, p-value > 0.05). If correlations exceeded this threshold, variables were considered to have high correlation and were mutually excluded.

To test the effect of metrics extracted at Scale 1 (200m buffer) we employed GLMMs, where fixed factors were landscape metrics extracted from the 200 meter-buffers and the random factor is the identity of the 1 km radius landscape (at scale 3). Models for scale 2 and 3 did not involve random factors.

All statistical framework was performed in R software v. 4.1. The explanatory variables were centered, scaled, and tested for best fitting distributions using package *fitdistrplus (*DELIGNETTE-MULLER, 2015). All models were fitted using gaussian distribution family and log as link function. We performed GLMMs using package *lme4's* function *"glmer",* and package *stats "glm"* function to perform GLM's. Best fit models were defined through model selection using AICc values (Akaike's Information Criterion penalized for small samples), lowest values indicating the most parsimonious models and ΔAICc < 2 models being considered equivalent. AICc values and ΔAICc were calculated using "*ICtab"* function from *bbmle* package. (BOLKER, 2017)

RESULTS

ASYMMETRY

Fluctuating asymmetry for shape was statistically significant for both *Cissia eous* (*Ind*Side* F =6.17, p < 0.0001, Table 2) and *Paryphthimoides poltys* (*Ind*Side* F = 6.07, p < 0.0001, Table 3). The sum of the squares of the error represents a small

fraction of the variation compared to the other factors (0.0226; 0,0228, for each species respectively), which means that the variation caused by measurement error does not heavily represent the morphometric variation captured and will not be a confounding factor in further analyses. The analysis indicates presence of directional asymmetry for shape in *C. eous* (*Side* F= 3.05; p < 0.0001, Table 2) and *P. poltys* (*Side* F = 1.70, p = 0.0072, Table 3) Other factors (landscape and trap) did not explain the observed variation.

Regarding allometry, 4.5% of shape variation was explained by size in *P. poltys* and 46.8% of shape variation was explained by size *C. eous* (P < 0.001). To correct for allometric effect we extracted the residuals of a regression of shape variables on centroid size and performed an ANOVA Procrustes on these residuals. That is the reason no variance is detected for centroid size in our ANOVA. Distribution of fluctuating asymmetry values can be found in Supplementary material (Figures 1S; 2S; 3S).

Table 2. ANOVA Procrustes table of *Cissia eous* distances matrix.

CENTROID SIZE:							
EFFECT	**SS**	**MS**	**df**	**F**	**P (param.)**		
LANDSCAPE	0,000010	0,000001	9	2,15	0,0485		
TRAP	0,000025	0,000001	42	1,15	0,3343		
INDIVIDUAL	0,000020	0,000001	38	3,10	<.0001		
SIDE	0,000000	0,000000	1	0,16	0,6916		
IND * SIDE	0,000015	0,000000	89	6,11	<.0001		
ERROR 1	0,000005	0,000000	180				
SHAPE, PROCRUSTES ANOVA:							
EFFECT	**SS**	**MS**	**df**	**F**	**P (param.)**	**Pillai tr.**	**P (param.)**
LANDSCAPE	0,03594779	0,0001174764	306	0,94	0,7608	5,56	0,9994
TRAP	0,13720931	0,0000960850	1428	0,77	1,0000	14,05	1,0000
INDIVIDUAL	0,16211652	0,0001254772	1292	5,44	<.0001	18,46	<.0001
SIDE	0,00239166	0,0000703429	34	3,05	<.0001	0,65	0,0001
IND * SIDE	0,06977642	0,0000230590	3026	6,17	<.0001	21,28	<.0001
ERROR 1	0,02287560	0,0000037378	6120				

Individual = individual effect on variance, Side = effect of variance of side factors (indicative of directional symmetry), Ind*Side = interaction between the effect of individual variance and the

effect of directional asymmetry variance, corresponds to the effect of fluctuating variation on morphometric data. Error1= scan error produced by the observer.

Table 3. *Paryphthimoides* poltys ANOVA Procrustes table

CENTROID SIZE:							
EFFECT	SS	MS	df	F	P(param.)		
TRAP	0,000001	0,000000	9	0,22	0,9911		
LANDSCAPE	0,000014	0,000000	43	0,74	0,8508		
INDIVIDUAL	0,000027	0,000000	63	7,15	<.0001		
SIDE	0,000000	0,000000	1	0,28	0,5999		
IND*SIDE	0,000007	0,000000	115	4,57	<.0001		
ERROR 1	0,000003	0,000000	232				
SHAPE, PROCRUSTES ANOVA:							
EFFECT	SS	MS	df	F	P (param.)	Pillai tr.	P (param.)
TRAP	0,04148825	0,0001355825	306	1,00	0,4935	3,92	0,9070
LANDSCAPE	0,12458131	0,0000852129	1462	0,63	1,0000	10,40	1,0000
INDIVIDUAL	0,29055163	0,0001356450	2142	7,78	<.0001	21,51	<.0001
SIDE	0,00100578	0,0000295818	34	1,70	0,0072	0,36	0,1234
IND*SIDE	0,06819397	0,0000174409	3910	6,07	<.0001	21,67	<.0001
ERROR 1	0,02266328	0,0000028731	7888				

Individual = effect of the individual on variance. Side = effect of side on variance (indicative of directional symmetry). Ind*Side = interaction between the effect of individual variance and the effect of directional asymmetry variance, corresponds to the Fluctuating variation effect on morphometric data. Error1= scan error produced by the observer

SPATIAL METRICS

Landscapes were defined in 3 scales at the sampling areas and spatial metrics were extracted from categorial maps based on land use and land cover in order to characterize sampling areas and serve as variables in our models to investigate how they are related to fluctuating asymmetry. In general sampling areas were very heterogenous, specially at the small scale (200 meters radius) where we can see gradients of forest edge density (Figure 4S) and spatial diversity (Figure 5S) We observe a subtle difference in the edge density range between the landscapes we sampled each species, seeming that *P. poltys* occurs in a slightly lower range of edge density than *C. eous* (Figure 4S). The difference between species spatial preference/tolerance becomes clearer when looking at the dominant class in each landscape at scale 1 (Figure 6S) with *P. poltys* being sampled in advanced forest dominated landscapes more frequently than *C. eous*. Connectivity at scale 3 (1 km

radius) shows a connectance gradient between 10% - 30% (considering the two forests classes as a single class) (Figure 10S). A more detailed report can be found in the *Characterization of Landscapes* section in Supplementary Material.

LANDSCAPE EFFECTS ON FLUCTUATING ASYMMETRY

Fluctuating asymmetry measured with Procrustes FA scores was not correlated with any landscape metric at scale 1 (200 meters buffers) in both species. When measured with Mahalanobis FA scores, fluctuating asymmetry was correlated with four of the 11 landscape metrics, but in many cases the associated parameter was not significantly different from zero, indicating that the relationship is uncertain. For *C. eous* Anthropic area percentage is a constantly reoccurring variable positively correlated to Mahalanobis FA scores at scale 1. The variable Forest edges was consistently positively correlated with FA scores. Fluctuating asymmetry in *Cissia eous* was not negatively associated with any of the variables. Conversely, agriculture percentage was negatively correlated to FA scores (Mahalanobis) in *P. poltys* for scales 1 and 2. Anthropogenic Transformation Index was only related to FA levels at wider scales (1 km – *C. eous*; 200 meters merged – *P. poltys)*, but the relationship diverged between species (positive for *C. eous* and negative for *P. poltys*). (Figure 7). A detailed description of the best-fit models is in the sections below.

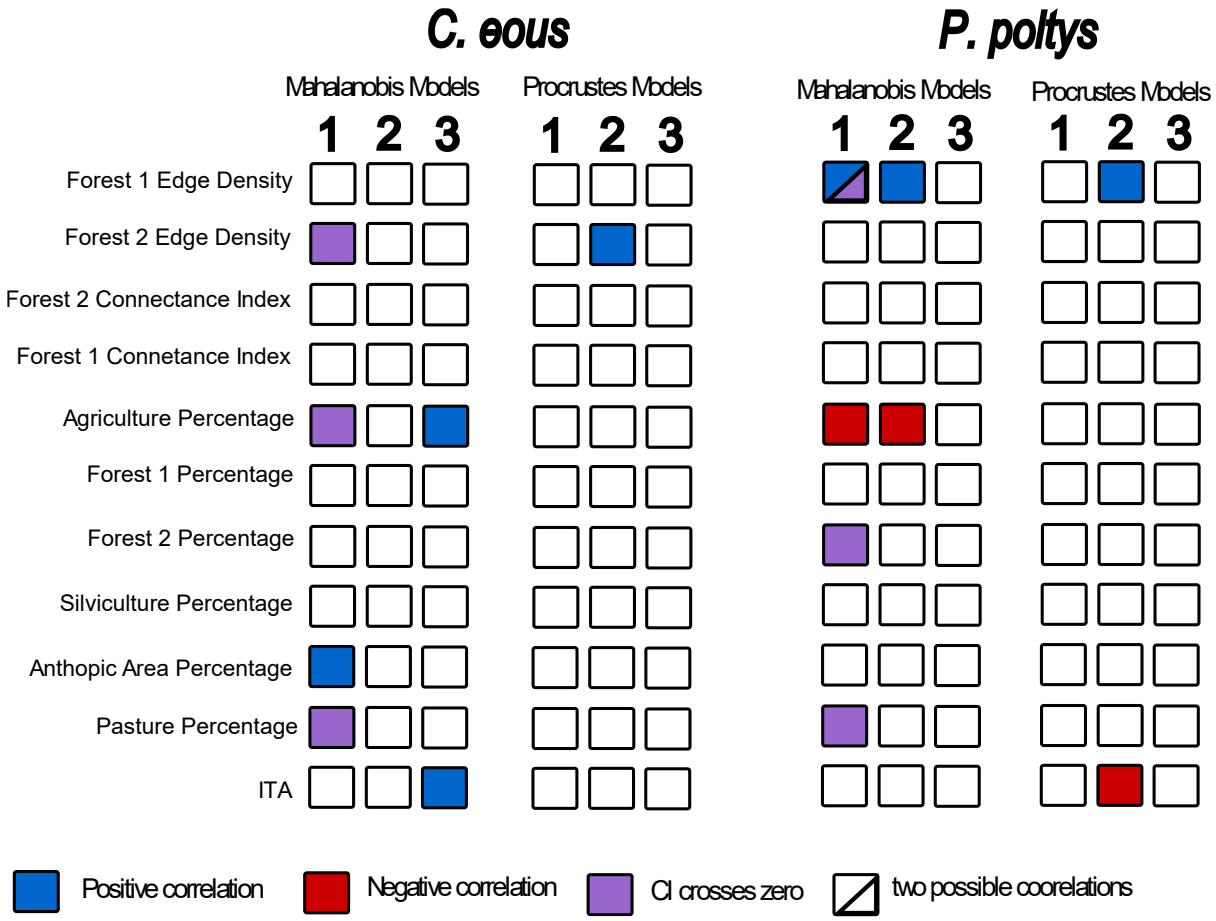

Figure 7. Models results overview. Colors indicate correlation type. Purple boxes mean that the confidence interval crosses zero so the correlation could be either positive, negative or non-existent. Divided boxes indicate two different correlations pointed out by different models. Models selections where the null hypothesis was equally plausible are not reported.

SCALE 1

- ***Cissia eous***

Generalized Linear Mixed Models were fitted using different combination of 10 landscapes variables (no silviculture at this scale). For Procrustes FA scores at scale 1 all models are equated to the null model, therefore we can't say any of the best fit models are more parsimonious than the null model (Table 4).

Table 4. Best models according to AICc selection for Procrustes Distances as dependent variable in *C. eous* at Scale 1. The table reports values for Log Likelihood (LogLik); Akaike Information Criterion for small samples (AICc); Delta Log Likelihoods (dLogLik); ΔAICc (dAICc); Degrees of Freedom (df); AIC weights (weights).

		logLik	*AICc*	*dLogLik*	*dAICc*	*df*	*weight*
Procrustes FA Scores	PLAND Anthropic area	146.0	-280.19	3.24	0.0	5	0.010
	ED. Forest 2	144.3	-279.41	1.55	0.8	4	0.071
	Connect Forest 1 + ED. Forest 2	145.4	-279.02	2.66	1.2	5	0.058
	PLAND Anthropic area	144.0	-278.92	1.30	1.3	4	0.055
	PLAND Anthropic area + Connect Forest 2	145.3	-278.81	2.56	1.4	5	0.053
	NULL	142.7	-278.80	0.00	1.4	3	0.052
	Connect Forest 2	143.8	-278.40	1.04	1.8	4	0.043

When Mahalanobis FA scores is set as dependent variable the null model is no longer included amongst the best models. Four models are considered as the most parsimonious with ΔAICc (dAICc) values below 2. Percentage of anthropic area is consistently shown as an explanatory variable. The sum of the AICc weights makes up for 78% of all variation encompassed by the universe of models fitted. The highest weight value was found in Percentage of Anthropic Area + edge density of advanced forests as fixed factors and *location* (landscape id) as random factor, it accounts for 32% of explained variation, almost twice the amount of explanatory power of the second best-fit model. Anthropic area alone accounted for 13% of explained variation, and when in combination with Percentage of Pasture, the variation explained goes to 15%, not a relevant increment, what leads us to conclude that Pasture percentage is not an important variable to explain asymmetry in *C. eous* at the finer scale. Finally, the second-best fit amounts to 18% of explained variation. It includes percentage of Anthropic Areas and percentage of Agriculture, where percentage of agricultural areas are negatively correlated, and a very short portion of the confidence interval do cross the zero line (Table 5).

Table 5. Best models according to AICc selection for Mahalanobis Distances as dependent variable in *C. eous* at Scale 1. The table reports values for Log Likelihood (LogLik); Akaike Information Criterion for small samples (AICc); Delta Log Likelihoods (dLogLik); Delta AICc (dAICc); Degrees of Freedom (df); AIC weights (weights).

		logLik	***AICc***	***dLogLik***	***dAICc***	***df***	***weight***
Mahalanobis FA Scores	1) PLAND Anthropic area + ED. Forest 2	-28.29	68.34	9.80	0.0	5	0.32
	2) PLAND Anthropic area + PLAND Agriculture	-28.84	69.45	9.20	1.1	5	0.18
	3) PLAND Anthropic area + PLAND Pasture	-29.03	69.82	9.01	1.5	5	0.15
	4) PLAND Anthropic area	-30.50	70.14	7.54	1.8	4	0.13

Confidence intervals for Advanced Forest edge, percentage of agriculture and percentage of pasture range from positive to negatives values, but possible values are overwhelmingly placed on the side of estimated values, so chances of 0 (zero) being the actual value are fewer. Fluctuating asymmetry in *C. eous* is positively correlated with Anthropic Areas which displays comparatively higher effect size, except for advanced forest edge density, since its confidence interval range is larger (Figure 8).

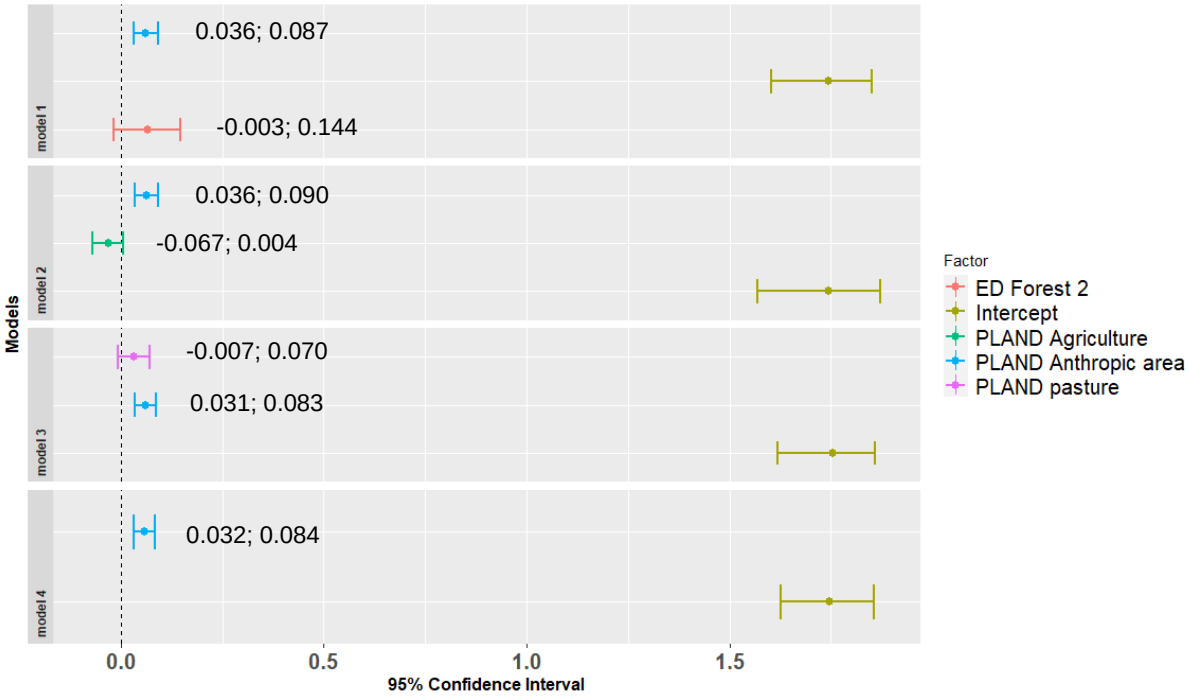

Figure 8. Confidence intervals and estimated values for fixed factors in best fit models when Mahalanobis FA Scores is the dependent variable. *Cissia eous*, scale 1. Obs. Forest 2 = Advanced Forest.

- ***Paryphthimoides poltys***

At Scale 1, the best-fit models with Procrustes FA Scores for *P. poltys* are all equivalent to the Null model. (Table 6)

Table 6. Best models according to AICc selection for Procrustes Distances as dependent variable in *P. poltys* at Scale 1. The table reports values for Log Likelihood (LogLik); Akaike Information Criterion for small samples (AICc); Delta Log Likelihoods (dLogLik); Delta AICc (dAICc); Degrees of Freedom (df); AIC weights (weights).

		logLik	*AICc*	*dLogLik*	*dAICc*	*df*	*weight*
Procrustes FA Scores	NULL	164.5	-322.5	0.00	0.00	3	0.10
	Connect. Forest 1	165.1	-321.1	0.53	1.37	4	0.05
	PLAND Agriculture	165.1	-321.1	0.52	1.39	4	0.05
	PLAND Pasture	165.0	-321.1	0.51	1.41	4	0.05

When Mahalanobis FA scores is the dependent variable, four models are ranked as the most parsimonious ones. Percentage of agriculture, percentage of pasture and forests edge are variables in these models. They account for 37% of variation explained by the universe of fitted models (Table 7).

Table 7. Best models according to AICc selection for Mahalanobis FA Scores as dependent variable in *P. poltys* at Scale 1. The table reports values for Log Likelihood (LogLik); Akaike Information Criterion for small samples (AICc); Delta Log Likelihoods (dLogLik); Delta AICc (dAICc); Degrees of Freedom (df); AIC weights (weights).

		logLik	*AICc*	*dLogLik*	*dAICc*	*df*	*weight*
Mahalanobis FA Scores	PLAND Agriculture + ED. Forest 1	-53.3	118.1	4.07	0.00	5	0.15
	PLAND Agriculture + PLAND Forest 2	-53.7	119.1	3.61	0.93	5	0.09
	ED. Forest 1 + PLAND Pasture	-53.8	119.2	3.52	1.10	5	0.08
	PLAND Pasture	-55.5	120.1	1.81	1.96	4	0.05

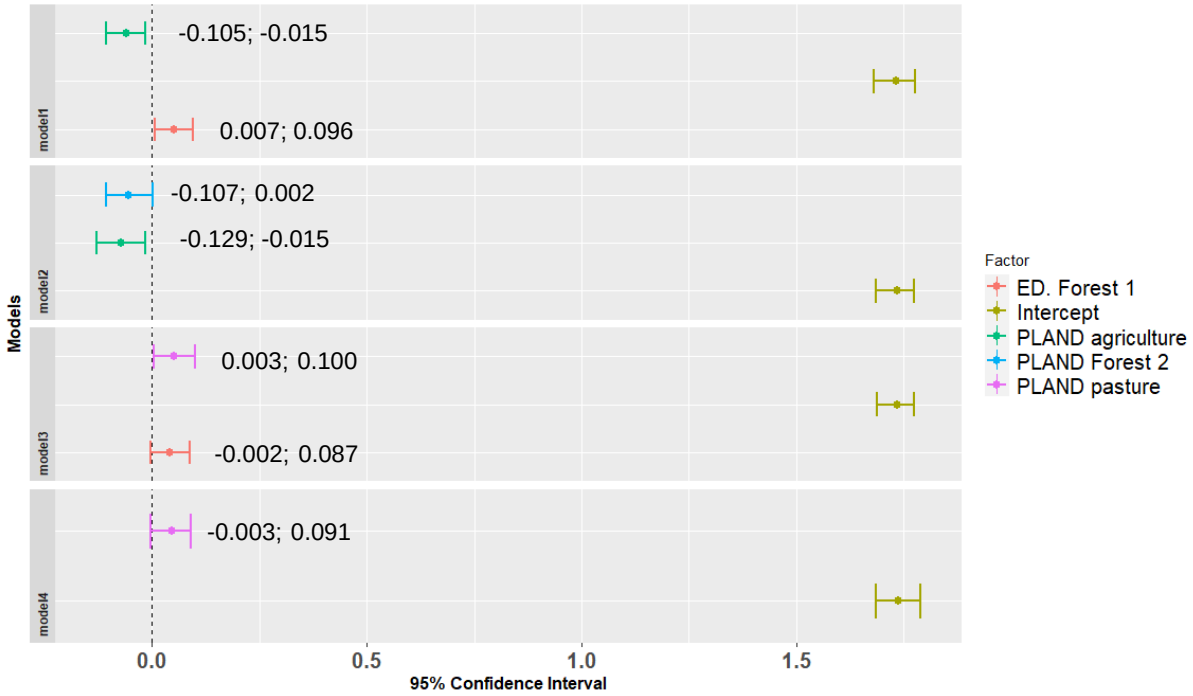

Figure 9. Confidence intervals and estimated values for fixed factors in best fit models when Mahalanobis FA Scores is the dependent variable. *P. poltys,* scale 1. Obs. Forest 1 = Initial Forest.

SCALE 2

- ***Cissia eous***

At scale 2, for *C. eous,* with Procrustes FA Scores as dependent variable one single model was selected as the most parsimonious one: advanced forest edge as the independent variable: LogLik = 45.2; AICc = -80.4; dLogLik = 3.81; df = 3; weight = 0.48. The model accounts for 48% of total variation explained by the whole set of models. Confidence intervals for the coefficients do not cross the value of 0 (zero) (Figure 10).

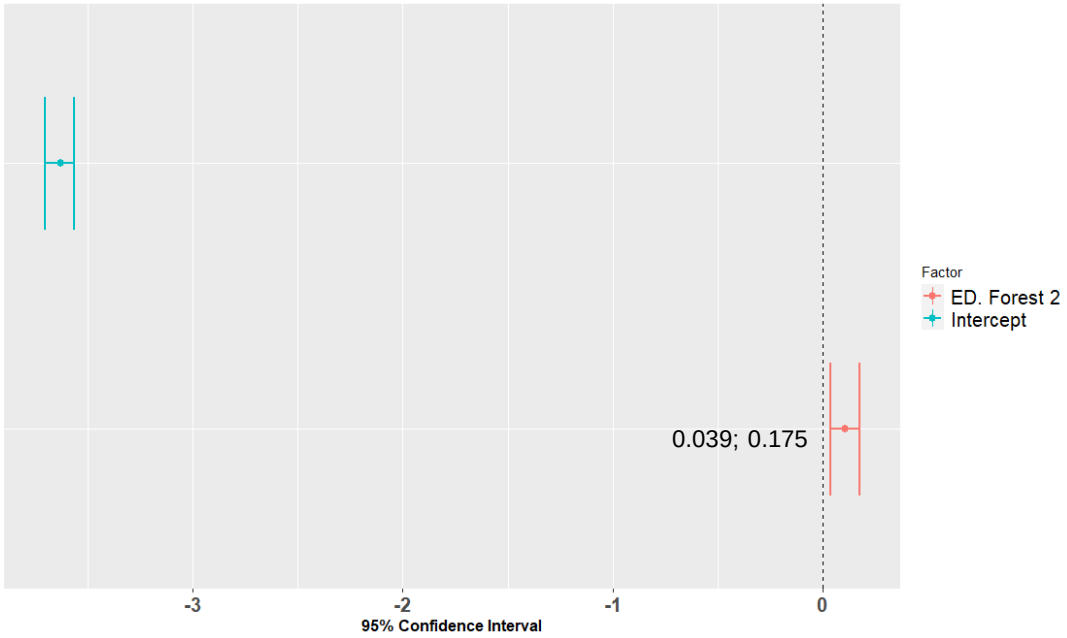

Figure 10. Confidence intervals and estimated values for independent variables in best fit models when Procrustes FA Scores is the dependent variable. *C. eous,* scale 2. Obs. Forest 2 = Advanced Forest.

Models fitted with Mahalanobis as dependent variable did not differ from the Null Model (Table 8).

Table 8. Best models according to AICc selection for Mahalanobis FA Scores as dependent variable in *C. eous* at Scale 2. The table reports values for Log Likelihood (LogLik); Akaike Information Criterion for small samples (AICc); Delta Log Likelihoods (dLogLik); Delta AICc (dAICc); Degrees of Freedom (df); AIC weights (weights).

		logLik	*AICc*	*dLogLik*	*dAICc*	*df*	*weight*
Mahalanobis FA Scores	NULL	-9.20	24.12	0.00	0.00	2	0.27
	PLAND Fores 1 + ED. Forest 2	-4.82	25.64	4.38	1.52	4	0.13
	PLAND Forest 1	-7.87	25.74	1.34	1.61	3	0.12

- ***Paryphthimoides poltys***

One model was top-ranked when Procrustes FA Scores are the dependent variable. In this model Initial Forests edge + ITA are the independent variables: LogLik = 56.29, AICc = -96.58, dLogLik = 15.01, df = 4, weight = 0.98.

The model accounts for 98% of total variation encompassed by the universe of models fitted and coefficients confidence intervals do not cross zero (Figure 11).

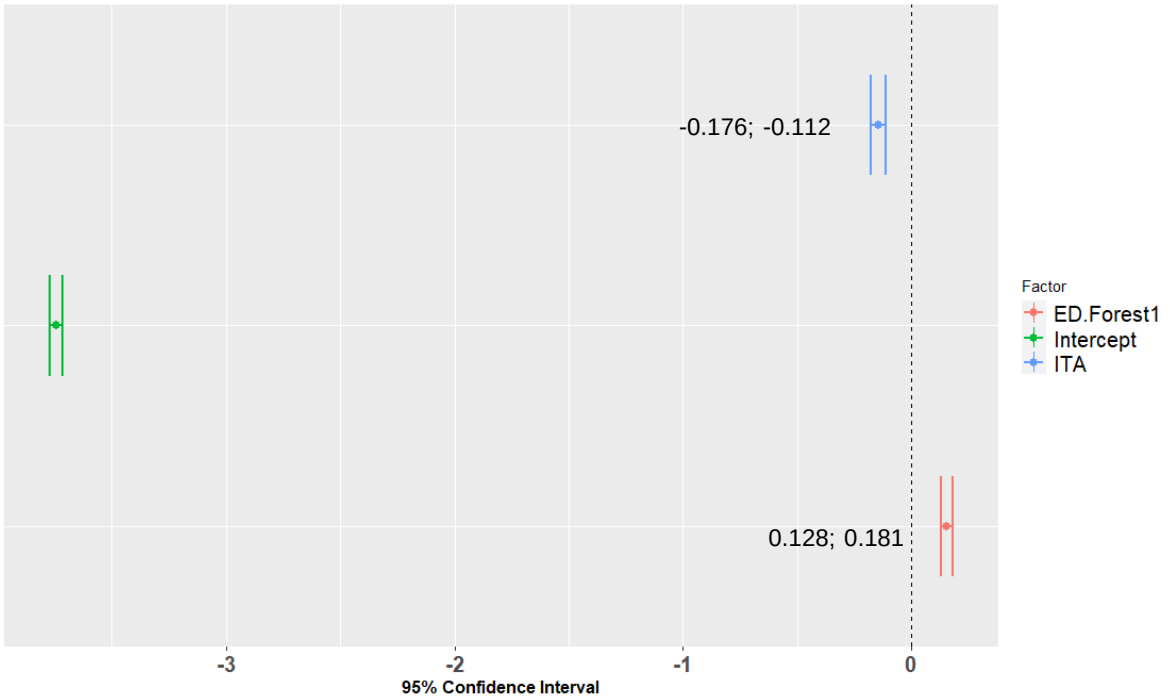

Figure 11. Confidence intervals and estimated values for independent variables in best fit models when Procrustes FA Scores is the dependent variable. *P. poltys,* scale 2. Obs. Forest 1 = Initial Forests.

For fits with Mahalanobis distances as dependent variable again only one model was among the most plausible ones. In this model, percentage of agriculture + Initial Forest edges were included as independent variables; LogLik = 3.3, AICc = 9.3, dLogLik = 10.3, weight = 0.94, df = 4. Confidence intervals did not cross Zero (Figure 12).

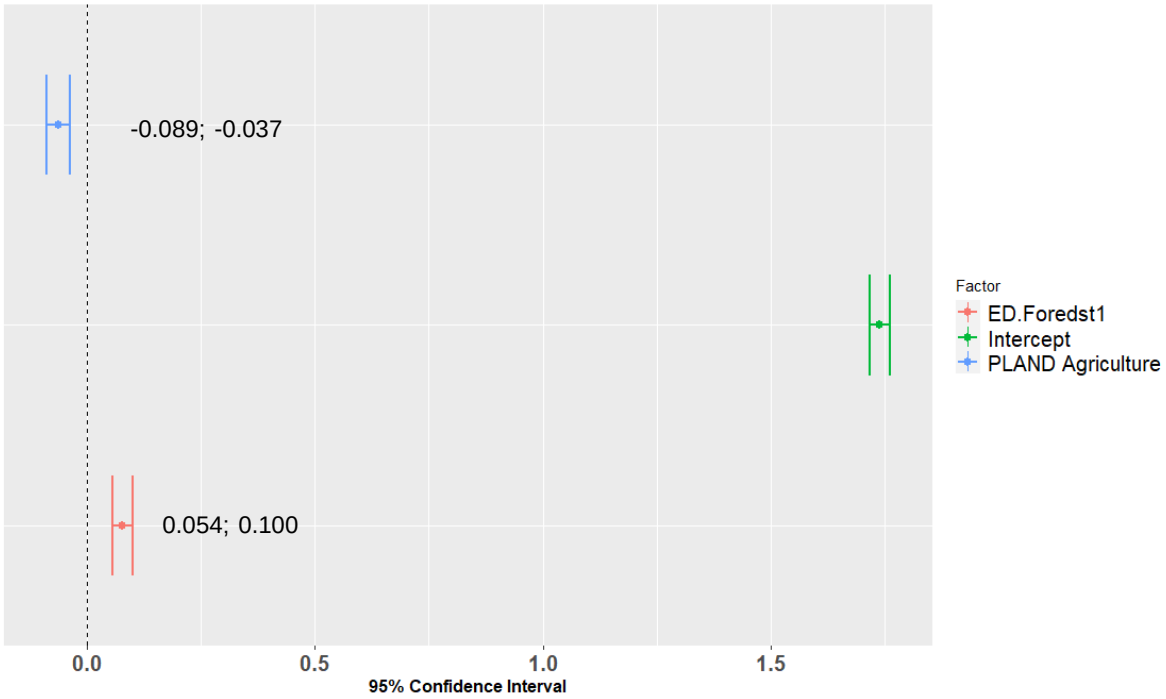

Figure 12. Confidence intervals and estimated values for independent variables in best fit models when Mahalanobis FA Scores is the dependent variable. *P. poltys,* scale 2.

SCALE 3

- ***Cissia eous***

At scale 3, models fitted for *C. eous* Procrustes FA scores did not differ from the Null model (Table 9).

Table 9. Best models according to AICc selection for Procrustes Distances as dependent variable in *C. eous* at Scale 3. The table reports values for Log Likelihood (LogLik); Akaike Information Criterion for small samples (AICc); Delta Log Likelihoods (dLogLik); Delta AICc (dAICc); Degrees of Freedom (df); AIC weights (weights).

		logLik	*AICc*	*dLogLik*	*dAICc*	*df*	*weight*
Procrustes FA Scores	NULL	41.38	-77.04	0.00	0	2	0.24
	PLAND Agriculture	43.07	-76.14	1.69	0.89	3	0.15

Two models were top ranked for *C. eous* Mahalanobis FA scores. These models' weight summed accounted for 47% for all variation explained.

Table 10. Best models according to AICc selection for Mahalanobis Distances as dependent variable in *C. eous* at Scale 3. The table reports values for Log Likelihood (LogLik); Akaike Information Criterion for small samples (AICc); Delta Log Likelihoods (dLogLik); Delta AICc (dAICc); Degrees of Freedom (df); AIC weights (weights).

		logLik	*AICc*	*dLogLik*	*dAICc*	*df*	*weight*
Mahalanobis FA Scores	PLAND Agriculture	-5.40	20.81	3.8	0	3	0.27
	ITA	-5.71	21.42	3.5	0.6	3	0.20

Confidence intervals of the selected models did not cross Zero, which means we can be 95% assured that the true estimate lies between the calculated interval and that it does not include zero (Figure 13).

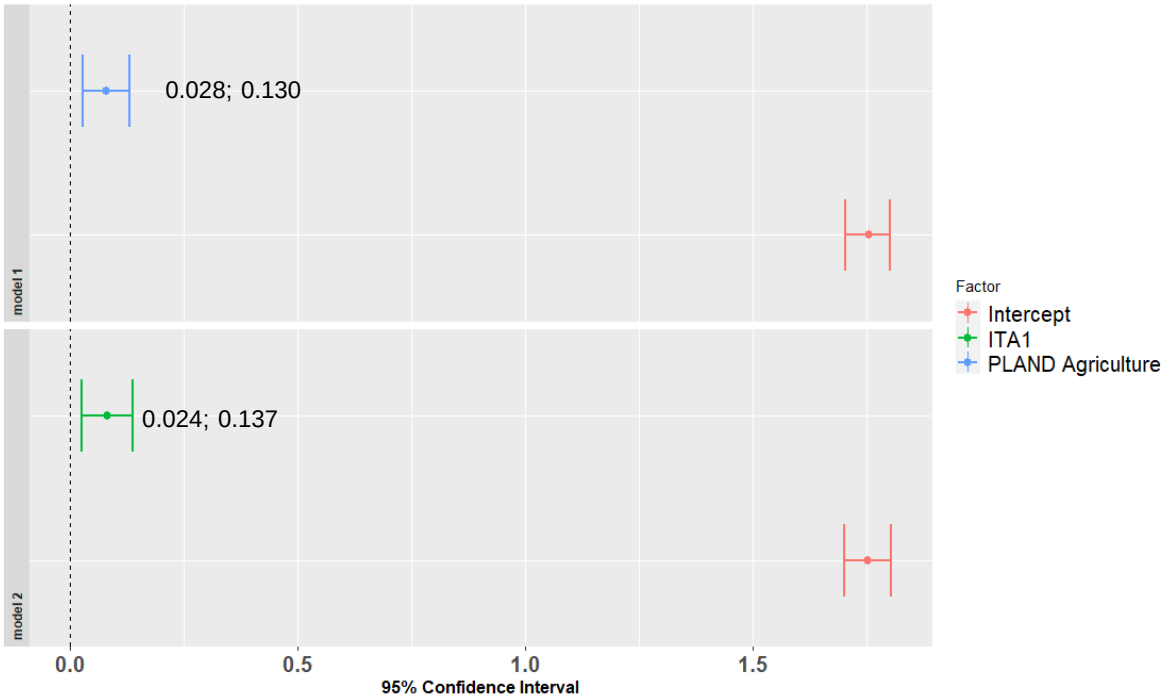

Figure 13. Confidence intervals and estimated values for independent variables in best fit models when Mahalanobis FA Scores is the dependent variable. *C. eous*, scale 3.

- ***Paryphthimoides poltys***

At scale 3, Procrustes FA scores in *P. poltys* is correlated with ITA and percentage of advanced forest: LogLik = 47.6, AICc = -79.2, dLogLik = 6.3, df = 4, weight = 0.27. This single model is responsible for 27% of all variation found. Coefficient's confidence interval values do not cross Zero (Figure 14).

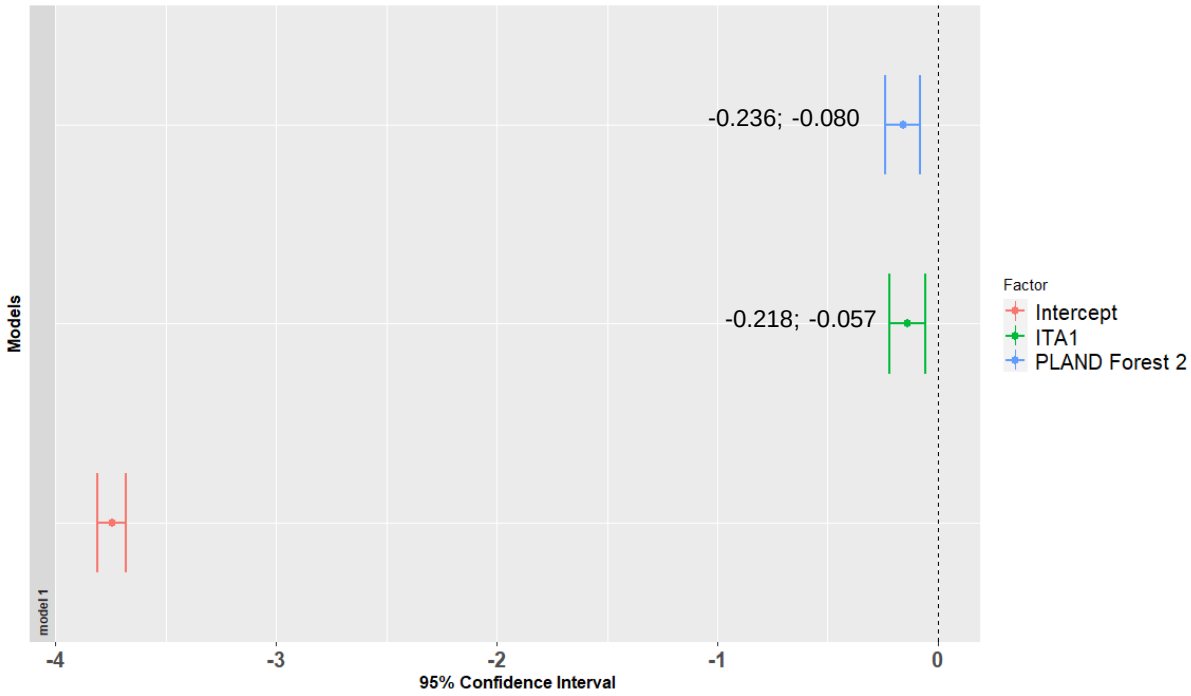

Figure 14. Confidence intervals and estimated values for independent variables in best fit models when Procrustes FA Scores is the dependent variable. *P. poltys,* scale 3.

Models with Mahalanobis FA scores as dependent variable did not differ from the Null model for *P. poltys* at this scale (Table 11).

Table 11. Best models according to AICc selection for Mahalanobis Distances as dependent variable in *P. poltys* at Scale 3. The table reports values for Log Likelihood (LogLik); Akaike Information Criterion for small samples (AICc); Delta Log Likelihoods (dLogLik); Delta AICc (dAICc); Degrees of Freedom (df); AIC weights (weights).

		logLik	*AICc*	*dLogLik*	*dAICc*	*df*	*weight*
Mahalanobis FA Scores	ED. Forest 1	-3.87	17.74	3.07	0.00	3	0.20
	PLAND Forest 2	-4.21	18.42	2.73	0.68	3	0.14
	NULL	-6.94	19.60	0.00	1.86	2	0.08

DISCUSSION

We studied how the wing phenotype of two species (*Cissia eous* and *Paryphthimoides poltys*) of lepidoptera (a well stablished bioindication group) is affected by different landscape elements and configuration at three spatial scales in agricultural landscapes. We used variations in bilateral symmetry between both wing sides in butterfly individuals to estimate fluctuating asymmetry as a proxy for developmental instability. We initially expected that more human modified landscapes would exert stronger effects on organismal development, resulting in higher fluctuating asymmetry. We also expected that this effect would be more detected at finer scales, giving the limited movement capacity of the study species. Our hypotheses were only partially corroborated.

The patterns found for *Cissia eous* and *Paryphthimoides poltys* were not consistent between species and across the scales of the study. A larger number of landscape features are correlated to fluctuating asymmetry at scale 1 (200 meter radius), however only percentage of anthropic area is significative for *Cissia eous* while only initial forests and agriculture have a clear effect over fluctuating asymmetry in *Paryphthimoides poltys*, other effects at this scale were unclear, meaning the null hypothesis could not be either rejected or accepted, since no-correlation was as plausible as negative or positive correlations. Still, that could be pointing out to what was concluded by Ribeiro and collogues (2012): Satyrini butterflies do respond more directly to the immediate environmental context (200 meters radius).

Higher percentages of anthropic area at small scales are shown to be reliably associated with more fluctuating asymmetry in *Cissia eous*. This result is in agreement with our initial expectations on the importance of anthropic areas as a source of extrinsic developmental instability. Similarly, the index of anthropic transformation and percentage of agriculture also associated positively with FA in *C. eous*. Both variables are associated with human land uses and may also relate with stressful conditions that affect organisms' phenotypes. Regarding agriculture, the most obvious source of environmental stress comes from human-made chemicals used as pesticides/insecticides, these molecules are being developed since the green revolution and are still a novel element in ecosystems from an evolutionary perspective. Since FA was indicated as a possible marker for developmental instability

from environmental stress, studies investigating FA's relationship with pesticides have been conducted with various groups such as dragonflies, butterflies, fishes and lizards (CHANG et al, 2007; KONOPKA et al, 2012; ALLENBACH, 1999; SIMBULA et al, 2021). Results are varied and there is evidence of higher FA levels in different traits of the same organism. Hence the hypothesis of human-induced transformations on the natural environment being a cause of stress that triggers instability processes during species development seems to be well supported and corroborated for *C. eous*, with the addition of evidence that indicates this effect also implicates species that are not particularly dependent on a more pristine environment.

For *Paryphthimoides poltys* smaller and younger forest edges and percentage of agriculture at the immediate scale (200 meters radius) reliably explained some of the fluctuating asymmetry detected. The positive correlation between edges of initial forests and FA extends to the scale 2. For *C. eous*, at scale 2 we observe a positive correlation between advanced forests' edge. *FA scores* increase in landscapes with more edges around forest patches. this comes off as an intriguing result, given the high affinity *C. eous* and *P. poltys* are reported to have to open areas (ZACCA et al, 2018; ZACCA et al, 2020). Then it seems logical to infer that forest edges do not pose an important source of stress for these species. In this scenario, It is possible that forest edges represent a refuge for adult butterflies because it offers more amenable microclimatic conditions, and substrate for sheltering against predators or climatic events. Then, it is likely that the more stable conditions in the edges allow for the survival of more asymmetric and less fit butterflies, compared to harsher environments. But it is important that we also take into account what these elements in the landscape mean to the development of these animals, not only during their adult phase, but also before. There are two likely (non-exclusive) reasons forest edges might represent a source of stress: increased competition for food in these areas and forest edges serving as atmospheric pollutants deposits.

Competition in prior life stages could be the driving interaction to produce stress that is resulting in developmental instability. Some Poacea are important to *C. eous* as host plant resource (*Digitaria sanguinalis, Stenotaphrum secundatum*) where eggs are laid, caterpillars feed off and pupae fix themselves until the last metamorphosis is complete. These plants are mainly found in pasturelands and grass fields. Host-plants

for *P. poltys* (*Eulesine*, *Cenchrus L* and *Stenotaphrum)* mostly inhabit open areas like pastures and may be an infrequent resource on edge areas as well. The decrease in food availability could mean food-stress for the species, which could also drive competition. Competition can be amplified by the fact that *P. poltys* usually lays a single egg per host plant and larvae are solitary (ZACCA et al, 2020). It was already shown that food stress can affect butterfly's wings morphology (JOHNSON, 2004; PELLEGROMS et al, 2009), even though FA itself is not quite reliable estimator of food stress, demonstrating quite varied results across different groups (STOKS, 2001; VANGESTEL 2011; GONZALEZ et al. 2014; SWADDLE & WITTER 1994). Another possible source of environmental stress could be a phenomenon that has being studied for decades: the concentration of pollutants (and nutrients) at forest edges (WEATHERS et al, 2001). Deposition of sodium, chloride and ions that cause soil acidification and eutrophication, sulfur, inorganic nitrogen and calcium has been found in edge areas, airborne pollutants are brought specially by throughfall in wet seasons (vertical flow) and by the wind in dry seasons (horizontal flow) (DRAAIJERS et al, 1988; DE SCHRIJVER et al, 2007). There is evidence of the impact anthropogenic pollution deposition at forest edges on other bioindicators (GLENN et al, 1998) and the increased accumulation of pollutants in areas close to agricultural and urban landscapes (WEATHERS et al, 2001). The contact with concentrated pollution might be the source of disruptive noise increasing developmental instability in butterflies along forest edges. In summary, forest edges might be functioning as an ecological trap (SEVERNS, 2011), being a landscape structure that formerly offered higher quality resource and attracts adult butterflies a preferable habitat to reproduce while this very structure has been modified by anthropogenic activity which is now negatively affecting butterflies in their immature stages.

Anthropic Transformation Index (ITA) is positively related to *C.eous'* FA levels at scale 3 (1 km radius) and negatively related to *P. poltys'* FA levels at scale 2 (200 meters merged buffers). The positive correlation to FA scores in *C. eous* reinforces anthropization as an important cause of developmental instability, as already supported by percentage of anthropic area being closely related to fluctuating asymmetry at small scale.

Except for the positive relationship with forest edges, FA in *P. poltys* was negatively related with percentage of agriculture and the index of anthropic transformation. Interestingly, these results diverge from *C. eous*, even though both species share similar habits. The negative correlation with FA indicates that asymmetry is higher is less anthropic landscapes. This seemingly contradictory evidence can potentially be explained by higher anthropization serving as a selective force favoring individuals which developmental stability is more robust in face of environmental stress, denoting that more symmetrical individuals are the ones surviving in harsh, anthropogenic landscapes. Fluctuating asymmetry in insects has been largely studied and robustly supports that FA is a good proxy for developmental instability induced by environmental factors and it does relate to fitness (DE ANNA ET AL, 2013). Therefore, we can find higher levels of asymmetry in less disturbed environments, not because those environments produce more stress, but because individuals with lower developmental stability (more asymmetrical ones) have higher chances to thrive in such conditions in comparison to more anthropized places where developmental instability is disruptive enough to affect individuals' fitness. A similar dynamic was found in a 2020 study carried by IVANKOVIĆ TATALOVIĆ and colleagues where it was found higher levels of asymmetry for carabids in agricultural areas with 'ecologically based pest management' in comparison to areas where a large spectrum of pesticides were used. A similar interaction was reported in BENÍTEZ et al (2018).

Indeed, in *Paryphthimoides poltys* fluctuating asymmetry is negatively corelated to agriculture (Scale 1 and 2), meaning that higher levels of asymmetry are found in landscapes with smaller amounts of agricultural area. this results and the fact that percentage of agriculture is negatively correlated with percentage of advanced forests (Figure 15S) reinforces the hypothesis that *P. poltys* is undergoing a selective pressure in anthropized areas. Data does not support the idea that less fragmented or less disturbed areas could impose more extrinsic noise, in reality *P. poltys* in its adult phase seems to have more affinity to larger forested areas than *C. eous* (Figure 6S) while also occurring in landscapes dominated by agriculture at a lesser extent in comparison to *C. eous*.

The divergencies we see between both species regarding how each one is being affected by landscape structures and anthropization might be due to differential levels of developmental instability and stability (distinct processes). *P. poltys* showed more sensitivity to habitat and landscape anthropization to the extent of possibly having its fitness deeply affected, it could be an indicative of a weaker noise buffering in this species. *C. eous,* on another hand, responded to anthropization at both, small and large scale, displaying an increase in its fluctuating asymmetry along the increase of anthropic areas (small scale) and anthropic transformation index (large scale) without undergoing an apparently strong selection process for more symmetrical individuals.

Mahalanobis models seemed to perform better than Procrustes models, that might be due to the fact that Mahalanobis distance is more sensitive to shape variation in unusual directions of the shape space (a more detailed explanation of morphometric spaces is in Supplementary Material), that means that even more subtle asymmetrical variation in being described by this measure. Nonetheless, Procrustes models were still important to capture correlations at the intermediate scale.

CONCLUSION

Our research investigated how landscape anthropization affects the development of two common and fairly abundant Lepidoptera species in an important biodiversity hotspot. We measured fluctuating asymmetry of these species through the geometric morphometrics method and approached anthropization processes through landscape metrics in 3 different scales. We found evidence for developmental instability in both species and also data that supports the case for this instability being related to human induced environmental transformations. We found small scales to be particularly influential in developmental instability processes and that *FA* measured in Mahalanobis distances seems to capture better the relationship between fluctuating asymmetry and the landscape, still we recommend the use of both metrics (Mahalanobis and Procrustes) in order to acquire a wider picture of the situation.

C. eous levels of asymmetry were consistently related to anthropic areas at the small scale (200-meter radius) suggesting a good potential as a bioindicator to assess

anthropization in the Atlantic Forest. *P. poltys* results suggest that it is more sensitive to developmental noise and it might have an impact in individuals' fitness. Studies are needed to test this hypothesis, especially regarding the role forest edges have on population maintenance and fitness. These results indicate that the intensity of modern anthropization is negatively affecting even species deemed as well adapted to human-transformed environments.

REFERENCES

ADAMS, Dean C.; ROHLF, F. James; SLICE, Dennis E. Geometric morphometrics: ten years of progress following the 'revolution'. Italian Journal of Zoology, v. 71, n. 1, p. 5-16, 2004.

ALLENBACH, Dawn M.; SULLIVAN, Karen Brown; LYDY, Michael J. Higher fluctuating asymmetry as a measure of susceptibility to pesticides in fishes. Environmental Toxicology and Chemistry: An International Journal, v. 18, n. 5, p. 899-905, 1999.

ANCIÃES, Marina; MARINI, M. A. The effects of fragmentation on fluctuating asymmetry in passerine birds of Brazilian tropical forests. Journal of Applied Ecology, v. 37, n. 6, p. 1013-1028, 2000.

BENÍTEZ, Hugo A. et al. Breaking symmetry: Fluctuating asymmetry and geometric morphometrics as tools for evaluating developmental instability under diverse agroecosystems. Symmetry, v. 12, n. 11, p. 1789, 2020.

BENÍTEZ, Hugo A. et al. Fluctuating asymmetry indicates levels of disturbance between agricultural productions: An example in Croatian population of Pterostichus melas melas (Coleptera: Carabidae). Zoologischer Anzeiger, v. 276, p. 42-49, 2018.

BIZARRO, Jorge Manuel Saraiva; CASAGRANDE, Mirna Martins; MIELKE, Olaf Hermanm Hendrik. Morfologia externa de Thyridia psidii cetoides (Rosenberg & Talbot). I. Cabeça e apêndices (Lepidoptera, Nymphalidae, Ithomiinae). Revista Brasileira de Zoologia, v. 20, n. 2, p. 279-284, 2003.

BOLKER, Ben; BOLKER, Maintainer Ben. Package 'bbmle'. Tools for General Maximum Likelihood Estimation, v. 641, 2017

BONEBRAKE, Timothy C. et al. More than just indicators: a review of tropical butterfly ecology and conservation. Biological conservation, v. 143, n. 8, p. 1831-1841, 2010.

BROWN JR, Keith S.; FREITAS, André Victor L. Atlantic forest butterflies: indicators for landscape conservation 1. Biotropica, v. 32, n. 4b, p. 934-956, 2000.

Canto-Dorow, T.S. 2020. Digitaria in Flora do Brasil 2020. Jardim Botânico do Rio de Janeiro.Disponível em: <http://floradobrasil.jbrj.gov.br/reflora/floradobrasil/FB13181>. Acesso em: 09 nov. 2021

CHANG, Xiaoli et al. Effects of temperature stress and pesticide exposure on fluctuating asymmetry and mortality of Copera annulata (Selys)(Odonata: Zygoptera) larvae. Ecotoxicology and environmental safety, v. 67, n. 1, p. 120-127, 2007

CRUZ, CARLA BERNADETE MADUREIRA et al. Carga antrópica da bacia hidrográfica da Baía de Guanabara. Simpósio Brasileiro de Sensoriamento Remoto, v. 9, p. 99-109, 1998.

DE ANNA, E. Beasley; BONISOLI-ALQUATI, Andrea; MOUSSEAU, Timothy A. The use of fluctuating asymmetry as a measure of environmentally induced developmental instability: A meta-analysis. Ecological Indicators, v. 30, p. 218-226, 2013

DELIGNETTE-MULLER, Marie Laure et al. fitdistrplus: An R package for fitting distributions. Journal of statistical software, v. 64, n. 4, p. 1-34, 2015.

DE SCHRIJVER, An et al. On the importance of incorporating forest edge deposition for evaluating exceedance of critical pollutant loads. Applied Vegetation Science, v. 10, n. 2, p. 293-298, 2007

DRAAIJERS, G. P. J.; IVENS, W. P. M. F.; BLEUTEN, W. Atmospheric deposition in forest edges measured by monitoring canopy throughfall. Water, Air, and Soil Pollution, v. 42, n. 1, p. 129-136, 1988

e-Flora of South Africa. v1.21. 2018. South African National Biodiversity Institute. http://ipt.sanbi.org.za/iptsanbi/resource?r=flora_descriptions&v=1.21

ELLIS, Rebecca D.; MCWHORTER, Todd J.; MARON, Martine. Integrating landscape ecology and conservation physiology. Landscape Ecology, v. 27, n. 1, p. 1-12, 2012.

EMBRAPA. Panorama Fitosanitário - Cultura do Milho. 2014. Disponível em: <http://panorama.cnpms.embrapa.br/plantas-daninhas/identificacao/folhas-estreitas/capim-colchao-digitaria-sanguinalis-l-scop>. Acesso em: 19 set. 2021.

FAHRIG, Lenore, et al. "Functional landscape heterogeneity and animal biodiversity in agricultural landscapes." Ecology letters 14.2 (2011): 101-112

FARINA, Almo. Principles and methods in landscape ecology: towards a science of the landscape. Springer Science & Business Media, 2008.

FILGUEIRAS, Tarciso S. O gênero Cenchrus L. no Brasil (Gramineae: Panicoideae). Acta Amazonica, v. 14, n. 1-2, p. 95-127, 1984.

FREITAS, André VL et al. Sampling Methods for Butterflies (Lepidoptera). In: Measuring Arthropod Biodiversity. Springer, Cham, 2021. p. 101-123.

GHALAMBOR, Cameron K. et al. Adaptive versus non-adaptive phenotypic plasticity and the potential for contemporary adaptation in new environments. Functional ecology, v. 21, n. 3, p. 394-407, 2007.

GLENN, Marian G.; WEBB, Sara L.; COLE, Mariette S. Forest integrity at anthropogenic edges: air pollution disrupts bioindicators. Environmental Monitoring and Assessment, v. 51, n. 1, p. 163-169, 1998.

GONZALEZ, Paula N.; LOTTO, Federico P.; HALLGRÍMSSON, Benedikt. Canalization and developmental instability of the fetal skull in a mouse model of maternal nutritional stress. American journal of physical anthropology, v. 154, n. 4, p. 544-553, 2014.

GOTTHARD, Karl; NYLIN, Sören. Adaptive plasticity and plasticity as an adaptation: a selective review of plasticity in animal morphology and life history. Oikos, p. 3-17, 1995.

GOWER, John C. Generalized procrustes analysis. Psychometrika, v. 40, n. 1, p. 33-51, 1975.

IVANKOVIĆ TATALOVIĆ, Lara et al. Fluctuating Asymmetry as a Method of Assessing Environmental Stress in Two Predatory Carabid Species within Mediterranean Agroecosystems. Symmetry, v. 12, n. 11, p. 1890, 2020.

JOHNSON, Haley et al. Does skipping a meal matter to a butterfly's appearance? Effects of larval food stress on wing morphology and color in monarch butterflies. PloS one, v. 9, n. 4, p. e93492, 2014.

KENDALL, David George et al. Shape and shape theory. John Wiley & Sons, 2009.
KEYS, Patrick W. et al. Anthropocene risk. Nature Sustainability, v. 2, n. 8, p. 667-673, 2019.

KLINGENBERG, Christian Peter. MorphoJ: an integrated software package for geometric morphometrics. Molecular ecology resources, v. 11, n. 2, p. 353-357, 2011

KLINGENBERG, Christian Peter. Size, shape, and form: concepts of allometry in geometric

KLINGENBERG, Christian Peter. Walking on Kendall’s shape space: Understanding shape spaces and their coordinate systems. Evolutionary Biology, v. 47, n. 4, p. 334-352, 2020.

KLINGENBERG, Christian Peter; MCINTYRE, Grant S. Geometric morphometrics of developmental instability: analyzing patterns of fluctuating asymmetry with Procrustes methods. Evolution, v. 52, n. 5, p. 1363-1375, 1998

KLINGENBERG, Christian Peter; MONTEIRO, Leandro R. Distances and directions in multidimensional shape spaces: implications for morphometric applications. Systematic Biology, v. 54, n. 4, p. 678-688, 2005

KLINGENBERG, Christian. Analyzing fluctuating asymmetry with geometric morphometrics: concepts, methods, and applications. Symmetry, v. 7, n. 2, p. 843-934, 2015.

KONOPKA, Joanna K.; SCOTT, Ian M.; MCNEIL, Jeremy N. Costs of insecticide resistance in Cydia pomonella (Lepidoptera: Tortricidae). Journal of economic entomology, v. 105, n. 3, p. 872-877, 2012..

LAWTON, John H.; JONES, Clive G. Linking species and ecosystems: organisms as ecosystem engineers. In: Linking species & ecosystems. Springer, Boston, MA, 1995. p. 141-150.

LEWIS, Simon L.; MASLIN, Mark A. Defining the anthropocene. Nature, v. 519, n. 7542, p. 171-180, 2015.

LIRA, Paula K. et al. Land-use and land-cover change in Atlantic Forest landscapes. Forest Ecology and Management, v. 278, p. 80-89, 2012.

MARCUS, Leslie F. et al. (Ed.). Advances in morphometrics. Springer Science & Business Media, 2013

MARKOW, Therese Ann (Ed.). Developmental instability: its origins and evolutionary implications: proceedings of the International Conference on Developmental Instability: Its Origins and Evolutionary Implications, Tempe, Arizona, 14–15 June 1993. Springer Science & Business Media, 2012, 334 p.

MATEO, J. (1991) Geoecologia de los Paisajes. Universidad Central de Caracas. Monografia

McGARIGAL, K., Cushman, S.A. and Ene, E., 2012. FRAGSTATS v4: spatial pattern analysis program for categorical and continuous maps. Computer software program produced by the authors at the University of Massachusetts, Amherst. http://www. umass. edu/landeco/research/fragstats/fragstats. html.

MILLER, Colleen R.; LATIMER, Christopher E.; ZUCKERBERG, Benjamin. Bill size variation in northern cardinals associated with anthropogenic drivers across North America. Ecology and evolution, v. 8, n. 10, p. 4841-4851, 2018.

MØLLER, Anders Pape; SWADDLE, John P. Asymmetry, developmental stability and evolution. Oxford University Press, UK, 1997.

MORELLATO, L. Patrícia C.; HADDAD, Célio FB. Introduction: The Brazilian Atlantic Forest 1. Biotropica, v. 32, n. 4b, p. 786-792, 2000

NUNES, Lorena Andrade; ARAÚJO, Edilson Divino de; MARCHINI, Luís Carlos. Fluctuating asymmetry in Apis mellifera (Hymenoptera: Apidae) as bioindicator of anthropogenic environments. Revista de biologia tropical, v. 63, n. 3, p. 673-682, 2015.

OBA, Shigeyuki et al. A Bayesian missing value estimation method for gene expression profile data. Bioinformatics, v. 19, n. 16, p. 2088-2096, 2003.

PALMER, A. Richard. Fluctuating asymmetry analyses: a primer. In: Developmental instability: its origins and evolutionary implications. Springer, Dordrecht, 1994. p. 335-

PALMER, A. Richard; STROBECK, Curtis. Fluctuating asymmetry: measurement, analysis, patterns. Annual review of Ecology and Systematics, v. 17, n. 1, p. 391-421, 1986.

PARSONS, P. A. Fluctuating asymmetry: an epigenetic measure of stress. Biological reviews, v. 65, n. 2, p. 131-145, 1990.

PEARSON, David L. Selecting indicator taxa for the quantitative assessment of biodiversity. Philosophical Transactions of the Royal Society of London. Series B: Biological Sciences, v. 345, n. 1311, p. 75-79, 1994.

PELLEGROMS, Boris et al. Larval food stress differentially affects flight morphology in male and female speckled woods (Pararge aegeria). Ecological Entomology, v. 34, n. 3, p. 387-393, 2009.

PINTO, Nelson Silva et al. Fluctuating asymmetry and wing size of Argia tinctipennis Selys (Zygoptera: Coenagrionidae) in relation to riparian forest preservation status. Neotropical Entomology, v. 41, n. 3, p. 178-185, 2012.

RÁKOSY, László; SCHMITT, Thomas. Are butterflies and moths suitable ecological indicator systems for restoration measures of semi-natural calcareous grassland habitats?. Ecological indicators, v. 11, n. 5, p. 1040-1045, 2011.

RIBEIRO, D.B.et al., 2012. “The importance of small scales to the fruit-feeding butterfly assemblages in a fragmented landscape”. Biodiversity and Conservation, 21(3), pp.811-827

RIBEIRO, Danilo Bandini et al. The importance of small scales to the fruit-feeding butterfly assemblages in a fragmented landscape. Biodiversity and Conservation, v. 21, n. 3, p. 811-827, 2012.

RIBEIRO, Milton Cezar et al. The Brazilian Atlantic Forest: a shrinking biodiversity hotspot. In: Biodiversity hotspots. Springer, Berlin, Heidelberg, 2011. p. 405-434.

ROHLF, F. J. 2017. tpsDig, digitize landmarks and outlines, version 2.31. Department of Ecology and Evolution, State University of New York at Stony Brook.

ROHLF, F. James. tpsDig, version 2.32. http://life. bio. sunysb. edu/morph/index. html, 2006.

ROHLF, F. James; MARCUS, Leslie F. A revolution morphometrics. Trends in ecology & evolution, v. 8, n. 4, p. 129-132, 1993

SCHÖNEMANN, Peter H.; CARROLL, Robert M. Fitting one matrix to another under choice of a central dilation and a rigid motion. Psychometrika, v. 35, n. 2, p. 245-255, 1970

SEVERNS, Paul M. Habitat restoration facilitates an ecological trap for a locally rare, wetland-restricted butterfly. Insect Conservation and Diversity, v. 4, n. 3, p. 184-191, 2011

SILVA, J.M.C. e CASTELETI, C.H.M., 2003. Status of the biodiversity of the Atlantic Forest of Brazil. The Atlantic Forest of South America: Biodiversity Status, Threats, and Outlook. CABS and Island Press, Washington, pp.43-59.

SIMBULA, Giulia et al. Fluctuating asymmetry as biomarker of pesticides exposure in the Italian wall lizards (Podarcis siculus). Zoology, v. 147, p. 125928, 2021.

SMALL, Christopher G. The statistical theory of shape. Springer Science & Business Media, 2012.

SMITH, Bruce D. The ultimate ecosystem engineers. SCIENCE-NEW YORK THEN WASHINGTON-, v. 315, n. 5820, p. 1797, 2007

Stoks, R. Food stress and predator-induced stress shape developmental performance in a damselfly. Oecologia 127, 222–229 (2001). https://doi.org/10.1007/s004420000595

SWADDLE, John P.; WITTER, Mark S. Food, feathers and fluctuating asymmetries. Proceedings of the Royal Society of London. Series B: Biological Sciences, v. 255, n. 1343, p. 147-152, 1994

SWADDLE, John P.; WITTER, Mark S.; CUTHILL, Innes C. The analysis of fluctuating asymmetry. Animal Behaviour, v. 48, n. 4, p. 986-989, 1994.

The GIMP Development Team, 2019. GIMP, Available at: https://www.gimp.org.

THOMAS, J. A. Monitoring change in the abundance and distribution of insects using butterflies and other indicator groups. Philosophical Transactions of the Royal Society B: Biological Sciences, v. 360, n. 1454, p. 339-357, 2005.

VANGESTEL, Carl; LENS, Luc. Does fluctuating asymmetry constitute a sensitive biomarker of nutritional stress in house sparrows (Passer domesticus)?. Ecological Indicators, v. 11, n. 2, p. 389-394, 2011

VU, Van Lien. Ecological indicator role of butterflies in Tam Dao National Park, Vietnam. Russian Entomological Journal, v. 16, n. 4, p. 479-486, 2007.

Watson, L., Macfarlane, T.D., and Dallwitz, M.J. 1992 onwards. The grass genera of the world: descriptions, illustrations, identification, and information retrieval; including synonyms, morphology, anatomy, physiology, phytochemistry, cytology, classification, pathogens, world and local distribution, and references. Version: 5th November 2021. delta-intkey.com'.

WEATHERS, Kathleen C.; CADENASSO, Mary L.; PICKETT, Steward TA. Forest edges as nutrient and pollutant concentrators: potential synergisms between fragmentation, forest canopies, and the atmosphere. Conservation Biology, v. 15, n. 6, p. 1506-1514, 2001

WEBSTER, M. A. R. K.; SHEETS, H. David. A practical introduction to landmark-based geometric morphometrics. The Paleontological Society Papers, v. 16, p. 163-188, 2010.

WFO (2021): Poa annua L. Published on the Internet;http://www.worldfloraonline.org/taxon/wfo-0000891536. Accessed on: 02 Sep 2021

ZACCA, Thamara et al. Systematics of the butterfly genus Cissia Doubleday, 1848 (Lepidoptera: Nymphalidae, Satyrinae) using an integrative approach. Arthropod systematics and phylogeny, v. 76, n. 2, p. 349-376, 2018.

ZACCA, Thamara et al. Systematics of the Neotropical butterfly genus Paryphthimoides Forster, 1964 (Lepidoptera: Nymphalidae: Satyrinae), with descriptions of seven new taxa. Insect Systematics & Evolution, v. 52, n. 1, p. 42-96, 2020.

ZALASIEWICZ, Jan et al. The Anthropocene: comparing its meaning in geology (chronostratigraphy) with conceptual approaches arising in other disciplines. Earth's Future, v. 9, n. 3, p. e2020EF001896, 2021.

ZELDITCH, Miriam Leah; SWIDERSKI, Donald L.; SHEETS, H. David. Geometric morphometrics for biologists: a primer. academic press, 2012.

SUPPLEMENTARY MATERIAL

Morphometric Spaces and Distance Measurements

The set of raw coordinate matrices produced by digitizing landmarks corresponds to the physical space (two-dimensional or three-dimensional) from which this information was extracted, this morphometric space is called figure-space. However, in order to analyze the geometric shape of a structure it is necessary as described above, to eliminate dimensions (variation) that are not of interest, so the various matrix operations applied to cartesian coordinates in the Figure-Space during Procrustes Fit characterize at the end a new morphometric space called Kendall's Shape Space, theorized by mathematician David Kendall in 1977, where he introduced the idea that shapes are elements in complex projective spaces. (KENDALL, 2009; SMALL, 2012) Shape Spaces are multidimensional, non-Euclidean spaces, difficult to visualize but through mathematical abstraction. For 2D forms these Spaces present themselves as hyperspheres which dimensionality is given by the formula: 2p-4, where p is the number of landmarks, in the case of this study, for example, the Shape Space that incorporates the procrustes coordinates of lepidopteran wings has 34 topological dimensions, produced by each possibility of variation in the configuration of the 19 digitized landmarks. Each of these possibilities is represented as a point in a Shape Space and the distance between two points is the difference of shape between two configurations, measured as the square root of the sum of squared distances between corresponding landmarks, this measure is called Procrustes Distance. (KLINGENBERG, 2020; MARCUS et al, 2013) The Procrustes Distance has a range of 0 to 1, and is dependent on the number of landmarks in the configuration. In any

case, in order to make it possible to use these distances in later analyses, it is necessary to project the points to a Euclidean space that allows the use of multivariate statistics, this projection is made to a Tangent Plane of dimensionality identical to that of Shape Space and that intersects it exactly at the point corresponding to the consensus calculated in the Procrustes Fit. Considering that the variations of biological data are very small, the scattering of the points in the Space-Form remains in the vicinity of the consensus shape, not suffering significant distortions in the projection process to the Tangent Plane. (KLINGENBERG, 2020). The Procrustes Distance between the two sides of an individual is used as a way to quantify the fluctuating asymmetry at the specimen scale (subtracting the variation of directional asymmetry when it is present in the population).

Fluctuating Asymmetry Distribution

The distribution of Fluctuating Asymmetry at the individual (figure 1), trap (Figure 2) and landscape-level (Figure 3) is presented as Procrustes distance and Mahalanobis distance. Mahalanobis distance seems to give the data a distribution closer to normal distribution. Correlation between both distance types were tested with a Spearman's test, for *C. eous* rho = 0.66, for *P. poltys* rho = 0.77.

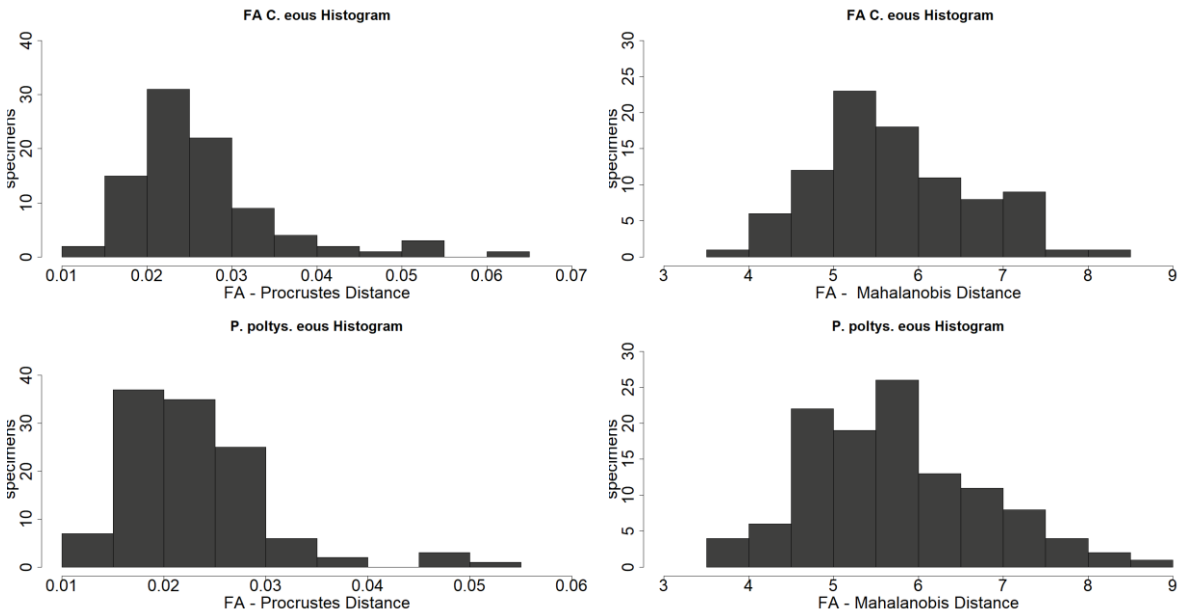

Figure 1. Frequency of individual asymmetry values for *C. eous* and *P. poltys*

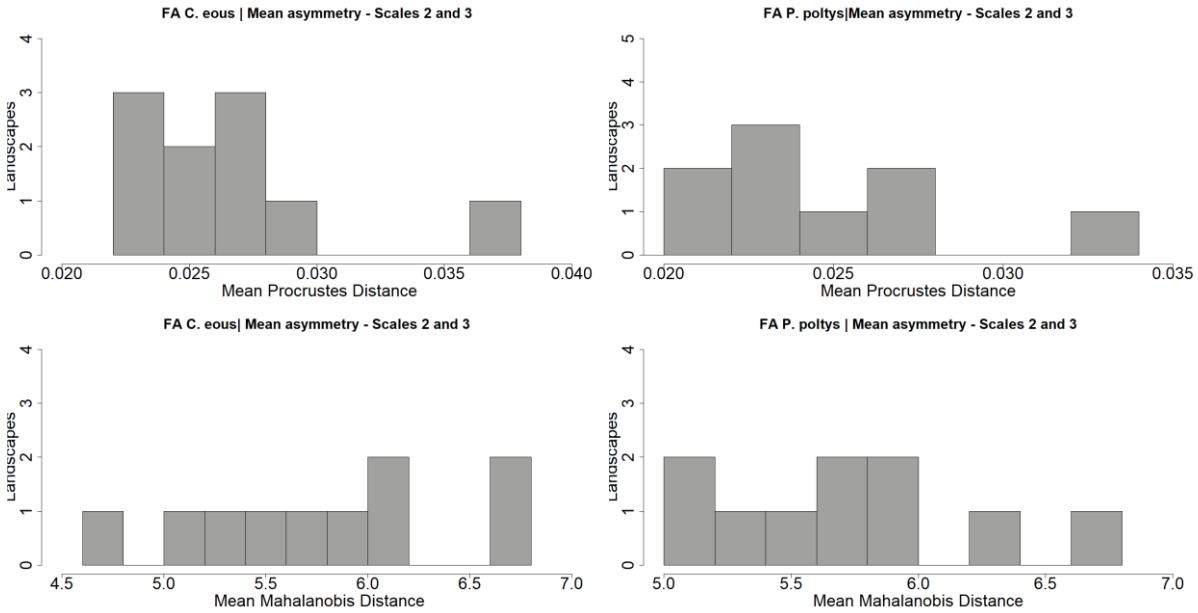

Figure 2. Frequency of mean asymmetry values of *C. eous* and *P. poltys* per trap (scale 1).

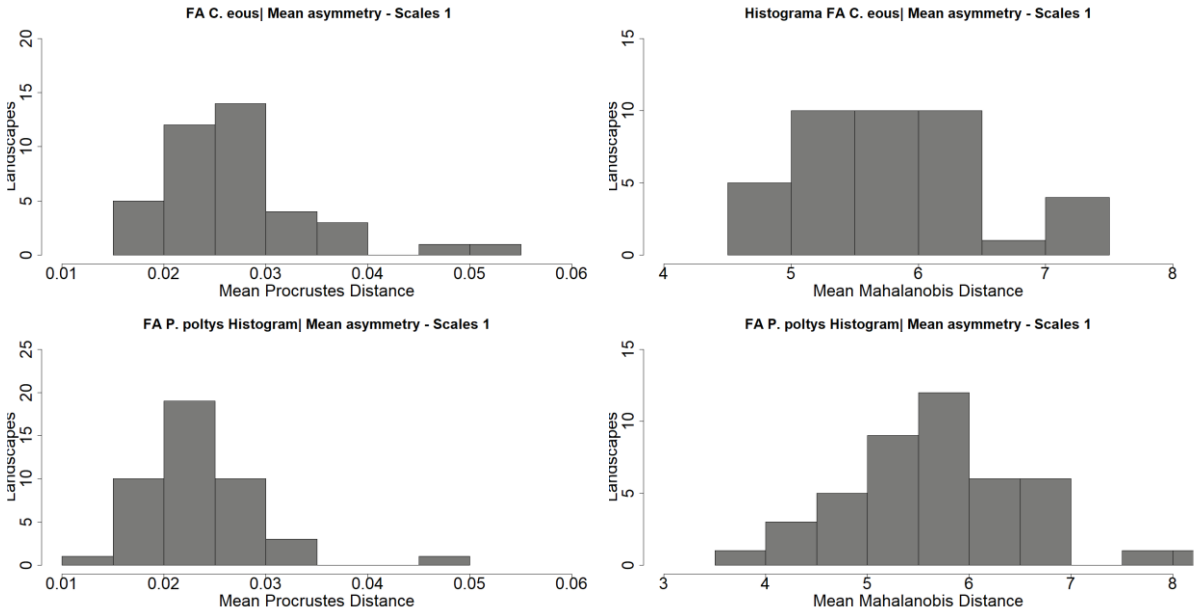

Figure 3. Frequency of mean asymmetry of *C. eous* and *P. poltys* per landscape (scales 2 and 3).

Characterization of landscapes

Scale 1 – 200 meters buffers

At scale 1 *P. poltys* seems to occur in places with both lower maximum (189 m/ha) and minimum (13 m/ha) values for edge density compared to *C. eous* (max -211 m/ha; min – 37 m/ha). (Figure 4).

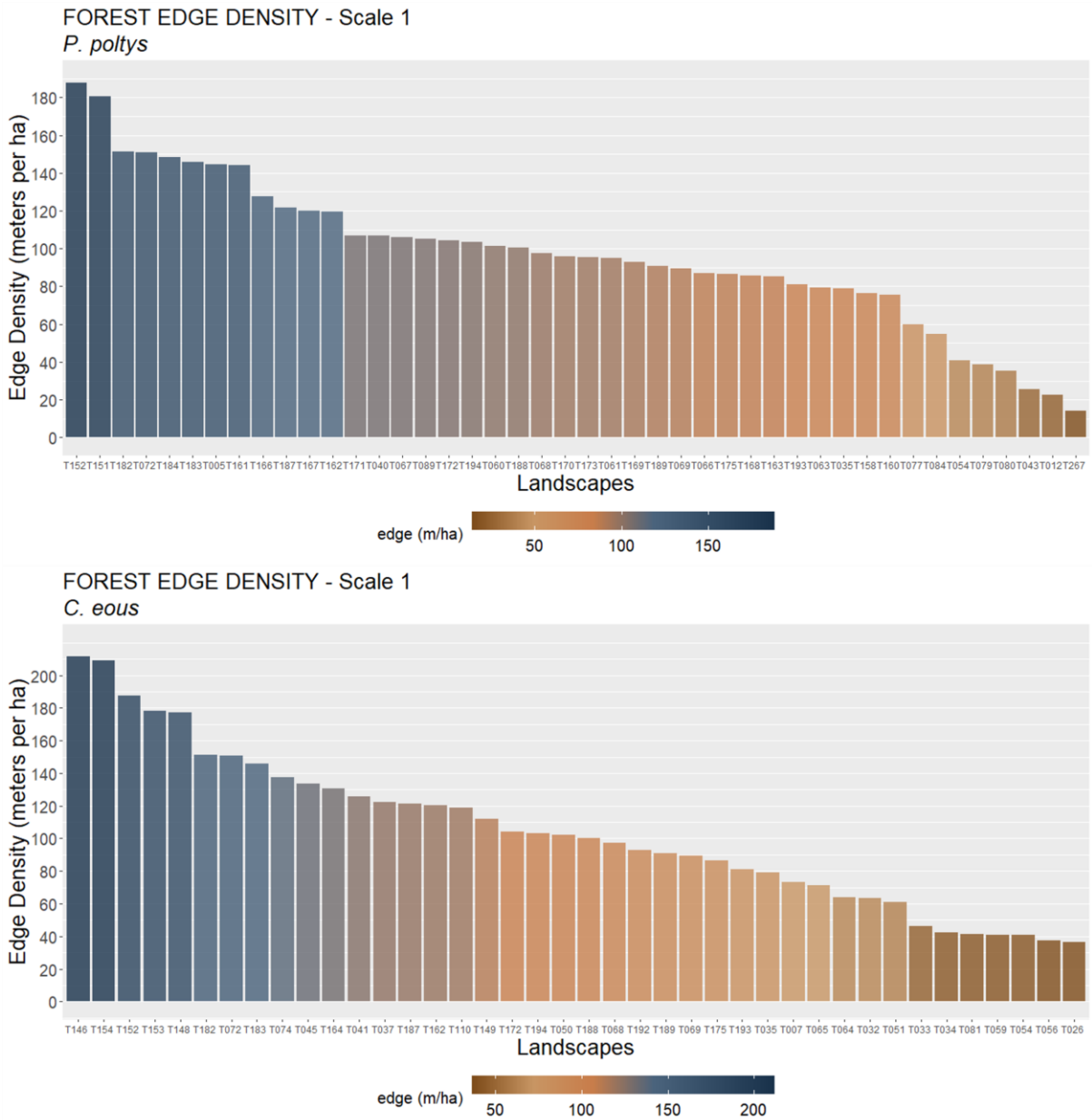

Figure 4. Edge density of general forest cover (both forest types counted as one single class)

Landscape heterogeneity is measured through Shannon-Weaver information index, also very popular for species diversity quantification. It is useful to inform about richness and equity among LULC (land use and land cover). We can use it to access how different landscapes are from each other when it comes to composition and proportions. It is important to consider what heterogeneity means in the context of the study, for its interpretation is tied to the LULC involved, since most of LULC (classes) in the present study is related somehow to anthropic spatial transformation, heterogeneity higher values are most likely indicative of anthropized classes sharing a fair amount of space with natural classes.

Scale 1 landscapes show somewhat of a heterogeneity gradient ranging from 0.5 to 1.25 with a few discrepant values on the extremes. (Figure 5).

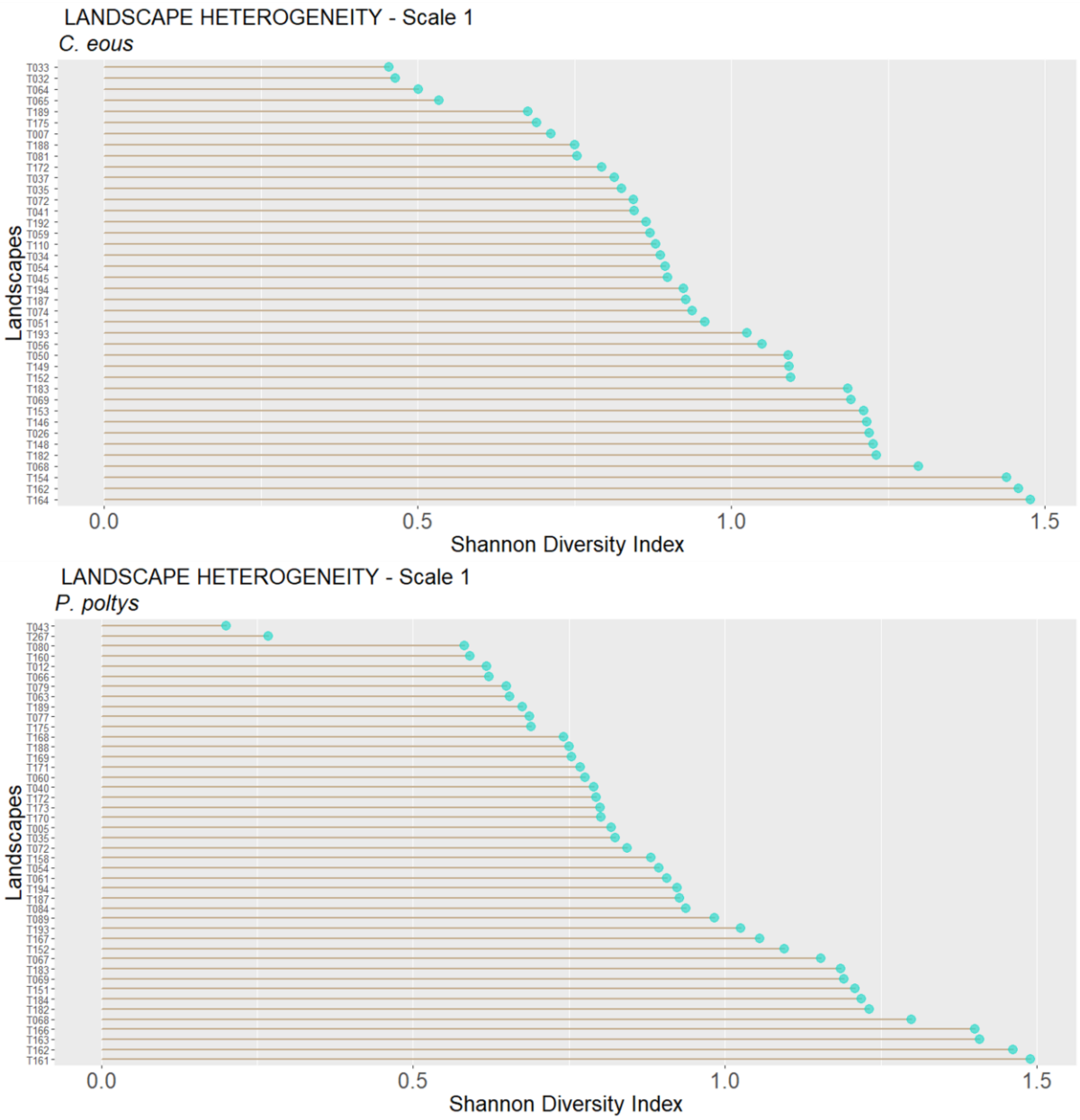

Figure 5. landscape heterogeneity measured as Shannon-Weaver diversity index. Higher values correspond to more classes composing the landscape and more balance in class proportions. Lower values indicate fewer classes of composition or greater unbalance in their proportions, resulting in overdominance of a particular class.

We can also evaluate how landscapes at scale 1 (200 meters radius) look like through the information on the largest patch to be found in each one, as a measure in

percentage unit of the landscape represented by a specific class. Largest Patch Index, then, offers us a glimpse of dominating classes throughout the scale. Four classes are shown to be the most representative: agriculture, Initial Forests (Forest 1), advanced Forests (Forest 2) and Pasture. At scale 1 landscapes where we sampled *C. eous,* agriculture and pasture seem to dominate more in landscape numbers (13 and 12 respectively). Where *P. poltys* was sampled, agriculture, advanced forest and pasture seem to be similarly represented, with agriculture dominated landscapes being more usual, however advanced forest is shown to be more prominent than in *C. eous* landscapes, in contrast to initial forest, which is less representative in landscape numbers and percentages (Figure 6).

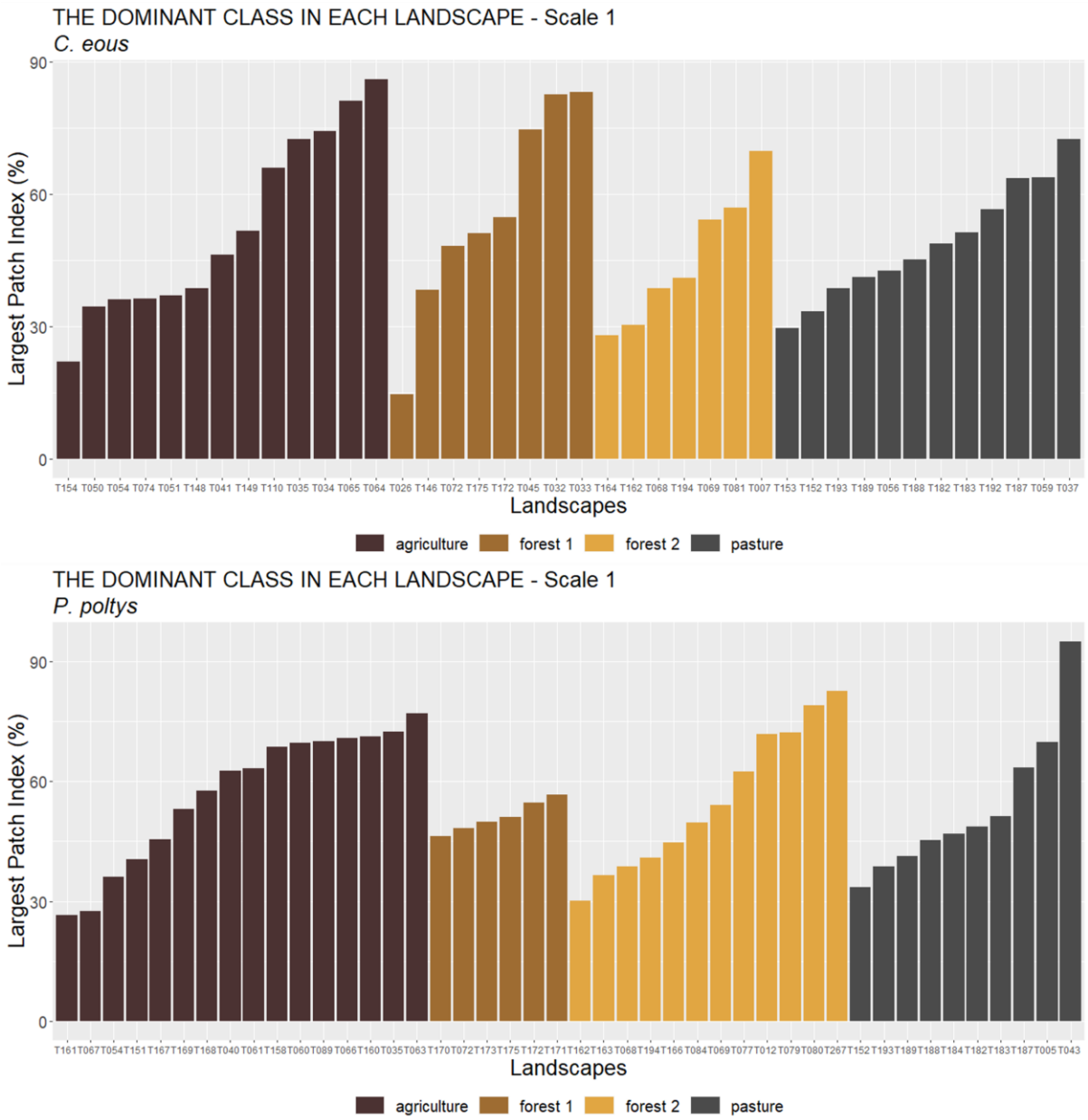

Figure 6. Most dominant LULC in each landscape at scale 1.

Scale 2 – 200 meters buffers merged & Scale 3 – 1km buffers

The classes distribution in Scale 2 is not particularly different between landscapes where we sampled each species, with the exception of a few sites where we can see major dissimilarities, like in LSi, for *C. eous* the landscape is composed mostly of pasture and initial forest (forest 1), for *P. poltys* LSi is overwhelmingly dominated by advanced forests (forest 2) (Figure 7)

Figure 7. Distribution in percentage of classes on scale 2 (200 meters buffers merged). The y-axis corresponds to the percentages, on the x-axis the landscapes are represented by each bar, and the colors show the proportions of each class in the landscapes.

Scale 3 - 1 km

The proportions of land use and land cover are quite heterogeneous in the scale 3 (Figure 8). Scale 3 encompasses 12 landscapes (Lsa, LSb, LSc LSd, LSe, LSf, LSg, LSh, LSi, LSj, LSk, LSl). Both subject species of the study were captured in the same

landscapes in this scale, except for LS*i - LSj*, where we only sampled *C. eous* and *LSh - LSk* where we only sampled *P. poltys*.

Agriculture, pastures and the two types of forest dominate the mosaic. Anthropic areas are not especially representative, except in landscapes *LSa, LSc, LSi* and *LSk* (Figure 8). Silviculture is more apparent in landscape *Lsa* and *LSh* only, 2 of the 3 landscapes where curiously agriculture represents its lowest proportions comparatively to the other study sites. There is no advanced forest (forest 2) in *LSd*, where pastures occupy almost 50% of the environment and water and wetlands (naturally underrepresented classes) display their highest percentages (Figure 8). Wetlands are represented in only 3 landscapes, as well as bodies of water (rivers, lakes). Forests 1 are present to a greater or lesser extent in all areas.

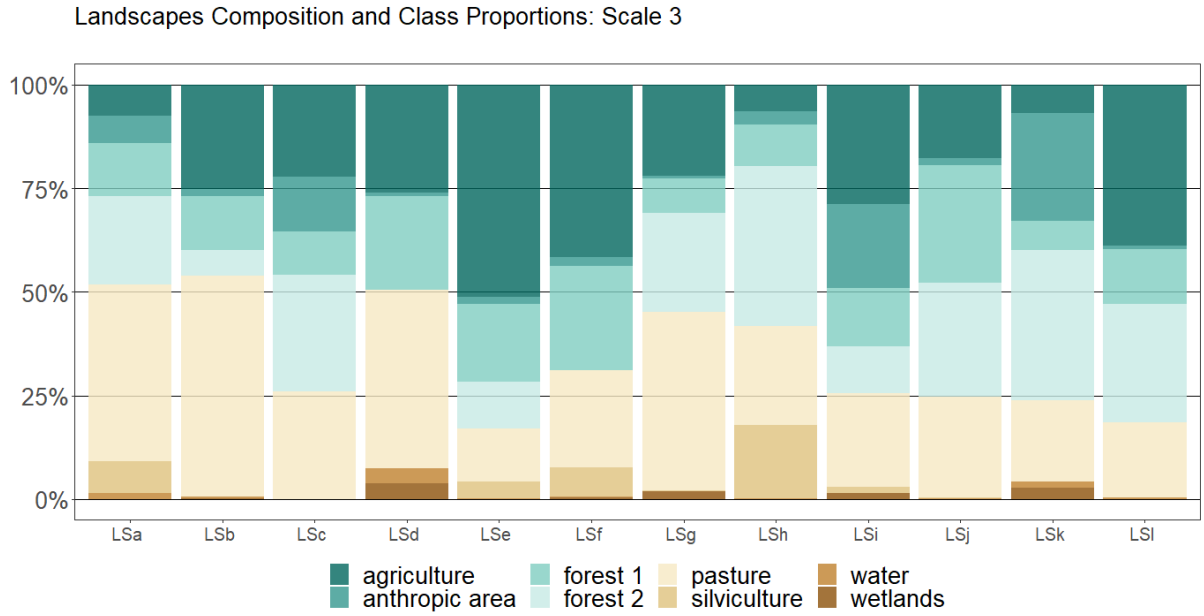

Figure 8. Distribution in percentage of classes on scale 3 (1 km). The y-axis corresponds to the percentages, on the x-axis the landscapes are represented by each bar, and the colors show the proportions of each class in the landscapes.

We address habitat availability as Edge Density, measured as meters per hectare of a particular class, in this case we measured initial and advanced forests (forest 1 and 2) as one single *Forest* class.

Cissia eous seems to occur in places with slightly higher values of forest edge density compared to *Paryphthimoides poltys* at the scale 2. (Figure 9).

Highest edge density levels are found in LSd at both scales (Scale 2: close to 175 m/ha for *C. eous*; 154 m/ha for *P. poltys.* Scale 3: 105 m/ha), in this case the forest

edge is entirely composed by initial forest class. The lowest values at Scale 2 are around 35 m/ha in LSi for *C. eous*; and around 12 m/ha in LSi for *P. poltys*. (Figure 9)

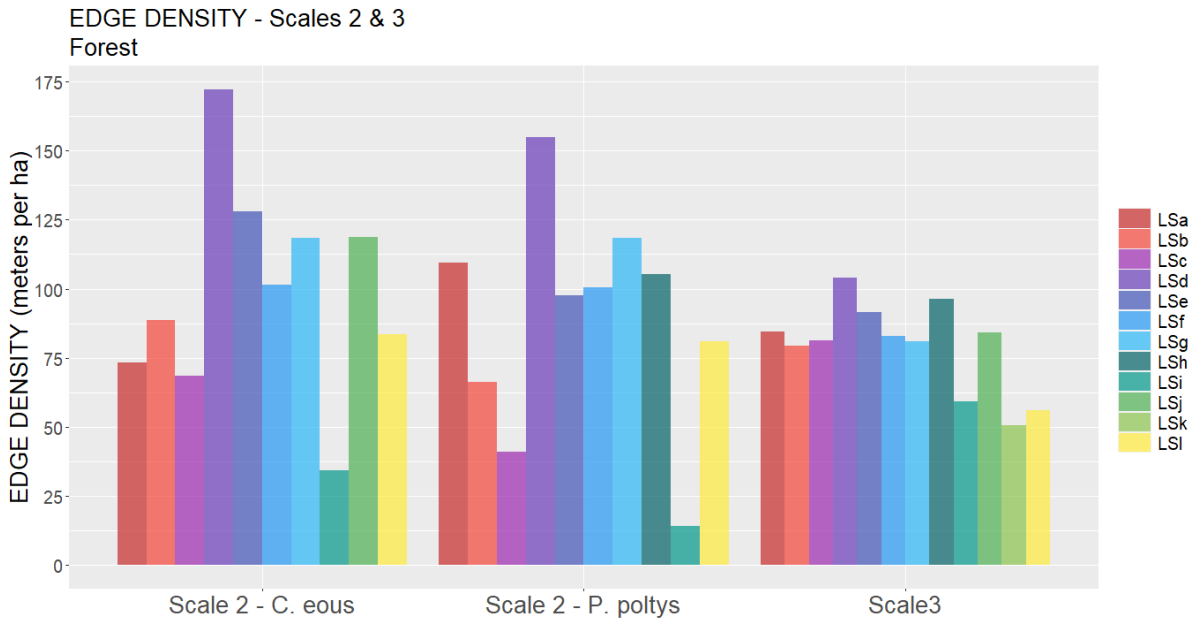

Figure 9. Meters per hectare of forest edges at the Scales 2 and 3.

Functional connectivity measured as the connectance Index informs us on the amount of patches of a class which are deemed to be connected from the perspective of a species or group of species. In this study the threshold is defined as 200 meters as maximum distance between two patches of forest (both types) so they can be considered connected. We observe in Scale 3 landscapes that the maximum connectance is around 34% in *LSk*, in despite of displaying the biggest proportion of anthropic areas across the scale, which may be compensated by a larger amount of advanced forests (forest 2). All the other landscapes present lower levels of connectance, the lowest being around 10% in *LSi*. (Figure 10)

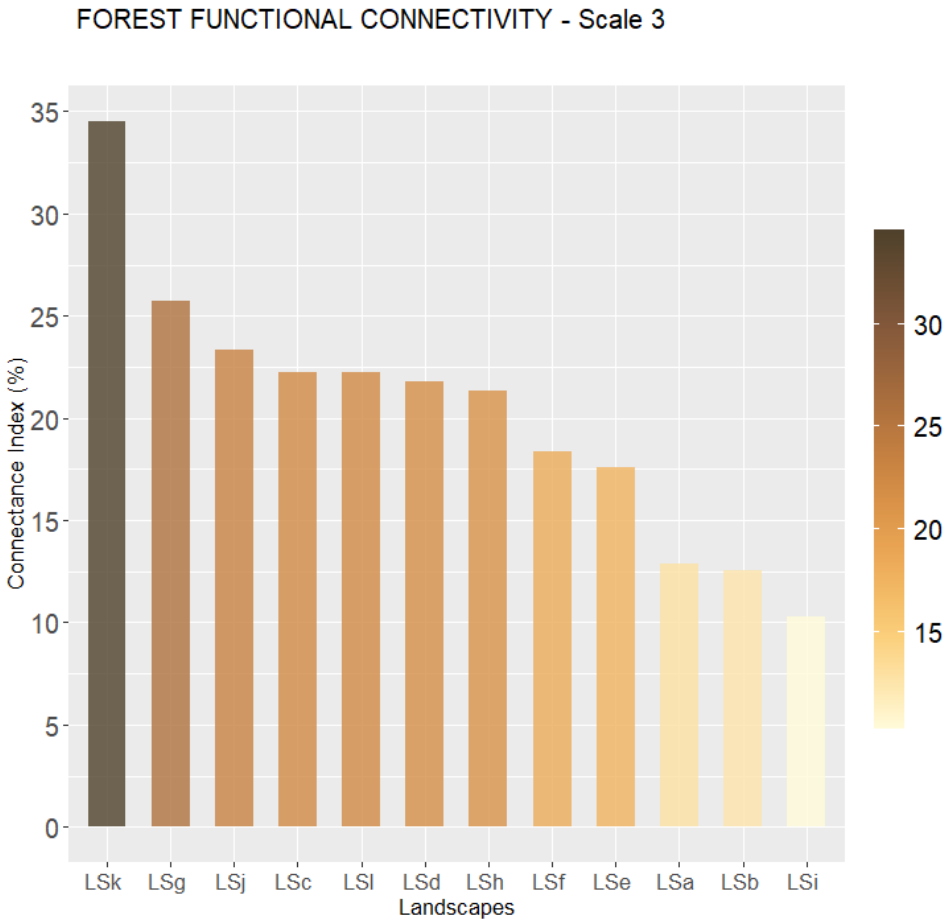

.

Figure 10. Forest functional connectivity in each scale 3's landscape. Values in percentage represent forest patches general proximity having 200 meters as threshold distance.

The Euclidean Nearest-Neighbor metric (Figure 11) is a simple way to assess the isolation between patches of a particular class. Since the Atlantic Forest is a biome mostly composed of forest in its native state, investigation on how forest cover is configured in this biome is an indicator of anthropic pressure. We evaluated isolation at the scale 3 to access a general context of the area we sampled the species.

Initial Forest type fragments are more common in the context of advanced fragmentation, since bigger fragments become rarer, most of the forest cover is made up of smaller patches, we can see that the range of distances goes from 15 meters minimum to 183 maximum distance (Figure 11).

For advanced forest (forest 2) LSh, LSc and LSk showed the shortest distances between forest fragments (between 25 and 72 meters), while in LSe the nearest neighbor forest fragment is met at 584 meters away.

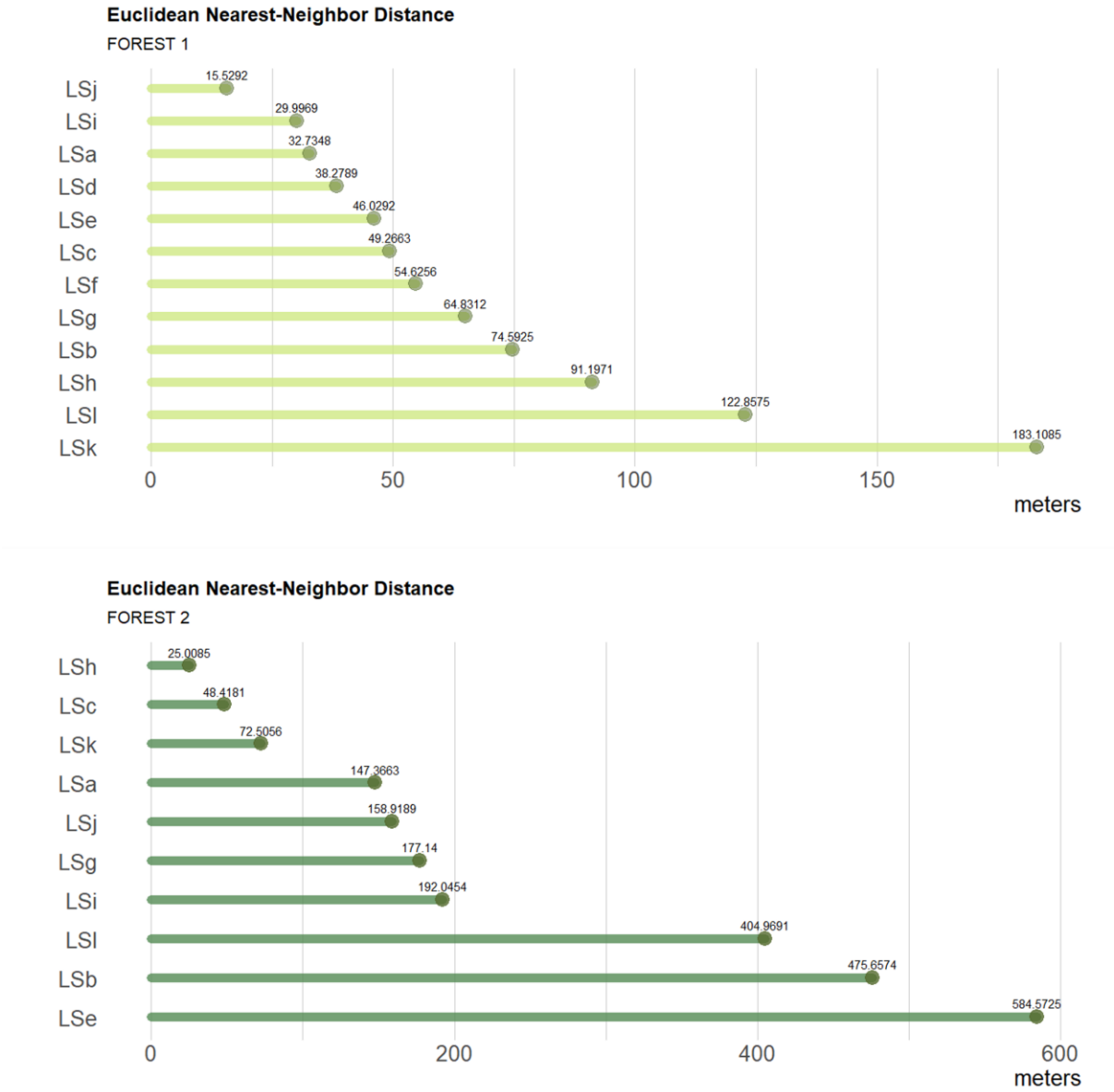

Figure 11. Average distance in meters between fragments of initial and advanced forests in each landscape at the scale 3.

Table 1. Anthropic Transformation Index (ITA) weights. 0 is not anthropized, 5 is maximum anthropization of referred class.

	0	1	2	3	4	5
Water		■	■			
Forest 1				■		
Forest 2				■		
Pasture					■	
Agriculture						■

Silviculture						
Wetlands						
Anthropic Area						

Correlograms

Escala 3

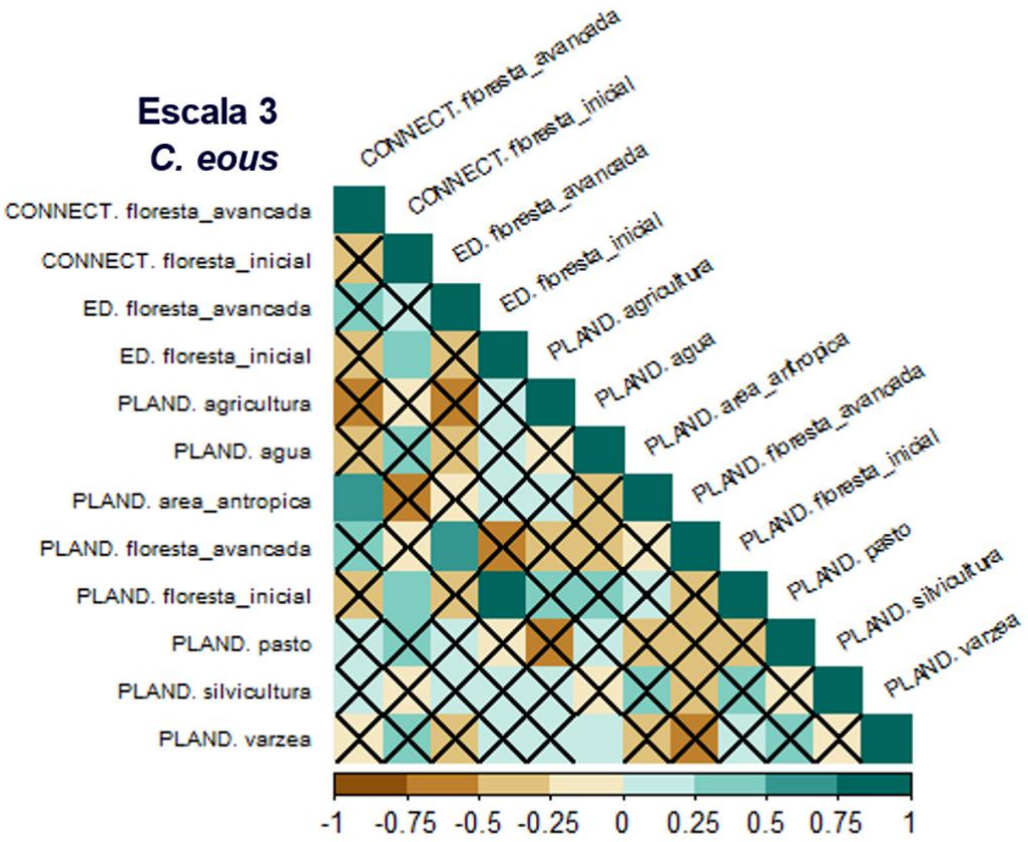

Figure 12. Correlogram for landscape metrics extracted from scale 3 landscapes where *C. eous* was sampled. X's indicate for non-significant correlations forces (p> 0.05). Variables association force above 0.5 was considered correlated.

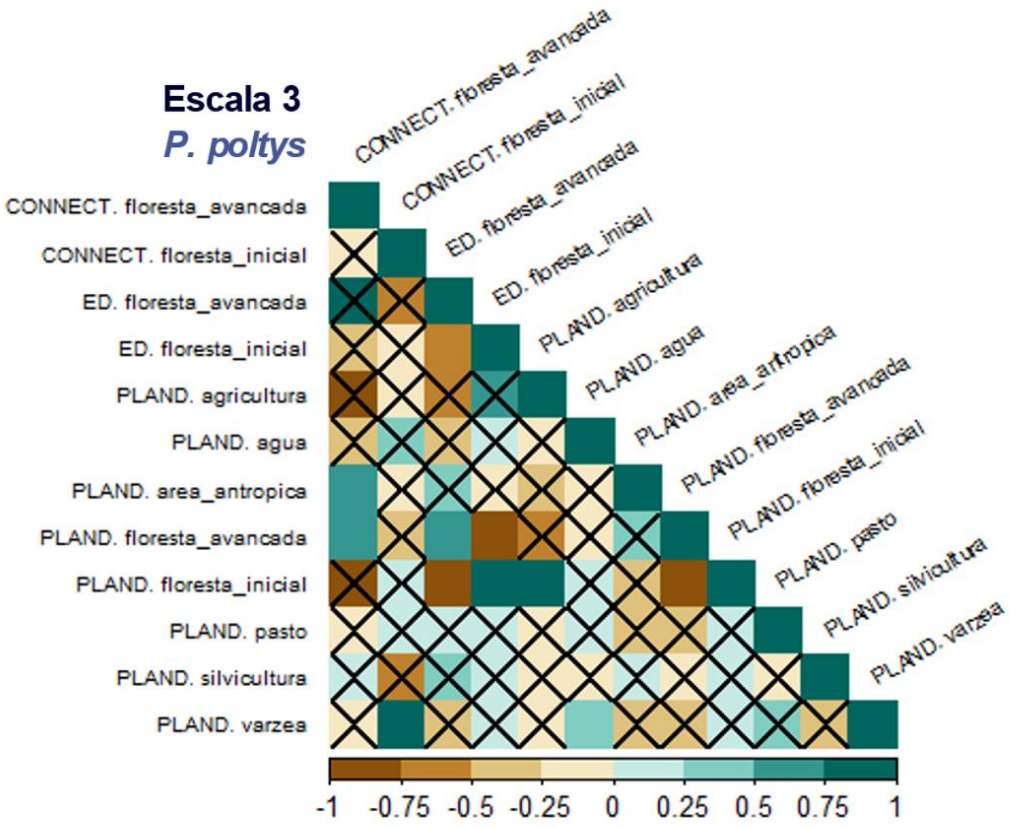

Figure 13. Correlogram for landscape metrics extracted from scale 3 landscapes where *P. poltys* was sampled. X's indicate for non-significant correlations forces (p> 0.05). Variables association force above 0.5 was considered correlated.

Escala 2

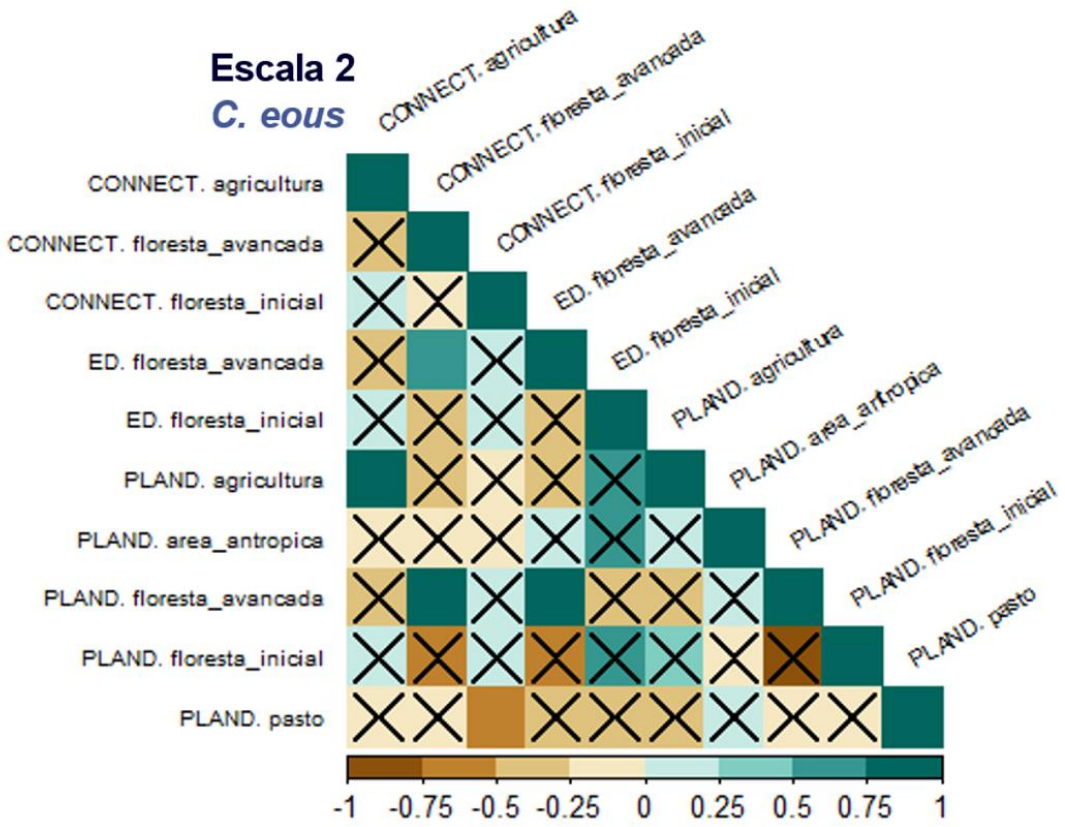

Figure 14. Correlogram for landscape metrics extracted from scale 2 landscapes where *C. eous* was sampled. X's indicate for non-significant correlations forces (p> 0.05). Variables association force above 0.5 was considered correlated.

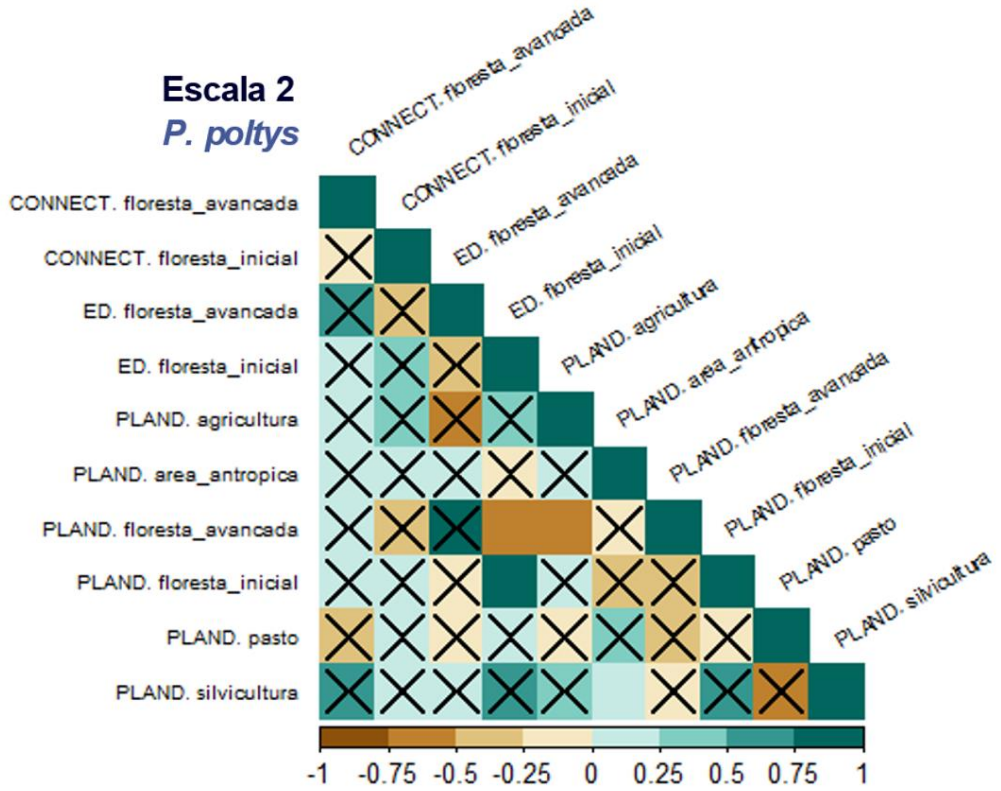

Figure 15. Correlogram for landscape metrics extracted from scale 2 landscapes where *P. poltys* was sampled. X's indicate for non-significant correlations forces (p> 0.05). Variables association force above 0.5 was considered correlated.

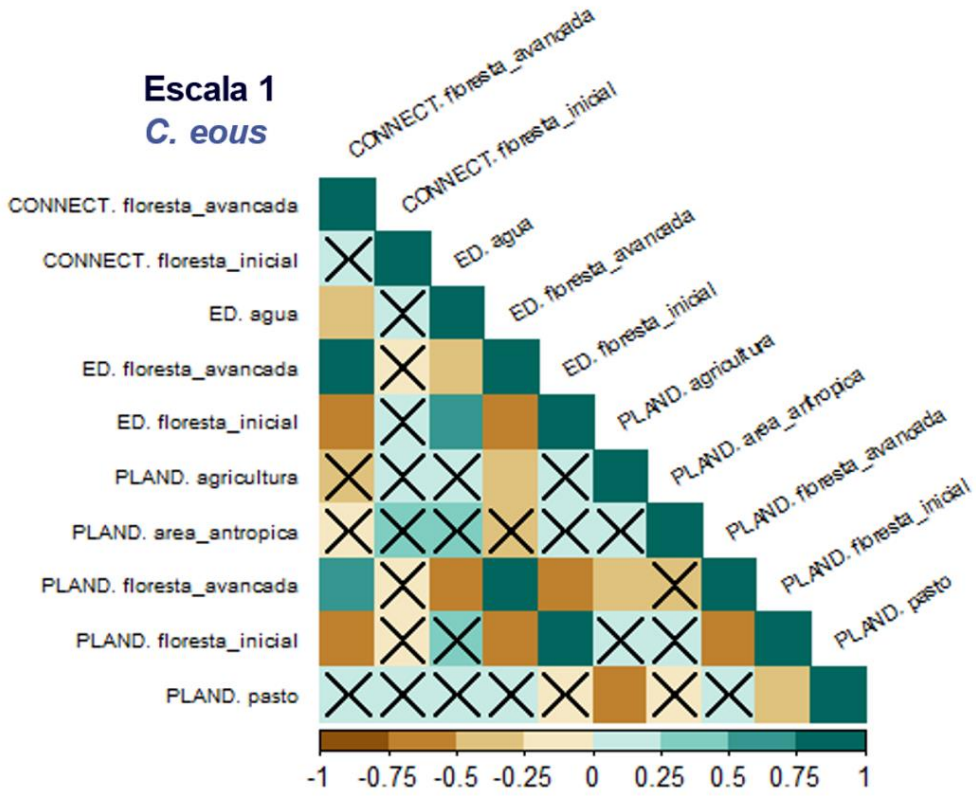

Figure 16. Correlogram for landscape metrics extracted from scale landscapes where *C. eous* was sampled. X's indicate for non-significant correlations forces (p> 0.05). Variables association force above 0.5 was considered correlated.

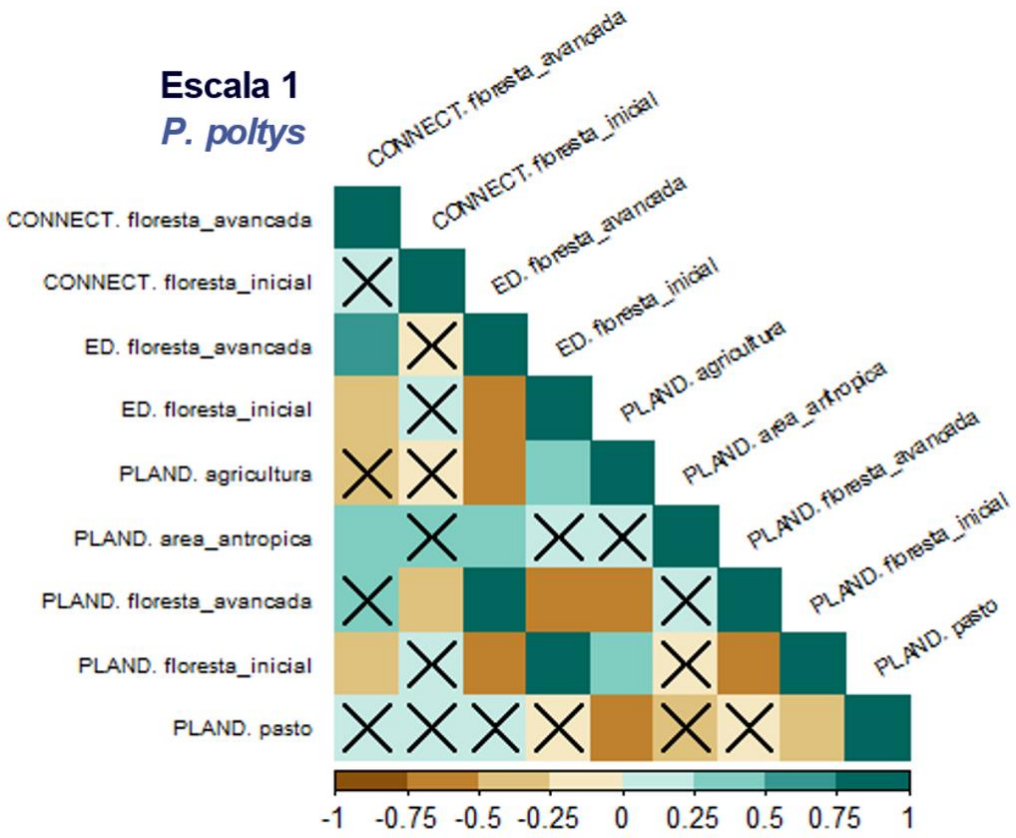

Figure 17. Correlogram for landscape metrics extracted from scale 1 landscapes where *P. poltys* was sampled. X's indicate for non-significant correlations forces (p> 0.05). Variables association force above 0.5 was considered correlated.

Fitted models

Abbreviations for models' variables: PANT: percentage of anthropic area, PFLO1: percentage of initial forest (forest 1), PFLO2: percentage of advanced forest (forest 2), PAGR: percentage of agriculture, PSILV: percentage of silviculture, PPAST: percentage of pasture, P EDFLO1: initial forest edge density, EDFLO2: forest 2 edge density, CONFLO1: initial forest connectance index, CONFLO2: advanced forest connectance index , RAN: random factor (1| SITE).

Example: PANT_EDFLO2_RAN represents:

X FA scores ~ percentage of anthropic area + forest 2 edge density + (1| SITE)

Table 2. *C. eous* -Scale 1 (Procrustes FA scores)

MODELS	LOGLIK	AICC	DLOGLIK	DAICC	DF	WEIGHT
PANT_EDFLO2_RAN	145.98	-280.19	3.24	0.00	5	0.11
EDFLO2_RAN	144.28	-279.41	1.55	0.77	4	0.07
CONFLO1_EDFLO2_RAN	145.39	-279.02	2.66	1.17	5	0.06
PANT_RAN	144.03	-278.92	1.30	1.27	4	0.06
PANT_CONFLO2_RAN	145.29	-278.81	2.56	1.37	5	0.05
NULO	142.73	-278.80	0.00	1.39	3	0.05
CONFLO2_RAN	143.77	-278.40	1.04	1.78	4	0.04
CONFLO1_RAN	143.61	-278.07	0.87	2.11	4	0.04
EDFLO2_PAST_RAN	144.65	-277.54	1.92	2.65	5	0.03
CONFLO1_CONFLO2_RAN	144.55	-277.34	1.82	2.85	5	0.03
PFLO1_RAN	143.19	-277.23	0.46	2.95	4	0.02
PPAST_RAN	143.17	-277.19	0.43	3.00	4	0.02
PANT_PPAST_RAN	144.47	-277.17	1.73	3.02	5	0.02
EDFLO2_CONFLO2_RAN	144.46	-277.15	1.72	3.04	5	0.02
ITA_EDFLO2_RAN	144.41	-277.06	1.68	3.12	5	0.02
PANT_CONGLO1_RAN	144.35	-276.94	1.62	3.24	5	0.02
PAGR_EDFLO2_RAN	144.28	-276.80	1.55	3.39	5	0.02
CONFLO2_PPAST_RAN	144.26	-276.75	1.52	3.44	5	0.02
CONFLO1_PPAST_RAN	144.22	-276.68	1.49	3.51	5	0.02
PANT_PAGR_RAN	144.21	-276.66	1.48	3.52	5	0.02
PANT_PFLO1_RAN	144.19	-276.62	1.46	3.57	5	0.02
PANT_EDFLO1_RAN	144.18	-276.59	1.45	3.59	5	0.02
CONFLO1_PAGR_RAN	144.15	-276.53	1.42	3.65	5	0.02
PAGR_RAN	142.81	-276.49	0.08	3.70	4	0.02
ITA_RAN	142.77	-276.40	0.04	3.78	4	0.02
PFLO2_RAN	142.77	-276.40	0.04	3.79	4	0.02
EDFLO1_RAN	142.73	-276.32	0.00	3.86	4	0.02
ITA_PANT_RAN	144.03	-276.29	1.30	3.89	5	0.02
CONFLO1_PFLO1_RAN	143.91	-276.05	1.18	4.13	5	0.01
PAGR_CONFLO2_RAN	143.84	-275.91	1.10	4.28	5	0.01
CONFLO2_PFLO2_RAN	143.83	-275.90	1.10	4.28	5	0.01
ITA_CONFLO2_RAN	143.80	-275.84	1.07	4.34	5	0.01
CONFLO1_EDFLO1_RAN	143.62	-275.48	0.89	4.70	5	0.01
ITA_CONFLO1_RAN	143.61	-275.46	0.88	4.73	5	0.01
ITA_PAGR_RAN	143.54	-275.31	0.80	4.88	5	0.01
PAGR_PFLO1_RAN	143.38	-274.99	0.64	5.20	5	0.01
PFLO1_PPAST_RAN	143.36	-274.96	0.63	5.23	5	0.01
ITA_PPAST_RAN	143.24	-274.71	0.50	5.48	5	0.01
ITA_PFLO1_RAN	143.20	-274.63	0.46	5.56	5	0.01
EDFLO1_PPAST_RAN	143.17	-274.57	0.43	5.62	5	0.01
ITA_PFLO2_RAN	142.86	-273.95	0.13	6.23	5	0.00
PAGR_EDFLO1_RAN	142.81	-273.86	0.08	6.32	5	0.00
ITA_EDFLO1_RAN	142.77	-273.78	0.04	6.40	5	0.00

Table 3. *C. eous* -Scale 1 (Mahalanobis FA scores)

MODELS	LOGLIK	AICC	DLOGLIK	DAICC	DF	WEIGHT
PANT_EDFLO2_RAN	-28.29	68.34	9.75	0.00	5	0.32
PANT_PAGR_RAN	-28.84	69.45	9.20	1.11	5	0.18
PANT_PPAST_RAN	-29.03	69.82	9.01	1.48	5	0.15
PANT_RAN	-30.50	70.14	7.54	1.80	4	0.13
ITA_PANT_RAN	-30.09	71.94	7.95	3.60	5	0.05
PANT_CONFLO2_RAN	-30.10	71.97	7.94	3.63	5	0.05
PANT_PFLO1_RAN	-30.43	72.63	7.61	4.29	5	0.04
PANT_EDFLO1_RAN	-30.49	72.74	7.55	4.40	5	0.04
PANT_CONGLO1_RAN	-30.50	72.76	7.54	4.42	5	0.04
NULO	-38.04	82.75	0.00	14.41	3	0.00
EDFLO2_RAN	-36.88	82.91	1.16	14.57	4	0.00
CONFLO1_EDFLO2_RAN	-36.09	83.95	1.95	15.61	5	0.00
CONFLO1_RAN	-37.41	83.97	0.63	15.63	4	0.00
EDFLO2_CONFLO2_RAN	-36.16	84.08	1.88	15.74	5	0.00
PPAST_RAN	-37.48	84.11	0.56	15.77	4	0.00
EDFLO1_RAN	-37.49	84.13	0.55	15.79	4	0.00
ITA_PAGR_RAN	-36.33	84.43	1.71	16.09	5	0.00
EDFLO2_PAST_RAN	-36.46	84.68	1.58	16.34	5	0.00
PFLO1_RAN	-37.82	84.78	0.22	16.44	4	0.00
PAGR_RAN	-37.88	84.91	0.16	16.57	4	0.00
CONFLO2_RAN	-37.90	84.95	0.14	16.61	4	0.00
ITA_RAN	-37.98	85.09	0.07	16.75	4	0.00
PFLO2_RAN	-38.03	85.21	0.01	16.87	4	0.00
ITA_EDFLO2_RAN	-36.75	85.26	1.30	16.92	5	0.00
CONFLO1_PPAST_RAN	-36.79	85.35	1.25	17.01	5	0.00
PAGR_EDFLO2_RAN	-36.86	85.49	1.18	17.15	5	0.00
CONFLO1_PAGR_RAN	-36.87	85.50	1.17	17.16	5	0.00
CONFLO1_EDFLO1_RAN	-36.99	85.74	1.05	17.40	5	0.00
EDFLO1_PPAST_RAN	-36.99	85.75	1.05	17.42	5	0.00
CONFLO1_CONFLO2_RAN	-37.16	86.09	0.88	17.75	5	0.00
CONFLO1_PFLO1_RAN	-37.30	86.36	0.74	18.02	5	0.00
CONFLO2_PPAST_RAN	-37.35	86.46	0.69	18.12	5	0.00
ITA_PPAST_RAN	-37.35	86.47	0.69	18.13	5	0.00
ITA_EDFLO1_RAN	-37.39	86.55	0.65	18.21	5	0.00
PAGR_EDFLO1_RAN	-37.40	86.57	0.64	18.23	5	0.00
ITA_CONFLO1_RAN	-37.41	86.59	0.63	18.25	5	0.00
PFLO1_PPAST_RAN	-37.44	86.65	0.60	18.31	5	0.00
PAGR_PFLO1_RAN	-37.51	86.79	0.53	18.45	5	0.00
PAGR_CONFLO2_RAN	-37.78	87.32	0.26	18.98	5	0.00
ITA_CONFLO2_RAN	-37.80	87.36	0.24	19.03	5	0.00

ITA_PFLO1_RAN	-37.82	87.40	0.22	19.06	5	0.00
CONFLO2_PFLO2_RAN	-37.90	87.57	0.14	19.23	5	0.00
ITA_PFLO2_RAN	-37.98	87.72	0.07	19.38	5	0.00

Table 4. *P. poltys* -Scale 1 (Procrustes FA scores)

MODELS	LOGLIK	AICC	DLOGLIK	DAICC	DF	WEIGHT
NULO	164.53	-322.46	0.00	0.00	3	0.10
CONFLO1_RAN	165.06	-321.09	0.53	1.37	4	0.05
PANT_RAN	165.05	-321.08	0.52	1.39	4	0.05
PPAST_RAN	165.04	-321.06	0.51	1.41	4	0.05
PAGR_RAN	164.72	-320.42	0.19	2.05	4	0.04
EDFLO2_RAN	164.67	-320.32	0.14	2.15	4	0.03
PFLO1_RAN	164.63	-320.23	0.10	2.23	4	0.03
ITA_RAN	164.60	-320.17	0.07	2.29	4	0.03
PSIL_RAN	164.56	-320.10	0.03	2.36	4	0.03
CONFLO2_RAN	164.55	-320.07	0.02	2.39	4	0.03
PFLO2_RAN	164.53	-320.04	0.00	2.42	4	0.03
EDFLO1_RAN	164.53	-320.04	0.00	2.43	4	0.03
PANT_CONFLO1_RAN	165.59	-319.60	1.06	2.86	5	0.02
CONFLO1_PPAST_RAN	165.35	-319.12	0.82	3.35	5	0.02
PANT_PPAST_RAN	165.32	-319.05	0.79	3.41	5	0.02
CONFLO1_PAGR_RAN	165.30	-319.02	0.77	3.44	5	0.02
CONFLO1_ITA_RAN	165.25	-318.92	0.72	3.55	5	0.02
CONFLO1_EDFLO2_RAN	165.21	-318.85	0.68	3.61	5	0.02
EDFLO2_PPAST_RAN	165.21	-318.85	0.68	3.61	5	0.02
PANT_PFLO1_RAN	165.19	-318.80	0.66	3.66	5	0.02
PANT_PAGR_RAN	165.18	-318.78	0.65	3.68	5	0.02
CONFLO1_PFLO1_RAN	165.16	-318.74	0.63	3.72	5	0.02
CONFLO1_CONFLO2_RAN	165.10	-318.63	0.57	3.83	5	0.01
PPAST_ITA_RAN	165.10	-318.63	0.57	3.84	5	0.01
CONFLO1_PFLO2_RAN	165.09	-318.61	0.56	3.85	5	0.01
EDFLO1_PPAST_RAN	165.09	-318.60	0.56	3.86	5	0.01
PANT_EDFLO2_RAN	165.08	-318.58	0.55	3.89	5	0.01
PANT_ITA_RAN	165.07	-318.56	0.54	3.90	5	0.01
CONFLO1_EDFLO1_RAN	165.07	-318.56	0.54	3.90	5	0.01
PFLO1_PPAST_RAN	165.05	-318.53	0.52	3.93	5	0.01
CONFLO2_PPAST_RAN	165.05	-318.53	0.52	3.93	5	0.01
PANT_CONFLO2_RAN	165.05	-318.53	0.52	3.94	5	0.01
PANT_EDFLO1_RAN	165.05	-318.52	0.52	3.94	5	0.01
PANT_PFLO2_RAN	165.05	-318.52	0.52	3.94	5	0.01
PPAST_PFLO2_RAN	165.05	-318.52	0.52	3.94	5	0.01
PAGR_PFLO2_RAN	164.94	-318.29	0.41	4.17	5	0.01

EDFLO2_ITA_RAN	164.87	-318.16	0.34	4.30	5	0.01
PAGR_EDFLO1_RAN	164.87	-318.16	0.34	4.30	5	0.01
ITA_PFLO2_RAN	164.86	-318.14	0.33	4.32	5	0.01
PAGR_CONFLO2_RAN	164.76	-317.95	0.23	4.51	5	0.01
PAGE_PFLO1_RAN	164.76	-317.94	0.23	4.52	5	0.01
PAGR_ITA_RAN	164.76	-317.94	0.23	4.52	5	0.01
EDFLO2_CONFLO2_RAN	164.69	-317.81	0.16	4.66	5	0.01
PFLO1_CONFLO2_RAN	164.67	-317.76	0.14	4.70	5	0.01
PFLO1_ITA_RAN	164.67	-317.76	0.14	4.70	5	0.01
EDFLO1_ITA_RAN	164.64	-317.71	0.11	4.75	5	0.01
CONFLO2_ITA_RAN	164.62	-317.66	0.09	4.80	5	0.01
EDFLO1_CONFLO2_RAN	164.55	-317.52	0.02	4.94	5	0.01
CONFLO2_PFLO2_RAN	164.55	-317.52	0.02	4.94	5	0.01

Table 5. *P. poltys* -Scale 1 (Mahalanobis FA scores)

MODELS	LOGLIK	AICC	DLOGLIK	DAICC	DF	WEIGHT
PAGR_EDFLO1_RAN	-53.28	118.14	4.07	0.00	5	0.15
PAGR_PFLO2_RAN	-53.74	119.06	3.60	0.93	5	0.09
EDFLO1_PPAST_RAN	-53.83	119.23	3.52	1.10	5	0.09
PPAST_RAN	-55.54	120.10	1.81	1.96	4	0.06
PAGR_RAN	-55.72	120.46	1.63	2.32	4	0.05
ITA_PFLO2_RAN	-54.63	120.83	2.72	2.69	5	0.04
CONFLO1_PAGR_RAN	-54.71	121.00	2.64	2.86	5	0.04
NULO	-57.31	121.30	0	3.20	3	0.02
PFLO1_PPAST_RAN	-54.89	121.47	2.45	3.23	5	0.03
EDFLO1_ITA_RAN	-54.95	121.49	2.39	3.35	5	0.03
CONFLO1_PPAST_RAN	-55.01	121.60	2.34	3.46	5	0.03
PAGE_PFLO1_RAN	-55.08	121.75	2.26	3.61	5	0.02
EDFLO1_RAN	-56.38	121.79	0.96	3.66	4	0.02
CONFLO1_RAN	-56.41	121.85	0.94	3.71	4	0.02
PPAST_ITA_RAN	-55.21	121.99	2.14	3.85	5	0.02
PAGR_ITA_RAN	-55.34	122.25	2.01	4.12	5	0.02
EDFLO2_PPAST_RAN	-55.42	122.42	1.93	4.28	5	0.02
ITA_RAN	-56.73	122.49	0.62	4.35	4	0.02
CONFLO1_ITA_RAN	-55.46	122.50	1.89	4.36	5	0.02
PPAST_PFLO2_RAN	-55.48	122.54	1.86	4.41	5	0.02
PANT_PPAST_RAN	-55.52	122.62	1.83	4.48	5	0.02
CONFLO2_PPAST_RAN	-55.53	122.64	1.81	4.51	5	0.02
PSIL_RAN	-56.91	122.85	0.43	4.72	4	0.01
PAGR_CONFLO2_RAN	-55.71	123.00	1.64	4.86	5	0.01
PANT_PAGR_RAN	-55.72	123.01	1.63	4.87	5	0.01
CONFLO1_EDFLO1_RAN	-55.74	123.06	1.61	4.92	5	0.01

EDFLO1_CONFLO2_RAN	-55.84	123.26	1.51	5.12	5	0.01
CONFLO2_RAN	-57.25	123.52	0.10	5.38	4	0.01
PFLO2_RAN	-57.25	123.53	0.10	5.39	4	0.01
PFLO1_RAN	-57.31	123.64	0.04	5.51	4	0.01
PANT_RAN	-57.34	123.70	0.01	5.56	4	0.01
EDFLO2_RAN	-57.35	123.72	0.00	5.58	4	0.01
PANT_CONFLO1_RAN	-56.24	124.05	1.11	5.92	5	0.01
PANT_EDFLO1_RAN	-56.36	124.30	0.99	6.16	5	0.01
CONFLO1_CONFLO2_RAN	-56.41	124.39	0.94	6.25	5	0.01
CONFLO1_PFLO2_RAN	-56.41	124.40	0.94	6.26	5	0.01
CONFLO1_PFLO1_RAN	-56.41	124.40	0.94	6.26	5	0.01
CONFLO1_EDFLO2_RAN	-56.41	124.40	0.94	6.26	5	0.01
PFLO1_ITA_RAN	-56.54	124.67	0.80	6.53	5	0.01
EDFLO2_ITA_RAN	-56.64	124.87	0.70	6.73	5	0.01
CONFLO2_ITA_RAN	-56.68	124.93	0.67	6.80	5	0.01
PANT_ITA_RAN	-56.73	125.03	0.62	6.89	5	0.00
CONFLO2_PFLO2_RAN	-57.09	125.75	0.26	7.62	5	0.00
PFLO1_CONFLO2_RAN	-57.13	125.83	0.22	7.70	5	0.00
EDFLO2_CONFLO2_RAN	-57.17	125.92	0.18	7.78	5	0.00
PANT_CONFLO2_RAN	-57.20	125.97	0.15	7.84	5	0.00
PANT_PFLO2_RAN	-57.24	126.05	0.11	7.91	5	0.00
PANT_PFLO1_RAN	-57.30	126.18	0.05	8.04	5	0.00
PANT_EDFLO2_RAN	-57.33	126.24	0.02	8.10	5	0.00

Table 6. *C. eous* -Scale 2 (Procrustes FA scores)

MODELS	LOGLIK	AICC	DLOGLIK	DAICC	DF	WEIGHT
EDFLO2	45.18	-80.37	3.81	0.00	3	0.49
PFLO1_EDFLO2	46.54	-77.08	5.16	3.29	4	0.09
NULO	41.38	-77.04	0.00	3.33	2	0.09
EDFLO1_EDFLO2	46.03	-76.05	4.65	4.32	4	0.06
CONFLO1_EDFLO2	45.45	-74.90	4.07	5.47	4	0.03
PANT_EDFLO2	45.35	-74.71	3.97	5.66	4	0.03
EDFLO2_PPAST	45.23	-74.46	3.85	5.91	4	0.03
PAGR_EDFLO2	45.21	-74.41	3.83	5.96	4	0.02
ITA_EDFLO2	45.19	-74.38	3.81	5.99	4	0.02
PFLO2	41.78	-73.57	0.41	6.80	3	0.02
PAGR	41.76	-73.51	0.38	6.86	3	0.02
CONFLO2	41.64	-73.28	0.26	7.09	3	0.01
PANT	41.54	-73.09	0.17	7.28	3	0.01
PPAST	41.45	-72.91	0.08	7.46	3	0.01

PFLO1	41.42	-72.85	0.04	7.52	3	0.01
EDFLO1	41.42	-72.83	0.04	7.54	3	0.01
CONFLO1	41.40	-72.80	0.02	7.57	3	0.01
ITA	41.38	-72.76	0.00	7.61	3	0.01
ITA_PAGR	42.47	-68.94	1.09	11.43	4	0.00
PAGR_PPAST	42.13	-68.27	0.76	12.10	4	0.00
PANT_CONFLO2	42.05	-68.10	0.67	12.27	4	0.00
PANT_EDFLO1	41.88	-67.77	0.51	12.60	4	0.00
PAGR_CONFLO2	41.87	-67.75	0.50	12.62	4	0.00
PFLO1_PFLO2	41.84	-67.67	0.46	12.70	4	0.00
EDFLO1_PFLO2	41.82	-67.64	0.44	12.73	4	0.00
ITA_PFLO2	41.81	-67.63	0.44	12.74	4	0.00
CONFLO1_PAGR	41.77	-67.54	0.39	12.83	4	0.00
PAGR_EDFLO1	41.76	-67.53	0.39	12.84	4	0.00
PAGR_PFLO1	41.76	-67.51	0.38	12.86	4	0.00
CONFLO1_CONFLO2	41.68	-67.37	0.31	13.00	4	0.00
CONFLO2_PPAST	41.66	-67.33	0.29	13.04	4	0.00
ITA_CONFLO2	41.65	-67.29	0.27	13.08	4	0.00
EDFLO1_CONFLO2	41.64	-67.29	0.27	13.08	4	0.00
PFLO1_CONFLO2	41.64	-67.29	0.27	13.08	4	0.00
PANT_PPAST	41.63	-67.25	0.25	13.12	4	0.00
ITA_PANT	41.61	-67.22	0.23	13.15	4	0.00
PFLO1_PPAST	41.57	-67.14	0.19	13.23	4	0.00
PANT_PAGR	41.57	-67.13	0.19	13.24	4	0.00
PANT_CONFLO1	41.57	-67.13	0.19	13.24	4	0.00
EDFLO1_PPAST	41.50	-66.99	0.12	13.38	4	0.00
CONFLO1_PFLO1	41.48	-66.96	0.10	13.41	4	0.00
ITA_PPAST	41.45	-66.91	0.08	13.46	4	0.00
PFLO1_EDFLO1	41.43	-66.87	0.06	13.50	4	0.00
CONFLO1_EDFLO1	41.43	-66.87	0.06	13.50	4	0.00
ITA_EDFLO1	41.43	-66.86	0.05	13.51	4	0.00
ITA_PFLO1	41.42	-66.85	0.04	13.52	4	0.00
ITA_CONFLO1	41.40	-66.81	0.02	13.56	4	0.00

Table 7. *C. eous* -Scale 2 (Mahalanobis FA scores)

MODELS	LOGLIK	AICC	DLOGLIK	DAICC	DF	WEIGHT
NULO	-9.20	24.12	0.00	0.00	2	0.28
PFLO1_EDFLO2	-4.82	25.64	4.38	1.52	4	0.13
PFLO1	-7.87	25.74	1.34	1.61	3	0.12
PPAST	-8.81	27.63	0.39	3.50	3	0.05
PFLO2	-8.82	27.65	0.38	3.52	3	0.05
EDFLO2	-8.88	27.76	0.32	3.64	3	0.04

CONFLO2	-8.99	27.97	0.22	3.85	3	0.04
CONFLO1	-9.09	28.18	0.11	4.06	3	0.04
PANT	-9.11	28.22	0.09	4.10	3	0.04
PAGR	-9.12	28.24	0.08	4.12	3	0.04
ITA	-9.18	28.36	0.02	4.24	3	0.03
EDFLO1	-9.20	28.41	0.00	4.28	3	0.03
PFLO1_EDFLO1	-7.49	30.98	1.72	6.85	4	0.01
PFLO1_PPAST	-7.79	31.58	1.42	7.45	4	0.01
ITA_PFLO1	-7.83	31.66	1.38	7.53	4	0.01
PFLO1_CONFLO2	-7.85	31.71	1.35	7.58	4	0.01
PANT_PAGR	-7.86	31.71	1.35	7.59	4	0.01
PFLO1_PFLO2	-7.86	31.73	1.34	7.60	4	0.01
CONFLO1_PFLO1	-7.86	31.73	1.34	7.60	4	0.01
PAGR_PFLO1	-7.87	31.73	1.34	7.61	4	0.01
CONFLO2_PPAST	-8.34	32.68	0.86	8.56	4	0.00
EDFLO2_PPAST	-8.56	33.11	0.65	8.99	4	0.00
PAGR_EDFLO2	-8.63	33.26	0.57	9.14	4	0.00
EDFLO1_PFLO2	-8.69	33.39	0.51	9.26	4	0.00
PANT_PPAST	-8.72	33.43	0.49	9.31	4	0.00
CONFLO1_EDFLO2	-8.72	33.44	0.48	9.32	4	0.00
PANT_CONFLO2	-8.75	33.50	0.45	9.38	4	0.00
PANT_EDFLO2	-8.75	33.50	0.45	9.38	4	0.00
EDFLO1_EDFLO2	-8.76	33.53	0.44	9.40	4	0.00
ITA_PPAST	-8.80	33.60	0.40	9.48	4	0.00
EDFLO1_PPAST	-8.81	33.62	0.39	9.50	4	0.00
PAGR_PPAST	-8.81	33.63	0.39	9.50	4	0.00
ITA_PFLO2	-8.82	33.65	0.38	9.52	4	0.00
ITA_EDFLO2	-8.86	33.72	0.34	9.60	4	0.00
CONFLO1_CONFLO2	-8.89	33.78	0.32	9.65	4	0.00
EDFLO1_CONFLO2	-8.94	33.87	0.27	9.75	4	0.00
PAGR_CONFLO2	-8.97	33.93	0.24	9.81	4	0.00
ITA_PANT	-8.97	33.94	0.23	9.82	4	0.00
ITA_CONFLO2	-8.98	33.96	0.23	9.83	4	0.00
ITA_CONFLO1	-9.00	33.99	0.21	9.87	4	0.00
PANT_CONFLO1	-9.00	34.00	0.20	9.88	4	0.00
CONFLO1_PAGR	-9.00	34.01	0.20	9.88	4	0.00
PANT_EDFLO1	-9.03	34.05	0.18	9.93	4	0.00

CONFLO1_EDFLO1	-9.09	34.17	0.12	10.05	4	0.00
ITA_PAGR	-9.10	34.21	0.10	10.09	4	0.00
PAGR_EDFLO1	-9.11	34.22	0.09	10.10	4	0.00
ITA_EDFLO1	-9.18	34.36	0.02	10.24	4	0.00

Table 8. *P. poltys* -Scale 2 (Procrustes FA scores)

MODELS	LOGLIK	AICC	DLOGLIK	DAICC	DF	WEIGHT
EDFLO1_ITA	56.29	-96.58	15.01	0.00	4	0.98
PAGR_EDFLO1	52.45	-88.90	11.17	7.68	4	0.02
EDFLO1	43.87	-77.74	2.59	18.84	3	0.00
NULO	41.28	-76.84	0.00	19.73	2	0.00
ITA_PFLO2	46.10	-76.19	4.82	20.38	4	0.00
PAGR_	42.34	-74.68	1.06	21.90	3	0.00
ITA	42.23	-74.47	0.96	22.11	3	0.00
CONFLO1_EDFLO1	44.71	-73.41	3.43	23.16	4	0.00
PFLO1	41.66	-73.31	0.38	23.26	3	0.00
CONFLO2	41.64	-73.29	0.37	23.29	3	0.00
EDFLO1_EDFLO2	44.56	-73.13	3.29	23.45	4	0.00
PANT	41.45	-72.90	0.17	23.68	3	0.00
PFLO2	41.39	-72.79	0.11	23.79	3	0.00
CONFLO1	41.36	-72.73	0.08	23.85	3	0.00
PPAST	41.33	-72.67	0.06	23.91	3	0.00
EDFLO2	41.30	-72.59	0.02	23.98	3	0.00
PSILV	41.28	-72.56	0.00	24.02	3	0.00
EDFLO1_CONFLO2	44.17	-72.33	2.89	24.24	4	0.00
PAGE_PFLO1	44.11	-72.21	2.83	24.36	4	0.00
PANT_EDFLO1	43.99	-71.99	2.72	24.59	4	0.00
EDFLO1_PPAST	43.92	-71.83	2.64	24.74	4	0.00
EDFLO1_PSILV	43.89	-71.78	2.61	24.79	4	0.00
PFLO1_ITA	43.42	-70.85	2.15	25.73	4	0.00
PAGR_EDFLO2	43.31	-70.61	2.03	25.96	4	0.00
EDFLO2_ITA	42.69	-69.37	1.41	27.20	4	0.00
PAGR_CONFLO2	42.49	-68.97	1.21	27.60	4	0.00
PAGR_PSILV	42.41	-68.81	1.13	27.76	4	0.00
PANT_PAGR	42.40	-68.81	1.13	27.77	4	0.00
PPAST_ITA	42.39	-68.78	1.11	27.80	4	0.00
PAGR_ITA	42.35	-68.71	1.08	27.87	4	0.00
CONFLO1_PAGR	42.35	-68.70	1.07	27.88	4	0.00
PAGR_PPAST	42.34	-68.68	1.06	27.90	4	0.00
PSILV_ITA	42.27	-68.55	1.00	28.03	4	0.00
CONFLO1_ITA	42.27	-68.55	1.00	28.03	4	0.00
PANT_ITA	42.26	-68.52	0.98	28.06	4	0.00
PFLO1_PFLO2	42.13	-68.26	0.85	28.31	4	0.00

PFLO1_CONFLO2	42.08	-68.15	0.80	28.43	4	0.00
PFLO1_PPAST	41.98	-67.96	0.70	28.62	4	0.00
PSILV_CONFLO2	41.86	-67.72	0.58	28.85	4	0.00
PANT_PSILV	41.84	-67.67	0.56	28.90	4	0.00
CONFLO1_CONFLO2	41.82	-67.65	0.55	28.93	4	0.00
PANT_PFLO1	41.80	-67.59	0.52	28.98	4	0.00
CONFLO2_ITA	41.80	-67.59	0.52	28.98	4	0.00
CONFLO1_PFLO1	41.78	-67.56	0.50	29.01	4	0.00
PANT_CONFLO2	41.73	-67.45	0.45	29.12	4	0.00
PFLO1_PSILV	41.68	-67.36	0.40	29.22	4	0.00
EDFLO2_CONFLO2	41.67	-67.35	0.40	29.23	4	0.00
PFLO1_EDFLO2	41.66	-67.31	0.38	29.26	4	0.00
CONFLO2_PPAST	41.65	-67.29	0.37	29.28	4	0.00
PANT_CONFLO1	41.57	-67.14	0.29	29.44	4	0.00
PPAST_PFLO2	41.52	-67.05	0.24	29.53	4	0.00
PANT_PFLO2	41.52	-67.04	0.24	29.53	4	0.00
EDFLO2_PFLO2	41.51	-67.03	0.24	29.55	4	0.00
PANT_PPAST	41.49	-66.99	0.22	29.59	4	0.00
CONFLO1_PPAST	41.46	-66.92	0.18	29.66	4	0.00
PANT_EDFLO2	41.45	-66.91	0.18	29.67	4	0.00
CONFLO1_EDFLO2	41.41	-66.83	0.14	29.75	4	0.00
CONFLO1_PFLO2	41.41	-66.82	0.13	29.76	4	0.00
PSILV_PFLO2	41.39	-66.79	0.12	29.79	4	0.00
CONFLO1_PSILV	41.36	-66.73	0.09	29.85	4	0.00
PSILV_PPAST	41.36	-66.73	0.08	29.85	4	0.00
EDFLO2_PPAST	41.36	-66.71	0.08	29.86	4	0.00
PSILV_EDFLO2	41.30	-66.60	0.02	29.98	4	0.00

Table 9*. P. poltys* -Scale 2 (Mahalanobis FA scores)

MODELS	LOGLIK	AICC	DLOGLIK	DAICC	DF	WEIGHT
PAGR_EDFLO1	3.35	9.31	10.29	0.00	4	0.94
EDFLO1	-4.02	18.04	2.92	8.73	3	0.01
ITA_PFLO2	-1.13	18.26	5.81	8.95	4	0.01
EDFLO1_ITA	-1.19	18.38	5.75	9.07	4	0.01
NULO	-6.94	19.60	0.00	10.29	2	0.01
EDFLO1_EDFLO2	-2.68	21.36	4.26	12.06	4	0.00
EDFLO1_PPAST	-2.70	21.41	4.24	12.10	4	0.00
PPAST	-5.97	21.94	0.97	12.63	3	0.00
PFLO1	-6.17	22.33	0.77	13.03	3	0.00
PAGR_	-6.23	22.47	0.71	13.16	3	0.00
CONFLO2	-6.49	22.98	0.45	13.67	3	0.00
PFLO1_PPAST	-3.52	23.03	3.42	13.73	4	0.00

EDFLO1_CONFLO2	-3.54	23.08	3.40	13.77	4	0.00
ITA	-6.80	23.61	0.14	14.30	3	0.00
PAGE_PFLO1	-3.81	23.61	3.13	14.31	4	0.00
PFLO2	-6.82	23.65	0.12	14.34	3	0.00
CONFLO1	-6.88	23.76	0.06	14.46	3	0.00
PANT	-6.91	23.81	0.03	14.51	3	0.00
EDFLO1_PSILV	-3.93	23.87	3.01	14.56	4	0.00
PSILV	-6.94	23.87	0.00	14.57	3	0.00
EDFLO2	-6.94	23.88	0.00	14.57	3	0.00
CONFLO1_EDFLO1	-3.96	23.92	2.98	14.61	4	0.00
PANT_EDFLO1	-4.01	24.01	2.93	14.70	4	0.00
PAGR_ITA	-5.30	26.59	1.64	17.29	4	0.00
PAGR_PPAST	-5.54	27.07	1.40	17.77	4	0.00
PFLO1_CONFLO2	-5.58	27.16	1.36	17.86	4	0.00
PFLO1_ITA	-5.63	27.26	1.31	17.95	4	0.00
PPAST_ITA	-5.67	27.33	1.28	18.02	4	0.00
PSILV_PPAST	-5.67	27.34	1.27	18.03	4	0.00
CONFLO1_PAGR	-5.74	27.47	1.20	18.17	4	0.00
PAGR_EDFLO2	-5.90	27.79	1.04	18.49	4	0.00
CONFLO2_PPAST	-5.91	27.81	1.04	18.50	4	0.00
PANT_PPAST	-5.96	27.92	0.98	18.62	4	0.00
EDFLO2_PPAST	-5.97	27.93	0.97	18.63	4	0.00
PPAST_PFLO2	-5.97	27.94	0.97	18.63	4	0.00
CONFLO1_PPAST	-5.97	27.94	0.97	18.63	4	0.00
PAGR_CONFLO2	-6.01	28.03	0.93	18.72	4	0.00
PFLO1_PSILV	-6.07	28.14	0.87	18.83	4	0.00
PFLO1_EDFLO2	-6.11	28.22	0.83	18.92	4	0.00
CONFLO1_PFLO1	-6.14	28.28	0.80	18.97	4	0.00
PANT_PFLO1	-6.14	28.28	0.80	18.98	4	0.00
PFLO1_PFLO2	-6.16	28.33	0.78	19.02	4	0.00
PAGR_PSILV	-6.21	28.43	0.73	19.12	4	0.00
PANT_PAGR	-6.23	28.46	0.71	19.15	4	0.00
PSILV_CONFLO2	-6.31	28.62	0.63	19.31	4	0.00
EDFLO2_CONFLO2	-6.36	28.71	0.58	19.41	4	0.00
CONFLO2_ITA	-6.39	28.77	0.55	19.47	4	0.00
CONFLO1_CONFLO2	-6.46	28.93	0.48	19.62	4	0.00
PANT_CONFLO2	-6.49	28.98	0.45	19.67	4	0.00
CONFLO1_ITA	-6.55	29.10	0.39	19.79	4	0.00
PANT_PFLO2	-6.76	29.53	0.18	20.22	4	0.00
EDFLO2_ITA	-6.77	29.54	0.17	20.23	4	0.00
EDFLO2_PFLO2	-6.79	29.57	0.15	20.27	4	0.00
PANT_ITA	-6.80	29.59	0.15	20.28	4	0.00
PSILV_ITA	-6.80	29.61	0.14	20.30	4	0.00
PSILV_PFLO2	-6.82	29.63	0.12	20.33	4	0.00
CONFLO1_PFLO2	-6.82	29.64	0.12	20.33	4	0.00

PANT_CONFLO1	-6.86	29.71	0.08	20.41	4	0.00
PANT_PSILV	-6.88	29.76	0.06	20.45	4	0.00
CONFLO1_EDFLO2	-6.88	29.76	0.06	20.45	4	0.00
CONFLO1_PSILV	-6.88	29.76	0.06	20.45	4	0.00
PANT_EDFLO2	-6.90	29.81	0.04	20.50	4	0.00
PSILV_EDFLO2	-6.94	29.87	0.00	20.57	4	0.00

Table 10. *C. eous* -Scale 3 (Procrustes FA scores)

MODELS	LOGLIK	AICC	DLOGLIK	DAICC	DF	WEIGHT
NULO	41.38	-77.04	0.00	0.00	2	0.24
PAGR	43.07	-76.14	1.69	0.90	3	0.15
ITA	42.43	-74.86	1.05	2.18	3	0.08
PPAST	42.01	-74.01	0.63	3.03	3	0.05
EDFLO1	41.65	-73.31	0.28	3.73	3	0.04
CONFLO1	41.62	-73.23	0.24	3.81	3	0.04
PFLO2	41.59	-73.18	0.21	3.86	3	0.04
EDFLO2	41.46	-72.92	0.08	4.12	3	0.03
CONFLO2	41.44	-72.89	0.07	4.15	3	0.03
PANT	41.42	-72.85	0.04	4.20	3	0.03
PAGR_EDFLO2	44.41	-72.82	3.03	4.22	4	0.03
PFLO1	41.40	-72.80	0.02	4.24	3	0.03
CONFLO1_EDFLO1	43.93	-71.86	2.55	5.18	4	0.02
PAGR_PSILV	43.52	-71.04	2.14	6.00	4	0.01
ITA_EDFLO2	43.37	-70.74	1.99	6.30	4	0.01
PAGR_CONFLO2	43.31	-70.63	1.94	6.41	4	0.01
CONFLO1_PAGR	43.28	-70.57	1.91	6.48	4	0.01
PAGR_EDFLO1	43.23	-70.45	1.85	6.59	4	0.01
PAGR_PFLO1	43.10	-70.20	1.72	6.84	4	0.01
PAGR_PPAST	43.09	-70.18	1.71	6.86	4	0.01
ITA_PAGR	43.08	-70.16	1.70	6.88	4	0.01
PANT_PAGR	43.08	-70.15	1.70	6.89	4	0.01
CONFLO1_PFLO1	42.85	-69.70	1.47	7.34	4	0.01
PSILV_ITA	42.83	-69.67	1.46	7.37	4	0.01
ITA_PPAST	42.82	-69.64	1.44	7.40	4	0.01
ITA_EDFLO1	42.73	-69.46	1.35	7.58	4	0.01
ITA_CONFLO1	42.49	-68.98	1.11	8.06	4	0.00
ITA_PANT	42.48	-68.96	1.10	8.08	4	0.00
PSILV_PPAST	42.47	-68.95	1.10	8.09	4	0.00
ITA_PFLO1	42.47	-68.94	1.09	8.11	4	0.00
ITA_CONFLO2	42.44	-68.87	1.06	8.17	4	0.00
ITA_PFLO2	42.43	-68.86	1.05	8.18	4	0.00
EDFLO1_PPAST	42.37	-68.75	1.00	8.29	4	0.00
CONFLO1_PPAST	42.23	-68.46	0.85	8.58	4	0.00
PANT_PPAST	42.20	-68.41	0.83	8.63	4	0.00
EDFLO2_PPAST	42.18	-68.36	0.80	8.68	4	0.00

CONFLO2_PPAST	42.16	-68.33	0.79	8.71	4	0.00
EDFLO1_PSILV	42.13	-68.26	0.75	8.79	4	0.00
PSILV_EDFLO2	42.12	-68.24	0.74	8.80	4	0.00
CONFLO1_PSILV	42.09	-68.17	0.71	8.87	4	0.00
PFLO1_PPAST	42.01	-68.02	0.63	9.02	4	0.00
PSILV_PFLO2	41.98	-67.96	0.60	9.08	4	0.00
PANT_PSILV	41.96	-67.92	0.58	9.12	4	0.00
PFLO1_PSILV	41.91	-67.83	0.54	9.21	4	0.00
PANT_CONFLO1	41.87	-67.74	0.49	9.30	4	0.00
CONFLO1_CONFLO2	41.85	-67.70	0.47	9.34	4	0.00
EDFLO1_PFLO2	41.69	-67.37	0.31	9.67	4	0.00
EDFLO1_CONFLO2	41.66	-67.32	0.28	9.72	4	0.00
PANT_EDFLO1	41.66	-67.32	0.28	9.73	4	0.00
CONFLO1_EDFLO2	41.64	-67.29	0.27	9.75	4	0.00
EDFLO2_CONFLO2	41.61	-67.22	0.23	9.82	4	0.00
CONFLO2_PFLO2	41.59	-67.19	0.22	9.85	4	0.00
PFLO1_PFLO2	41.59	-67.18	0.21	9.86	4	0.00
PFLO1_EDFLO2	41.56	-67.12	0.18	9.92	4	0.00
PANT_EDFLO2	41.50	-67.01	0.13	10.03	4	0.00
PFLO1_CONFLO2	41.45	-66.89	0.07	10.15	4	0.00
PANT_PFLO1	41.43	-66.86	0.05	10.18	4	0.00

Table 11. *C. eous* -Scale 3 (Mahalanobis FA scores)

MODELS	LOGLIK	AICC	DLOGLIK	DAICC	DF	WEIGHT
PAGR	-5.40	20.81	3.80	0.00	3	0.28
ITA	-5.71	21.42	3.49	0.61	3	0.20
PAGR_CONFLO2	-4.00	24.00	5.21	3.19	4	0.06
NULO	-9.20	24.12	0.00	3.31	2	0.05
ITA_PPAST	-4.33	24.66	4.87	3.85	4	0.04
PPAST	-7.47	24.95	1.73	4.14	3	0.03
PANT_PAGR	-4.79	25.58	4.42	4.77	4	0.03
ITA_PFLO1	-4.80	25.59	4.41	4.78	4	0.03
ITA_CONFLO1	-5.06	26.12	4.14	5.31	4	0.02
ITA_PAGR	-5.11	26.23	4.09	5.42	4	0.02
PAGR_PSILV	-5.16	26.31	4.05	5.50	4	0.02
PAGR_PPAST	-5.21	26.42	4.00	5.61	4	0.02
ITA_EDFLO1	-5.24	26.48	3.97	5.67	4	0.02
PAGR_EDFLO1	-5.25	26.50	3.95	5.69	4	0.02
PAGR_PFLO1	-5.27	26.53	3.94	5.72	4	0.02
CONFLO1_PAGR	-5.29	26.58	3.92	5.77	4	0.02
PAGR_EDFLO2	-5.33	26.66	3.87	5.85	4	0.01
ITA_CONFLO2	-5.46	26.93	3.74	6.12	4	0.01
PSILV_ITA	-5.53	27.06	3.67	6.25	4	0.01
ITA_EDFLO2	-5.64	27.28	3.57	6.47	4	0.01

ITA_PANT	-5.65	27.29	3.56	6.48	4	0.01
PFLO2	-8.71	27.42	0.50	6.61	3	0.01
ITA_PFLO2	-5.71	27.42	3.49	6.61	4	0.01
PFLO1	-8.78	27.57	0.42	6.76	3	0.01
EDFLO1	-8.88	27.76	0.32	6.96	3	0.01
EDFLO2	-8.96	27.92	0.25	7.11	3	0.01
CONFLO2	-9.17	28.34	0.03	7.53	3	0.01
PANT	-9.19	28.37	0.02	7.56	3	0.01
CONFLO1	-9.20	28.41	0.00	7.60	3	0.01
EDFLO1_PPAST	-6.96	29.91	2.25	9.11	4	0.00
EDFLO2_PPAST	-7.26	30.52	1.94	9.71	4	0.00
PSILV_PPAST	-7.28	30.57	1.92	9.76	4	0.00
CONFLO2_PPAST	-7.32	30.65	1.88	9.84	4	0.00
PFLO1_PPAST	-7.34	30.68	1.86	9.87	4	0.00
PANT_PPAST	-7.44	30.89	1.76	10.08	4	0.00
CONFLO1_PPAST	-7.45	30.89	1.76	10.08	4	0.00
CONFLO1_PFLO1	-7.88	31.76	1.32	10.95	4	0.00
PFLO1_PFLO2	-8.53	33.05	0.68	12.24	4	0.00
CONFLO1_EDFLO1	-8.56	33.12	0.64	12.31	4	0.00
PSILV_PFLO2	-8.58	33.16	0.62	12.35	4	0.00
PFLO1_PSILV	-8.59	33.18	0.62	12.37	4	0.00
PANT_PFLO1	-8.62	33.24	0.58	12.43	4	0.00
EDFLO1_PSILV	-8.65	33.30	0.56	12.49	4	0.00
EDFLO1_PFLO2	-8.68	33.35	0.53	12.54	4	0.00
CONFLO2_PFLO2	-8.69	33.38	0.51	12.57	4	0.00
PFLO1_EDFLO2	-8.73	33.46	0.47	12.65	4	0.00
PSILV_EDFLO2	-8.74	33.48	0.47	12.67	4	0.00
PANT_EDFLO1	-8.76	33.53	0.44	12.72	4	0.00
PFLO1_CONFLO2	-8.78	33.56	0.43	12.75	4	0.00
EDFLO1_CONFLO2	-8.88	33.76	0.32	12.95	4	0.00
CONFLO1_PSILV	-8.91	33.83	0.29	13.02	4	0.00
PANT_PSILV	-8.92	33.84	0.29	13.03	4	0.00
PANT_EDFLO2	-8.94	33.88	0.27	13.07	4	0.00
CONFLO1_EDFLO2	-8.94	33.88	0.26	13.07	4	0.00
EDFLO2_CONFLO2	-8.96	33.92	0.25	13.11	4	0.00
CONFLO1_CONFLO2	-9.17	34.34	0.04	13.53	4	0.00
PANT_CONFLO1	-9.17	34.34	0.03	13.53	4	0.00

Table 12. *P. poltys* -Scale 3 (Procrustes FA scores)

MODELS	LOGLIK	AICC	DLOGLIK	DAICC	DF	WEIGHT
ITA_PFLO2	47.58	-79.16	6.30	0.00	4	0.30
NULO	41.28	-76.84	0.00	2.32	2	0.09
EDFLO1_ITA	45.98	-75.95	4.70	3.21	4	0.06
CONFLO1	42.97	-75.94	1.69	3.22	3	0.06

PFLO2	42.77	-75.54	1.49	3.62	3	0.05
EDFLO1	42.70	-75.40	1.42	3.76	3	0.05
CONFLO2	42.48	-74.96	1.20	4.20	3	0.04
EDFLO2	42.47	-74.94	1.19	4.22	3	0.04
PFLO1_ITA	45.42	-74.83	4.14	4.33	4	0.03
PFLO1	42.08	-74.17	0.81	4.99	3	0.02
CONFLO1_PFLO2	44.99	-73.97	3.71	5.19	4	0.02
CONFLO1_EDFLO1	44.92	-73.84	3.64	5.32	4	0.02
PANT_CONFLO1	44.80	-73.60	3.52	5.56	4	0.02
ITA	41.75	-73.49	0.47	5.67	3	0.02
EDFLO2_ITA	44.63	-73.26	3.35	5.90	4	0.02
PPAST	41.50	-73.01	0.22	6.16	3	0.01
CONFLO1_CONFLO2	44.34	-72.69	3.06	6.48	4	0.01
PANT	41.34	-72.67	0.06	6.49	3	0.01
PSILV	41.33	-72.65	0.05	6.51	3	0.01
CONFLO1_PFLO1	44.29	-72.58	3.01	6.58	4	0.01
PAGR	41.29	-72.58	0.01	6.59	3	0.01
PAGR_CONFLO2	44.28	-72.56	3.00	6.61	4	0.01
CONFLO1_EDFLO2	43.77	-71.54	2.49	7.63	4	0.01
CONFLO1_PPAST	43.72	-71.43	2.44	7.73	4	0.01
PAGR_EDFLO1	43.50	-70.99	2.22	8.17	4	0.01
PAGR_PFLO2	43.45	-70.89	2.17	8.27	4	0.00
EDFLO1_CONFLO2	43.31	-70.62	2.03	8.55	4	0.00
CONFLO1_PSILV	43.18	-70.37	1.91	8.80	4	0.00
PANT_PFLO2	43.18	-70.36	1.90	8.81	4	0.00
PAGR_ITA	43.11	-70.23	1.84	8.93	4	0.00
CONFLO1_ITA	43.05	-70.10	1.77	9.07	4	0.00
CONFLO1_PAGR	42.97	-69.95	1.69	9.22	4	0.00
EDFO2_CONFLO2	42.95	-69.90	1.67	9.27	4	0.00
PAGR_EDFLO2	42.92	-69.83	1.64	9.33	4	0.00
PSILV_PFLO2	42.91	-69.81	1.63	9.35	4	0.00
EDFLO1_PPAST	42.90	-69.80	1.62	9.37	4	0.00
EDFLO2_PPAST	42.89	-69.79	1.62	9.38	4	0.00
PANT_EDFLO1	42.82	-69.63	1.54	9.53	4	0.00
PPAST_PFLO2	42.79	-69.57	1.51	9.59	4	0.00
EDFLO1_PSILV	42.74	-69.48	1.46	9.69	4	0.00
PFLO1_CONFLO2	42.67	-69.34	1.39	9.82	4	0.00
CONFLO2_PPAST	42.65	-69.31	1.37	9.86	4	0.00
PSILV_EDFLO2	42.59	-69.17	1.31	9.99	4	0.00
PFLO1_PPAST	42.53	-69.07	1.26	10.10	4	0.00
PSILV_CONFLO2	42.48	-68.96	1.20	10.20	4	0.00
PANT_EDFLO2	42.47	-68.95	1.20	10.22	4	0.00
PANT_ITA	42.47	-68.93	1.19	10.23	4	0.00
PFLO1_PSILV	42.43	-68.86	1.15	10.30	4	0.00
PANT_PFLO1	42.16	-68.32	0.88	10.84	4	0.00
PPAST_ITA	41.93	-67.86	0.65	11.30	4	0.00

PSILV_ITA	41.85	-67.70	0.57	11.46	4	0.00
PSILV_PPAST	41.53	-67.06	0.25	12.10	4	0.00
PANT_PPAST	41.51	-67.02	0.23	12.15	4	0.00
OAGR_PPAST	41.51	-67.01	0.23	12.15	4	0.00
PANT_PAGR	41.41	-66.81	0.13	12.35	4	0.00
PANT_PSILV	41.39	-66.79	0.12	12.38	4	0.00
PAGR_PSILV	41.36	-66.73	0.09	12.43	4	0.00

Table 13. *P. poltys* -Scale 3 (Mahalanobis FA scores)

MODELS	LOGLIK	AICC	DLOGLIK	DAICC	DF	WEIGHT
EDFLO1	-3.87	17.74	3.07	0.00	3	0.20
PFLO2	-4.21	18.42	2.73	0.68	3	0.15
NULO	-6.94	19.60	0.00	1.86	2	0.08
ITA_PFLO2	-2.14	20.28	4.80	2.55	4	0.06
EDFLO1_ITA	-2.15	20.30	4.79	2.56	4	0.06
CONFLO2	-5.28	20.57	1.66	2.83	3	0.05
PFLO1	-5.52	21.04	1.42	3.30	3	0.04
PANT	-5.62	21.24	1.32	3.50	3	0.04
EDFLO2	-5.84	21.67	1.10	3.93	3	0.03
EDFLO1_PPAST	-2.97	21.93	3.97	4.19	4	0.03
PPAST	-6.12	22.23	0.83	4.49	3	0.02
EDFLO1_CONFLO2	-3.12	22.24	3.82	4.51	4	0.02
PAGR_EDFLO1	-3.55	23.09	3.39	5.35	4	0.01
PANT_EDFLO1	-3.59	23.18	3.35	5.44	4	0.01
CONFLO1_EDFLO1	-3.66	23.31	3.28	5.57	4	0.01
PANT_CONFLO1	-3.68	23.35	3.26	5.61	4	0.01
EDFLO1_PSILV	-3.70	23.40	3.24	5.66	4	0.01
PAGR	-6.77	23.54	0.17	5.80	3	0.01
CONFLO1	-6.77	23.54	0.17	5.80	3	0.01
PSILV	-6.80	23.59	0.14	5.85	3	0.01
PSILV_PFLO2	-3.80	23.60	3.14	5.86	4	0.01
ITA	-6.94	23.88	0.00	6.14	3	0.01
PPAST_PFLO2	-3.96	23.92	2.98	6.18	4	0.01
CONFLO1_PFLO2	-4.00	24.00	2.94	6.26	4	0.01
PFLO1_PPAST	-4.06	24.13	2.88	6.39	4	0.01
PAGR_PFLO2	-4.06	24.13	2.88	6.39	4	0.01
PANT_PFLO2	-4.09	24.17	2.86	6.43	4	0.01
PFLO1_ITA	-4.44	24.87	2.50	7.13	4	0.01
CONFLO2_PPAST	-4.49	24.97	2.46	7.23	4	0.01
PANT_ITA	-4.57	25.15	2.37	7.41	4	0.01
EDFLO2_PPAST	-4.59	25.18	2.35	7.45	4	0.00
PFLO1_PSILV	-4.68	25.37	2.26	7.63	4	0.00

PFLO1_CONFLO2	-4.81	25.62	2.13	7.88	4	0.00
PANT_EDFLO2	-4.86	25.72	2.08	7.98	4	0.00
PAGR_CONFLO2	-4.88	25.76	2.06	8.02	4	0.00
EDFO2_CONFLO2	-4.96	25.93	1.98	8.19	4	0.00
PANT_PFLO1	-5.08	26.15	1.87	8.41	4	0.00
CONFLO1_CONFLO2	-5.19	26.37	1.75	8.64	4	0.00
CONFLO1_PFLO1	-5.22	26.45	1.72	8.71	4	0.00
PANT_PPAST	-5.26	26.53	1.68	8.79	4	0.00
PSILV_CONFLO2	-5.27	26.53	1.67	8.79	4	0.00
PANT_PSILV	-5.34	26.69	1.60	8.95	4	0.00
OAGR_PPAST	-5.47	26.95	1.47	9.21	4	0.00
PANT_PAGR	-5.57	27.13	1.37	9.39	4	0.00
PSILV_EDFLO2	-5.59	27.17	1.35	9.43	4	0.00
EDFLO2_ITA	-5.59	27.18	1.35	9.44	4	0.00
CONFLO1_PPAST	-5.75	27.50	1.19	9.76	4	0.00
CONFLO1_EDFLO2	-5.82	27.63	1.12	9.89	4	0.00
PAGR_EDFLO2	-5.84	27.67	1.10	9.93	4	0.00
PAGR_ITA	-5.98	27.96	0.96	10.22	4	0.00
PSILV_PPAST	-6.03	28.05	0.91	10.32	4	0.00
PPAST_ITA	-6.11	28.22	0.83	10.48	4	0.00
CONFLO1_PAGR	-6.57	29.13	0.38	11.39	4	0.00
PAGR_PSILV	-6.71	29.41	0.24	11.67	4	0.00
CONFLO1_PSILV	-6.73	29.46	0.21	11.72	4	0.00
CONFLO1_ITA	-6.76	29.52	0.18	11.78	4	0.00
PSILV_ITA	-6.79	29.58	0.15	11.84	4	0.00